Water Yield in the Southern Appalachian Mountains

A DISSERTATION
SUBMITTED TO THE FACULTY OF THE GRADUATE SCHOOL
OF THE UNIVERSITY OF MINNESOTA
BY

Katherine Marie Kove

IN PARTIAL FULFILLMENT OF THE REQUIREMENTS
FOR THE DEGREE OF
DOCTOR OF PHILOSOPHY

Paul V. Bolstad, Thomas E. Burk

May 2011

Acknowledgements

This work would not have been possible without the guidance of my committee members, encouragement from my friends, and support of my family. So many people have been an inspiration to me, encouraged me to follow my dreams and have helped me to get to where I am.

I would like to express my deepest gratitude to my co-advisor, Dr. Paul Bolstad for his guidance, patience, and providing me with an excellent atmosphere for doing research throughout my degree. Also, his tireless edits of my dissertation developed this work into something I am truly proud of and I could not have done it without him. To my other co-advisor, Dr. Thomas Burk, I want to especially thank you for your continued intellectual challenges. Though I learned a lot from you about teaching, and leading field and lab courses, I am most thankful for the content that you have taught me. Your courses, especially those with three or fewer students, were my favorite courses of all time. Another special thanks to Dr. Alan Ek for inspiring me as an educator, mentor and scientist; his cheerfulness always brightened my day. Thank you also to Dr. Tracy Twine and Dr. Kenneth Brooks for serving on my dissertation committee, and always being so encouraging throughout the process.

A many thanks to all of my wonderful friends for their constant positive encouragement when I needed it most. I would like to thank my Dad for always truly believing that I could do anything, whether it was true or not, and my mom for teaching me to always stop and smell, paint, or sculpt the roses. I would like to thank my parents-in-love for their continued support, encouragement, advice and love. They are both true teachers in my life. Lastly, I would like to thank my husband for giving me support I did not know was possible. Finally, honey, it's time for you to get to sleep with the windows open.

Abstract

With over 55% forest cover, the southern Appalachians (SA) are a main water resource for the surrounding areas. These water resources are at risk due to changing climate and precipitation regimes as well as changes in forest cover. Understanding the implications of these risks will help to develop management strategies for an increasingly valuable resource. Evapotranspiration (ET), the combination of plant transpiration and surface evaporation, can vary across space and time, and is a significant component of the hydrological cycle in densely forested regions. Quantifying ET is critical to understanding the available water resource, especially in the SA. In the SA, ET averages 50% of annual precipitation in forested watersheds and can climb to 85%. However, ET is among the most difficult and complex component of the water cycle to measure and model. This dissertation addresses these complexities by investigating the ability of sap flow models to estimate ET and examining the impact of potential temperature and compositional shifts on water yield. We also examined sap flow input variables to determine the best methods for the SA including the spatial estimation of climatological variables, phenological dates, and leaf area index (LAI) estimates all of which would particularly enhance the development of our hydrological models.

The input variable analysis shows interpolating temperature requires elevation dependent interpolations, whereas precipitation is more spatially dependent. The Bristow and Campbell method had the lowest overall RMSE of 302 $\mu mol\ m^{-2}\ s^{-1}$ in the prediction of photosynthetically active radiation and vapor pressure deficit was best estimated by the temperature-based method. Phenologies were best estimated by growing degree day

models for spring and mean dates for fall. LAI estimates impact ET more than phenological estimates with a 3.1% change in ET from phenology estimates and an 11.5% change from LAI estimates.

Sap flow models underestimated catchment water balance ET by -11%. Although sap flow derived ET error was larger, advantages include increased flexibility in examining species composition and changes in future forests with only a 4% absolute difference in mean error compared to our best model.

ET increased with increasing temperature, 12% for 3.5 ^{o}C and 20% for 7 ^{o}C , except when temperatures increased more at night than the day (-2.8% for night biased 3.5 ^{o}C). Changes to a more mesic species composition increased ET by 8% whereas and a more xeric composition decreased ET by 2%.

Table of Contents

List of Tables

Chapter 1

Chapter 2

Chapter 3

Chapter 4

List of Figures

Introduction

Chapter 1

Chapter 2

Chapter 3

Chapter 4

Introduction

Water is essential to life on earth. Every ecosystem is dependent on water, and it is vital for all known forms of life. The majority of water, 96.5%, is found in oceans, with 1.74% in glaciers and ice caps. The remaining 1.76% is found in ground water (1.7%), soil moisture (0.001%), lakes (0.013%), atmosphere (0.001%), rivers (0.0002%), and other (0.045%), with only 1% accessible for human use (USGS, 2010). Water is dynamic and continually changing form, yet the amount on earth remains relatively constant.

The need for water is increasing, but the supply is declining. With decreasing surface and groundwater stores, the amount of water for human and ecological resources is in decline (Alley et al., 2002; Konikow and Kendy, 2005). Furthermore, the increasing human population, agricultural practices and industrial demand is requiring an ever increasing supply (USGS, 2006). With so much water used for human practices, less is available for the natural environment (Konikow and Kendy, 2005), and in some areas of the county human intervention has degraded or destroyed ecosystems from the removal of water (Whigham, 1999).

The southern Appalachians (SA) are a critical water resource for the surrounding region. Consisting of nearly 2 million square kilometers, the SA provides over 30 million people in the southeast with water. Additionally, this region contains unique habitat for rare and endangered plants and animals that rely on the regions high annual rainfall (Murdock, 1994). Limited water availability from drought and increased demand has led

to conflict over water rights in the southeast (Vest, 1993; Arrandale, 1999; Feldman, 2001; Dellapenna, 2005). For example, Georgia recently argued their boarder with Tennessee was executed incorrectly by surveyors in 1818, and its correct position would allow Georgia access to the Tennessee River (Copeland, 2008).

Pressure on the SA water resource requires increased understanding of the hydrological variability from year to year. The hydrological cycle encompasses precipitation, evaporation, plant transpiration, subsurface storage, subsurface flow and surface flow (Eisenbies et al., 2007). Evapotranspiration (ET), the combination of plant transpiration and surface evaporation, can vary across space and time, and is a significant component of the hydrological cycle in densely forested areas, such as the SA. Quantifying ET is critical to understanding the available water resource in this region. In the SA, ET rates average 50% of annual precipitation in forested watersheds and can climb to 85% (Lu et al., 2003). Due to high annual rainfall from this region, over 1000 mm of water return to the atmosphere annually (Zhang et al., 2001). Recent droughts across the southeast US attest to the potential impacts of changes in water availability, underscoring the need to better quantify the water cycle, and improve ET estimates (Moorhead, 2003).

ET is among the most difficult and complex components of the water cycle to model (Morton, 1983). Current models are extensive, ranging from temperature based models such as the Thornthwaite (1948) or the Hargreaves (1975), to radiation-based

models such as the Priestly–Taylor (1972) or Turc (1961), to more accurate combination equations including the Penman-Monteith model (Monteith, 1965).

Current ET models need improvement, particularly for estimating ET on forested catchments. One reason is that current models lack detailed species components. Some combination equations allow for a species term denoting general covertypes (forests, grassland, etc.), however, few general models include species-specific components. Including species compositions in ET modeling is indispensable due to the impact species composition has on ET. Studies have shown that transpiration varies among tree taxa on a leaf and tree basis. Consistent differences in rates between conifers and hardwoods have been measured (Ewers et al., 2002). Transpiration rates have also been measured across a variety of species, including red and silver birch (*Betula lenta and B. pendula*) (Kelliher et al., 1992), willow (*Salix spp.*) (Lindroth et al., 1995), oak (*Quercus spp.*) (Granier et al., 1996), beech (*Fagus spp.*) (Granier et al., 2000), cottonwood (*Populus spp.*) (Schaeffer et al., 2000) red maple (*Acer rubrum*), loblolly pine (*Pinus taeda*), chestnut oak (*Q. prinus*), white oak (*Q. alba*), red oak (*Q. rubra*), yellow-poplar (*Liriodendron tulipifera*) (Wilson et al., 2001), black gum (*Nyssa sylvatica*) (Wullschleger et al., 2001), Japanese cedar (*Cupressus japonica*) (Kumagai et al., 2005), apricot (*Prunus armeniaca*) (Nicolas et al., 2005) and white pine (*Pinus strobus*) (Ford et al., 2007).

Variation in species transpiration results from differences in physiological factors, including stomatal conductance and responsiveness to climate, and in structural

characteristics such as rooting depth, leaf area, canopy architecture, and the amount and permeability of sapwood (Vose et al., 2003). Differences in transpiration rates among woody species may impact total catchment transpiration and alter streamflow. Previous studies have shown that changes in species composition can impact stand ET and total catchment yield (Bosch and Hewlett, 1982; Ford and Vose, 2007, Wattenbach et al., 2007).

The development of sap flow models has addressed the need for a species driven ET model. Since sap flow is measured on an individual tree basis, sap flow equations can be derived for any measured tree species. In addition, they can be combined to estimate ET for a particular species composition. Studies, however, are limited as to the accuracy of scaling sap flow models to a variety of watersheds in the SA.

In order to use sap flow models to estimate catchment ET, we first need to calculate climate variables across the landscape, for use as model inputs. Climate variables required include precipitation, minimum temperature, and maximum temperature. Interpolating precipitation and temperature within small spatial and temporal scales is problematic, especially in mountainous regions (Skirvin et al., 2003). Low gauge density, particularly at high elevations, and incomplete periods of record, compound the need for accurate methods of interpolation (Willmott et al., 1991; Willmott et al., 1996; Costa and Foley, 1997). In addition, variance of precipitation and temperature are higher in mountainous regions. These further complexities are primarily due to changes in elevation, but also to slope, terrain shape and forest cover type (Chua

and Bras, 1982; Kyriakidis, 2001; Clark and Slater, 2006). A number of techniques for interpolating precipitation and temperature should be compared to determine the best available method.

Additional inputs required include vapor pressure deficit (VPD) and photosynthetically active radiation (PAR). VPD and PAR are sparsely measured both temporally and spatially (Alados et al., 1996). It is often not an option to interpolate VPD and PAR across the landscape, rather spatial layers are derived from interpolated surfaces of minimum and maximum temperature along with elevation (Blackburn and Proctor, 1983; Tanner, 1990; Zhang et al., 2000; Piri, 2009). Determining the best methods for estimating VPD and PAR across the landscape is important for developing the best methods in scaling sap flow models to the catchment.

Estimating the amount and duration of leaf area index (LAI) across the landscape is also required for use in sap flow models. Phenology, the timing of reoccurring biological events, drives ecosystem processes because leaves produce energy through photosynthesis, thereby impacting annual growth (Kramer et al., 2000). Since phenologies determine growing season length, they are also primary factors in determining annual net primary production and annual water consumption (Linderholm, 2006). The main drivers of spring phenology are temperature and photo period (Menzel, 2002). Spring leaf development is primarily estimated using growing degree-days, or the thermal sum, a sum of the variation in temperature from a threshold (Hunter and

Lechowicz, 1992). Determining the best starting date and threshold temperature is critical in estimating spring phenology.

Autumn phenology has not been studied as extensively as spring phenology (Menzel, 2002). The added complexities of senescence makes modeling autumn phenology more complicated, and the controls are less well-known (Fracheboud, 2009). Consequently, there is no consensus on the best modeling practices (Schaber and Badeck, 2005), probably due to the weak relationships between simple meteorological factors and autumn senescence (Menzel, 2002). To best utilize sap flow models, the best method for estimating fall phenology across the landscape should be determined for the SA.

Determining the best methods for interpolating and estimating inputs is essential for developing the best process in scaling sap flow to the watershed. Once these methods are determined, the accuracy in scaling sap flow models can be analyzed. Finally, models can be utilized for predicting the impacts of climate and species changes on watershed ET.

Study Area

Our study area, herein called the southern Appalachian region (SAR), encompasses western North Carolina, northern Georgia, and eastern Tennessee (Figure 1). Climate across the SAR is temperate, moist, and humid. Average annual temperatures range from 10 ^{o}C in the north to 18 ^{o}C in the south, with average annual precipitation ranging from 850 mm to over 2500 mm (NCDC, 2006). The region is

composed of Paleozoic and Precambrian bedrock deposited approximately 800 million years ago (Sankovski and Pridnia, 1995). Overstory composition and forest communities vary strongly with terrain and elevation across the SAR (Whittaker, 1956; Bolstad et al., 1998), and communities include mixed-deciduous (*Q. alba, Q. rubra, R. psuedoaccacia,* and *Carya* spp.), northern hardwoods (*A. saccharum, Tilia spp., B. aleghaniensis, A. octandra*), xeric oak-pine (*Q. coccinea, Q. prinus, O. arboretum,* and *P. rigida*), and cove (*L. tulipifera, B. lenta, Magnolia* spp.).

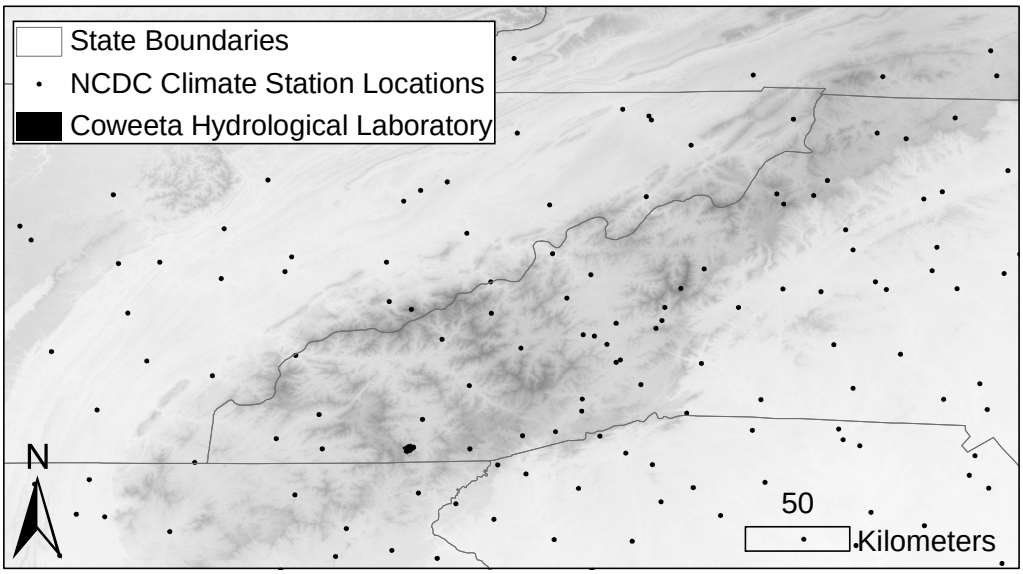

Figure 1: Southern Appalachian study area with locations of NCDC climate station locations and the Coweeta Hydrological Laboratory.

Understory most commonly includes *Rhododendron* spp. and *Kalmia* spp (Bolstad et al., 2001). Soils in this region vary considerably even at small scales and are most often represented by the orders ultisol and inceptisol where ultisols are found in basins, ridges, and areas of gentle topography, and inceptisols are found on steeper slopes (Swank and Crossley, 1988).

The second study area is the USDA Forest Service's Coweeta Hydrological Laboratory (CHL) and is located in southwestern North Carolina near the Georgia border (Figure 1). CHL is composed of a 2185 ha watershed with over 80 years of intact hydrological and climatologically data (Figure 2).

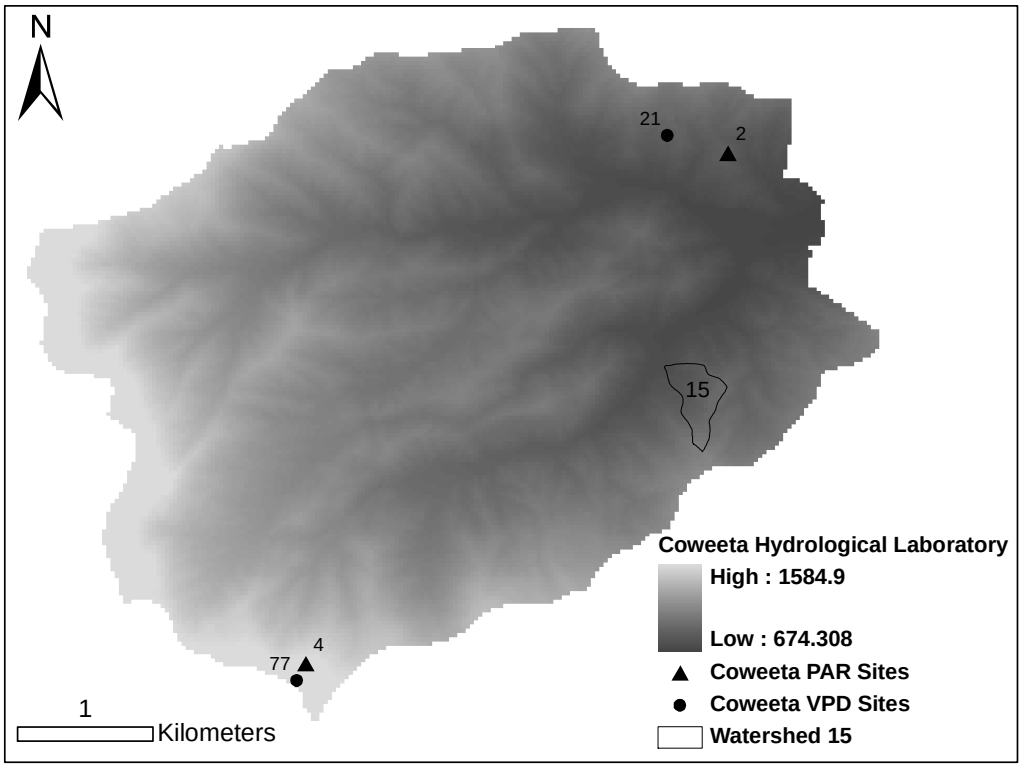

Figure 2: Coweeta Hydrological Laboratory digital elevation model with WS15, VPD climate station locations CS21 and CS77, and PAR locations S2 and S4.

Objectives

The goal of this dissertation is to establish the best ET model inputs for the region, determine ET model accuracy, and finally, use these tools to demonstrate the impacts of climate and species changes on regional water resources. This work is organized into four interrelated chapters written as manuscripts to be submitted to peer-reviewed journals. Chapters 1 through 3 focus on the development and modeling of inputs for ET models, and the accuracies of such models. Chapter 4 focuses on using the models for predictions of climate and species change impacts.

My dissertation is organized in the four chapters as follows:

1) Chapter one focuses on climate variable inputs to ET models. We establish the best interpolation method for precipitation and temperature within the SA by evaluating current methods and making comparisons using cross validation techniques. In addition, we establish the best VPD and PAR estimation techniques for the region by evaluating current methods and comparing to measured CHL data.

2) Chapter three examines the ability of sap flow models to estimate catchment ET. We first scale up species-specific sap flow models to a variety of watersheds in the SA and compare to catchment water balance estimates of ET. Then, we use three additional ET models, a regional multiple regression model, a PET/ET model, and a linear regression with precipiation and compare the predictive ability

to scaled sap flow equations and catchment water balance ET in estimating annual ET for the SA.

3) Chapter two looks at leaf phenology of the SA. This includes examining how leaf phenology changes seasonally, annually and across elevations. In addition, we propose to model leaf phenology (bud burst, leaf senescence) using climate variables, and as a function of above and below canopy PAR. Finally, we determine how the variability in leaf phenology and LAI impacts our sap flow estimates of ET.

4) Chapter four addresses the impacts of species and climate changes on ET in the SA. Using our sap flow models from Chapter 2, and the best input variables from Chapters 1 and 3, we study the impacts on ET estimates from increases in temperature and changes in species composition to more mesic or more xeric species.

Chapter 1: Estimating climate variables across the landscape

Accurate climate layers are important in a variety of fields including ecology, hydrology, forestry and climatology. Development of hydrological models is particularly enhanced by improvements in the spatial estimation of climatological input variables, because temperature, precipitation, solar radiation and atmospheric humidity are the main drivers in models that estimate evapotranspiration (ET) and hence catchment water yield. The best methods for interpolating minimum and maximum temperature and estimating photosynthetically active radiation (PAR) and vapor pressure deficit (VPD) for the southern Appalachians (SA) are not clearly defined in the literature. Our goal was to determine the best interpolation methods for temperature and precipitation and the best estimation methods for VPD and PAR for the SA. Analysis implemented regional regression (RR), ordinary kriging (OK) and kriging with external drift (KED) in the daily interpolation of minimum and maximum temperature and precipitation across 134 National Climatic Data Center (NCDC) stations from 1985-2005. PAR analysis compared the modified Hargreaves-Samani model and the Bristow and Campbell model to PAR data measured at the Coweeta Hydrological Laboratory (CHL) at two elevations. One temperature-based and one RH-based VPD model were also compared to data at CHL. Overall, KED and RR outperformed OK for interpolating temperature because elevation is included in the model and temperature and elevation are strongly correlated in the SA. Whereas, KED and OK out performed RR in interpolating precipitation, due to the strong spatial dependence of precipitation and the weak relationship between precipitation and elevation in our study region. PAR was best estimated using the

Bristow and Campbell method with an RMSE of 302 $\mu mol\ m^{-2}\ s^{-1}$, compared to 324 $\mu mol\ m^{-2}\ s^{-1}$ for the Hargreaves-Samani model. The VPD analysis shows that overall the temperature-based method had the lowest RMSE and mean error compared to the relative humidity-based method.

Introduction

Accurate climate layers are important to a variety of fields including ecology, hydrology, and forestry. Hydrological models are particularly enhanced by improvements in the spatial estimation of climatological input variables, because temperature, precipitation, and atmospheric humidity are the main drivers in models that estimate ET and hence catchment water yield (Krajewski et al., 1991; Shah et al., 1996; Koren et al., 1999; Carpenter et al., 2001; Xu et al., 2006). Therefore, for the improvement of ET models, it is essential to determine the best possible methods for estimating climate variables (Fekete et al., 2004).

Interpolating precipitation and temperature within small spatial and temporal scales is problematic, especially in mountainous regions (Book et al., 1992; Skirvin et al., 2003). Low gauge density, particularly at high elevations, and incomplete periods of record, compound the need for accurate methods of interpolation (Willmott et al., 1991; Willmott et al., 1996; Costa and Foley, 1997). In addition, variance of precipitation and temperature are higher in mountainous regions. These further complexities are primarily due to changes in elevation, but also to slope, terrain shape and forest cover type (Chua and Bras, 1982; Kyriakidis, 2001; Clark and Slater, 2006).

Many hydrological models require spatially distributed estimates of precipitation, temperature, vapor pressure deficit (VPD), and photosynthetically active radiation (PAR). VPD and PAR are sparsely measured both temporally and spatially (Alados et al., 1996). It is often not an option to interpolate VPD and PAR across the landscape, rather spatial layers are derived by predicting VPD and PAR from interpolated surfaces of minimum and maximum temperature, elevation, latitude and DOY (Blackburn and Proctor, 1983; Tanner, 1990; Zhang et al., 2000; Piri, 2009). Even with the limited accuracy these models bring, this method is still beneficial since both VPD and PAR are main drivers to modeling ET (Mulligan and Wainwright, 2004).

Studies have shown that radar-based precipitation estimates may be better than solely ground-based estimates (Johnson et al., 1999; Bellerby et al., 2000). However, terrain interference in mountainous areas may reduce accuracies or preclude radar (Ahrens, 2006; Clark and Slater, 2006; Antonio, 2009; Germann, 2009). Spatial time series require long periods of record, but the radar record is substantially shorter than the observational record. For these reasons, rain gauge data remains an important source for precipitation information across the country and thus the focus of this article.

A number of techniques for interpolating precipitation and temperature have been suggested. Classical approaches include Thiessen's (1911) nearest neighbor technique or Theissen polygons, where lines are drawn halfway between points and connected to make polygons with the center point value used to represent the polygon area (Thiessen, 1911).

Although appropriate on a more homogenous landscape or in less rigorous applications, single nearest neighbor techniques are inferior across mountainous areas and for highly detailed data requirements (Goovaerts, 2000; Buytaert et al., 2006).

Inverse distance weighted averages, developed by the US National Weather Service, weight points inversely based on their distance to the unsampled coordinate (Bedient and Huber, 1992). Although an improvement to Thiessens' simpler nearest neighbor technique, geographical distance in mountainous areas is not indicative, in and of itself, to correlations of temperature or precipitation. This is due to the influence that elevation has on both temperature and precipitation, which can lead to considerable changes in temperature and precipitation over small geographical distances.

Regional regression is a deterministic spatial interpolation technique using multiple predictors, including elevation, latitude/longitude, and/or terrain variables, in a regression function to estimate precipitation or temperature (Russo et al., 1993). These methods are greatly improved over earlier methods in mountainous regions due to the addition of elevation and terrain predictors (Carrera-Hernandez and Gaskin, 2007). A generally strong relationship between temperature and elevation and precipitation lead these methods to better represent the data. As elevation increases, temperature decreases, and orographic uplift often leads to an increase in precipitation (Pacl, 1972). Consequently, including elevation in the interpolation of precipitation often improves the accuracy, especially in mountainous areas (Chua and Bras, 1982; Hevesi et al., 1992; Phillips et al., 1992; Borga and Vizzaccaro, 1997; Skirvin et al., 2003; Haberlandt, 2007).

Spatial autocorrelation is the correlation of a variable with itself through space, and is the basis of geostatistics (Cliff and Ord, 1981). Based on the theory of regionalized variables, geostatistics allows for the optimization of weights assigned to neighboring points using a covariation between the data values of those points and their distances apart (Cressie, 1993; Goovaerts, 1997). Kriging with external drift also increases the complexity of the estimation procedure by introducing a secondary attribute, often more densely sampled, which generally improves the estimates. Numerous studies have shown the advantages to using kriging with external drift to interpolate precipitation, maximum temperature, and minimum temperature (Ishda and Kawashima, 1992; Phillips et al., 1992; Skirvin et al., 2003; Carrera-Hernandez and Gaskin, 2007; Haberlandt, 2007). Yet another study found regional regression (Bolstad et al., 1998) provided better estimates for temperature. For precipitation, Goovaerts, (2000) found ordinary kriging to be superior over kriging with external drift.

Although geostatistics have generally improved upon the estimation of precipitation and temperature, some have found that the results are dependent on gauge density and that with a low resolution network, geostatistics did not improve upon alternate methods (Dirks et al., 1998). Some results show that kriging with external drift using the co-predictor of elevation shows greater improvement over ordinary kriging when gauge density is low (Raspa et al., 1997). A study by Goovaerts (2000) used the correlation between elevation and precipitation to determine the best geostatistical method. He compared numerous geostatistical methods in a mountainous region of

Portugal, concluding that those with elevation as a covariate outperformed those without elevation only when the correlation between precipitation and elevation was greater than 0.75 (Lloyd, 2005). However, Carrera-Hernandez and Gaskin (2007) found that in the mountains of Mexico, kriging with elevation improved on ordinary kriging even in areas with a low correlation between elevation and precipitation.

PAR and VPD are sparsely measured and are thus hard to estimate by interpolation. Literature for PAR shows many complex models using sparsely-measured variables such as average annual radiation (Cooter and Dhakhwa, 1995), relative humidity (Thornton and Running, 1999), and radar return (Hashimoto, 2008). Without measurements of these variables, simpler models must be used. Minimum temperature and maximum temperature are the most spatially and temporally available variables. For this reason, temperature-based models estimating PAR and VPD are the best alternative (Blackburn and Proctor, 1983; Alados, 1996; Zhang et al., 2000). Consequently, instead of interpolating PAR and VPD, minimum temperature and maximum temperature are interpolated and PAR and VPD are estimated from the interpolated temperature values.

In general, PAR is a proportion of solar radiation calculated from the product of incoming daily extraterrestrial irradiance and a transmission coefficient (Tt). Tt represents the amount of solar radiation incident on the surface, and is generally modeled from the change in maximum and minimum daily temperature. Models sometimes include elevation (Diodato and Bellocchi, 2007). Hargreaves and Samani (1982) and Bristow and Campbell (1984) were among the first to model solar radiation using

minimum and maximum temperature. Both use nonlinear models to estimate transmittance based on change in temperature, and are still applied today. Arrandale (2002) created a more recent improvement in the Hargreaves-Samani model by adding elevation as an auxiliary variable, creating the modified Hargreaves-Samani model. PAR is extensively studied and a wide range of models are in the literature including empirical relationships (Cooter and Dhakhwa, 1995; Udo, 2002; Ball et. al., 2004) and physically based models (Hargreaves and Samani, 1982; Bristow and Campbell, 1984; Thornton and Running, 1999; Diodato and Bellocchi, 2007). However, even with the abundance of approaches, solar radiation models perform poorly, especially in mountainous terrain using temperature data as the primary predictor (Ranzi and Rosso, 1995). The best methods for predicting PAR have not been determined for many regions.

VPD is the difference between saturation vapor pressure (e_s) and actual vapor pressure (e_a) of atmospheric humidity. Estimation of VPD suffers from problems similar to PAR, primarily low measurement density. Further, many VPD models include minimally accessible climate variables such as minimum and maximum dew point temperatures and relative humidity (RH) (Howell and Dusek, 1995). It is not known how much these additional variables improve the estimates of VPD. More comparisons of the more complex RH model with that of a temperature model is needed.

Our study focuses on the SA, a critical water resource consisting of nearly two million square kilometers providing over 30 million people in the southeast with water. Limited water availability from drought and increased demand has led to conflict over

water rights in the southeast (Vest, 1993; Arrandale, 1999; Feldman, 2001; Dellapenna, 2005). For example, Georgia recently argued their border with Tennessee was executed incorrectly by surveyors in 1818, and its correct position would allow Georgia access to the Tennessee River (Copeland, 2008). Pressure on the SA water resource requires increased understanding of the hydrological variability from year to year of this region. Establishing the best methods for interpolating climate variables and better understanding the variability of those climate variables in the SA, ultimately leads to the improvement of ET models, a goal of this work.

There have been relatively few comparative studies for estimating climate variables across the SA. Determining the best methods using readily accessible data will allow for improvements in hydrological and ecological models throughout the region. The four objectives in this study are to (1) compare three methods for interpolating precipitation and temperature across the SA including a) regional regression, b) ordinary kriging and c) kriging with external drift using elevation as the auxiliary variable, (2) compare two temperature based PAR models, a) the modified Hargreaves-Samani and b) the Bristow and Campbell model for their predicative abilities across the SA at both a high and low elevation site, (3) compare two VPD models, one temperature based and one RH based for their predictive abilities in the SA at both high and low elevation sites, (4) characterize variability in measured precipitation, temperature, VPD and PAR.

Methods

Study Regions and Data Collection

Our study consists of two study areas. The first is the southern Appalachian region (SAR), consisting of the southern Appalachian Mountains and adjacent lands in western North Carolina, northern Georgia, and eastern Tennessee (Figure 1). Data from the SAR was used to interpolate climate variables including precipitation, minimum temperature, and maximum temperature. For interpolation, daily climate data was gathered for 134 climate stations across the SAR (Figure 1). Total daily precipitation, minimum temperature, and maximum temperature for each station from 1985-2005 was downloaded from the National Climatic Data Center (NCDC) website (NCDC, 2006). NCDC used a variety of instruments to measure temperature including glass thermometers, thermistors and thermocouples. Daily maximum temperature and minimum temperature were recorded in degrees Fahrenheit and converted to degrees Celsius. Precipitation was recorded in 15-min intervals and summed over 24 hour periods by the NCDC. Precipitation measurements were most commonly made using either tipping bucket or standard weighing gauges and were presented by NCDC in hundredths of inches and converted for our study to millimeters (NCDC, 2009). Gauge sites ranged in elevation from 100 m to 1980 m and ranged in annual precipitation from 854 mm $year^{-1}$ to 2418 mm $year^{-1}$.

The second study area is the USDA Forest Service's Coweeta Hydrological Laboratory (CHL) and is located in southwestern North Carolina near the Georgia border (Figure 1). CHL is composed of a 2185 ha watershed with over 80 years of intact

hydrological and climatologically data. Two datasets were developed at CHL to test PAR estimation methods and compare VPD estimation methods at high and low elevation sites. The first dataset consists of VPD data from two climate stations in CHL, climate station 21 (CS21) and climate station 77 (CS77) (Figure 2). CS21 is located on a southeast-facing, 21% sideslope at an elevation of 848 m and CS77 is located on a northwest-facing ridge, with an 18% slope at an elevation of 1439 m.

The second dataset consists of PAR data from two sites in CHL, PAR site 2 (S2) and PAR site 4 (S4). S2 is located adjacent to CS21 at an elevation of 810 m and S4 is located near CS77 at an elevation of 1380 m (Figure 2). S2 is a sideslope site with approximately 21% slope and with overstory trees primarily composed of chestnut oak and red maple. S4 is northwest facing sideslope, near a high ridge with approximately 18% slope and with overstory trees composed of chestnut oak and red oak.

Climate variables measured at CS21 and CS77 for use in the VPD analysis includes mean daily saturation vapor pressure, mean daily relative humidity, daily minimum temperature, and daily maximum temperature. Daily measured VPD was calculated using mean daily saturation vapor pressure and mean daily relative humidity following Castellvi et al. (1996). All climate variables at CS21 and CS77 were collected with a Campbell Scientific, Inc. automated data logger, Model CR10. Air temperature and relative humidity were measured using Campbell Model 207 and taken 1.3 m above the forest floor. PAR was measured from 2003 through 2009 at S2 and S4 using the Licor 190 quantum sensor, calibrated every few years and mounted above the canopy.

Measurements were taken every min and averaged hourly. Since we were interested in distinguishing leaf on/leaf off periods, and there was greater likelihood of stem or branch shading at lower solar angles, hourly values from 10am through 3pm of PAR in $\mu mol\ quanta\ J^{-1}$ were averaged to obtain daily values. There was a total of 8% missing data for S2 and 6% for S4 due to equipment failure over the study period, 2003-2009, though most was not during the leaf-out and senescence periods.

Climate in the study areas is temperate, moist and humid with average annual temperatures ranging from 10 ^{o}C in the north to 18 ^{o}C in the south. Average annual precipitation ranges from 850 mm in valleys to over 2500 mm across peaks. The region is composed of Paleozoic and Precambrian bedrock deposited approximately 800 million years ago (Sankovski and Pridnia, 1995). Overstory composition and forest communities vary strongly with terrain and elevation across the SA (Whittaker, 1956; Bolstad et al., 1998). Communities include mixed-deciduous (*Q. alba*, *Q. rubra*, *R. psuedoaccacia*, and *Carya* spp.), northern hardwoods (*A. saccharum*, *Tilia spp*., *B. aleghaniensis*, *A. octandra*), xeric oak-pine (*Q. coccinea*, *Q. prinus*, *O. arboretum*, and *P. rigida*), and cove (*L. tulipifera*, *B. lenta*, *Magnolia* spp.). Understory most commonly includes *Rhododendron* spp. and *Kalmia* spp (Bolstad et al., 2001). Soils in this region vary considerably even at small scales and are most often represented by the orders ultisol and inceptisol where ultisols are found in basins, ridges, and areas of gentle topography, and inceptisols are found on steeper slopes (Swank and Crossley, 1988).

Interpolation

This section provides a brief overview of the three interpolation methods used in this study, regional regression (RR), ordinary kriging (OK) and kriging with external drift (KED). Each model was applied to precipitation, minimum temperature and maximum temperature across the SAR. Regional regression was performed following a second degree polynomial model:

$$C_i = a + \beta_1 \cdot X + \beta_2 \cdot Y + \beta_3 \cdot Z + \beta_4 \cdot X^2 + \beta_5 \cdot Y^2 + \beta_6 \cdot Z^2$$

Where C_i's are the daily predicted climate variables, X is easting for a Cartesian projected coordinate system, Y is northing for a Cartesian coordinate system, and Z is elevation, flowing methods similar to Bolstad et al. (1998). In this work all data were projected to the universal transverse Mercator (UTM) zone 17 north, NAD83 (1986) coordinate system, and elevation in meters determined from a USGS National Elevation Dataset (NED) obtained at a 1-arc-second resolution (approximately 10 meters), with reported 2.44 m in root mean squared error (RMSE) of vertical accuracy.

Geostatistical techniques, in particular kriging, are based on a generalized least squares regression that model the spatial relationship of variables, in this case precipitation, minimum temperature, and maximum temperature. Unsampled locations are then estimated using a linear combination of neighboring observations.

Kriging models were based on:

$$C_i = \sum_{j=1}^{n} \lambda_j C_j$$

where C_i is the predicted climate variable, λ_j is the weight assigned by the variogram model, and C_j is the observed climate variable measured at each station. To apply the kriging method, observed variograms are fit following:

$$\gamma(h) = \frac{1}{2N(h)} \sum_{i=1}^{N(h)} [z(x_i) - z(x_i + h)]^2$$

Where $\hat{\gamma}(h)$ is the semivariance, h is the distance between observations, N is the number of locations, and $z(x_i)$ and $z(x_i + h)$ are the measured climate variables at location x_i and $x_i + h$.

Our two kriging variants can be distinguished by assumptions on the mean function. In OK we assume the expectation is constant, whereas in KED we assume the mean function is a linear combination with the auxiliary attribute, elevation. For a more detailed description of OK and KED refer to Goovaerts (1997).

Each interpolation method was performed to estimate precipitation and maximum and minimum temperature across the SAR using all available climate stations for each day from 1985-2005. In addition, using daily estimates of precipitation, we calculated monthly and annual aggregates to determine the predictive power across different temporal scales. Temperature was analyzed for daily estimates only, but error was averaged over monthly and annual time steps to analyze if seasonal or annual patterns existed.

Leave-one-out cross-validation was implemented to compare the performance among OK, KED and regional regression (Efron and Gong, 1983). The procedure involved removing a target climate station for that day and using the remaining dataset and a given method to estimate a value and prediction error at the target climate station. The process was repeated for all stations and all days. Precipitation, maximum temperature, and minimum temperature were predicted for each climate station across the SAR using this method. Error was computed as measured values minus predicted values. Summary statistics were calculated for daily total precipitation, monthly total precipitation, annual total precipitation, and daily minimum and maximum temperature. These summary statistics included bias or mean error, calculated as the average of the error, RMSE computed as the square-root of the averaged squared errors and linear relationship strength, computed as Pearson's correlation coefficient (ρ) between the predicted and explanatory variable. Spatial patterns of the error surfaces were visually inspected and if clustering was suspected, Moran's I was computed.

VPD

Two methods were used to estimate VPD, both described in Yoder et al. (2005). The first method, M_{Temp}, makes the assumption that in the calculation of ambient vapor pressure, minimum temperature can be substituted for dew point temperature. This substitution for dew point temperature appears valid in areas of high humidity, such as the SAR (Thornton et al., 1997). The second method, M_{RH}, assumed relative humidity can be used in the estimation of ambient vapor pressure. Relative humidity is defined as ambient vapor pressure divided by saturation vapor pressure multiplied by 100. Using

this definition, relative humidity multiplied by an estimation of saturation vapor pressure is used as an estimation of ambient vapor pressure.

M_{Temp} and M_{RH} VPD were both calculated by subtracting saturation vapor pressure, e_s, and ambient vapor pressure, e_a, following:

$$VPD = e_s - e_a$$

Both methods were calculated with the same e_s, but differed based on the calculation for e_a.

M_{Temp} and M_{RH} calculated saturation vapor pressure by averaging the saturation vapor pressure at the maximum daily temperature, T_{max} (^oC), and the minimum daily temperature, T_{min} (^oC) (Howell and Dusek 1995, Castellvi et al. 1996, Yoder et al., 2005). Saturation vapor pressure was found following Murray (1967) as:

$$e_s = \frac{e^o(T_{\max}) + e^o(T_{\min})}{2}$$

$$e^o(T) = 0.6108 \exp\left[\frac{17.27 \cdot T}{T + 237.3}\right]$$

M_{Temp} calculated e_a assuming dew point temperatures were equivalent to minimum temperatures following:

$$e_a = 0.6108 \exp\left[\frac{17.27 \cdot T_{\min}}{T_{\min} + 237.3}\right] \text{ (Thornton et al., 1997)}$$

M_{RH}, calculated e_a using relative humidity, following:

$$e_a(T) = \frac{RH_{mean}}{100}\left[\frac{e^o(T_{\max}) + e^o(T_{\min})}{2}\right]$$

Estimates of VPD were computed using M_{Temp} and M_{RH}, and temperature data measured at CS21 and CS77. VPD estimates were compared to measured VPD at both CS21 and CS77 for 17 years from 1993 to 2009.

PAR

PAR was estimated using daily extraterrestrial solar radiation, R_e (MJ m^{-2} s^{-1}), and was calculated from Bristow and Campbell (1984) using latitude and DOY. For the modified Hargreaves-Samani model (M_{HS}) global solar radiation, R_{g1} ,(MJ m^{-2} s^{-1}) was found by calculating the transmittance, T_{t1}, using elevation, E, change of temperature, $\Delta T = T_{\max} - T_{\min}$, and multiplying by R_e, where:

$$T_{t1} = 0.162 \cdot (1 + 2.7 \times 10^{-5} E) \cdot \sqrt{\Delta T}$$

The same process was used to calculate global solar radiation from Bristow and Campbell (M_{BC}) where global solar radiation, R_{g2} ,(MJ m^{-2} s^{-1}) was found by calculating the transmittance, T_{t2}, using change of temperature , ΔT , and multiplying by R_e, where:

$$T_{t2} = 0.7 \cdot \left(1 - \exp\left(-0.004 \cdot \Delta T^{2.4}\right)\right)$$

PAR was converted from R_g assuming 4.608 $\mu mol\ quanta\ J^{-1}$ (Campbell and Norman, 1998) and the assumption that 50% of global solar radiation fell in the range of 400-700 nm (Landsberg and Waring, 1997; Ford et al., 2007). PAR was estimated at S2 and S4 in CHL using methods, M_{HS} and M_{BC}, and data, elevation and daily temperature. Measured PAR data from S2 and S4 within CHL was used to compare estimated PAR predicted values from 2003 to 2009.

Predictive potential was analyzed for both VPD and PAR. Prediction error was computed as predicted values minus measured values. Summary statistics were calculated including mean error, RMSE and standard deviation. Further error analysis was continued with the examination of error against site variables including mean temperature, precipitation and elevation.

Analysis

All data analysis was performed in the statistical environment R. Statistical analysis of model performance was executed using equivalence testing to put the burden of proof on the model instead of using a null hypothesis that assumes the model is acceptable, reducing type I errors (Freese, 1960; Robinson and Froese, 2004). This was executed using a two one-sided t-test (TOST), requiring a normal distribution of the errors (Schuirmann, 1981; Westlake, 1981). Our test hypothesis is that the model mean errors are different than zero. This method requires the modeler to subjectively select a region between which the errors are considered negligible. This critical constant was chosen using guidelines described in Wellek (2003) which described 36% of the sample standard deviation as a strict test. All tests were at $\alpha=0.01$. If the null hypothesis was rejected, the model error was considered not significantly different than zero.

Results and Discussion

Temperature

Average monthly minimum and maximum temperature peaked in July and reached minimums in January. Average annual minimum and maximum temperature

ranged from 6.1 ^{o}C to 8.3 ^{o}C and 19.2 ^{o}C to 21.5 ^{o}C respectively. Average annual maximum and minimum temperatures covaried through time, peaking in 1986, 1990, and 1998. Mean annual standard deviation was 2.7 ^{o}C for minimum temperature and 3.1 ^{o}C for maximum temperature. Mean annual maximum temperatures varied more than mean annual minimum temperatures. Minimum and maximum temperatures had similar standard deviations each month. Monthly standard deviations of daily minimum and maximum temperatures decreased in summer months to minimum values in July near 1.6 ^{o}C and 2.1 ^{o}C respectively. Maximum monthly standard deviations were reached in January with 5.4 ^{o}C for minimum temperature and 5.3 ^{o}C for maximum temperature.

Temperatures typically decreased as elevation increased (F-test, $P<0.001$; Figure 3). Daily maximum temperature had a strong negative relationship with elevation with a correlation coefficient of 0.94. Daily minimum temperature had a moderately strong negative relationship with elevation with a correlation of 0.77. Correlations between mean monthly temperatures and elevation were consistently strong, ranging from 0.77 to 0.97 for maximum temperature and 0.62 and 0.87 for minimum temperature, with the strongest correlations during the summer months. Lower correlations occurred in spring and fall months for minimum temperature and in winter months for maximum temperature.

Overall, KED outperformed OK and RR in estimating both minimum and maximum temperature. The best method differed when daily errors were averaged over annual or monthly time scales. Cross validation of minimum and maximum temperature

interpolated daily and averaged annually showed KED with the lowest mean error compared with OK and RR. Mean error from interpolating maximum temperature was near zero for both KED and RR, with KED less than RR (Table 1). KED overestimated maximum temperature, RR underestimated, and OK underestimated over 10 times more than RR. Minimum temperature mean errors were near zero for all methods and none had a strong bias.

TOST was performed for minimum and maximum temperature model validation. All models were reasonable estimates of minimum and maximum temperature at the 36% level, though KED and RR were acceptable at the level of 15%. RMSE results for both minimum and maximum temperature showed KED with the lowest value, but very close to RR (Table 1). Both were smaller than OK which was 14% (0.2 ^{o}C) higher on average than RR and KED for minimum temperature and 28% (0.6 ^{o}C) higher for maximum temperature averaged annually.

The standard deviations of our temperature estimates underestimated the standard deviations of the measured temperatures. Annual standard deviations of predicted minimum and maximum temperature for all methods were smaller than standard deviations from measured minimum and maximum temperature, as one would expect. Measured maximum temperature standard deviations were most similar to those predicted by KED and least similar to those predicted by OK. For minimum temperature, KED standard deviations were most similar to observed and RR were least similar. Standard deviation from predicted temperature data had a similar temporal pattern across

our study period compared to standard deviations of measured temperatures. Even the larger differences in standard deviation are still practically insignificant.

Estimates improved, and ranks of the best estimation method were different for monthly averages when compared to daily averages. Monthly RMSEs were half that of the daily RMSEs, an improvement of 1.8 ^{o}C on average. Mean error for maximum temperature dipped in the summer months and peaked in the winter months. KED and OK overestimated maximum temperature across all months, and RR overestimated maximum temperature during the summer months and underestimated during the winter months. All methods overestimated minimum temperature for all months yet still dipped in the summer months and peaked in the winter months. KED mean error for minimum temperature averaged monthly was significantly smaller than RR and OK (t-test, $P<0.001$). RR maximum temperature mean error was smaller than OK and KED showing it had the smallest bias.

Monthly RMSE ranged from 1.4 ^{o}C to 2.7 ^{o}C for minimum temperature and 1.4 ^{o}C to 3.0 ^{o}C for maximum temperature, peaking in the winter months and dipping in the summer months. KED and RR RMSE were less than OK for maximum temperature averaged monthly.

The best methods for interpolating temperature in the southern Appalachian Mountains from our study are KED and RR. Methods differed little in RMSE, however biases show significant differences. Maximum temperature errors from KED

overestimated, and RR underestimated measured values. Minimum temperature showed opposite results with KED underestimating and RR overestimating measured values. A similar result from Bolstad et al. (1998) showed maximum temperature was primarily overestimated by RR and minimum temperature was primarily underestimated by RR for the SA. However, magnitude of error found here was significantly smaller than that of Bolstad et al. (1998), with a bias of -0.46 ^{o}C and 1.75 ^{o}C for maximum and minimum temperature respectively, compared to our biases of -0.0027 ^{o}C and 0.0046 ^{o}C, respectively. One possible explanation is the larger sample size used in our study compared to Bolstad et al. (1998), reducing mean error.

Our study found that OK underestimated both minimum and maximum temperature nearly ten times greater than the other methods. These results confirm those of a similar study from Jolly et al. (2005) that found OK underestimated predictions for both minimum and maximum temperature. Bias estimates were again larger in Jolly et al., (2005) possibly due to their broader study region, the continental United States. Additionally, sample size differences may be responsible. Their study consisted of only one year of data. Cerrera-Hernandez and Gaskin (2007) found KED interpolated minimum and maximum temperature across Mexico better than OK with similar RMSE to ours, but with a 12% lower RMSE for minimum temperature. This may be a result of the differing elevational range between our study areas. Cerrera-Hernandez and Gaskin studied an area of Mexico ranging from 2000 to 5500 m, where our study only reached 2000 m.

KED and RR are the best interpolators for temperature in our study possibly due to the strong relationship between temperature and elevation across the SAR. Since KED and RR include elevation in their interpolations, they would benefit from the increased strength in relationship. Goovaerts (2000) found elevation increased predictive power in interpolation as long as the correlation between the climate variable and elevation was above 0.75. For our study, the correlations are both above 0.75 for minimum and maximum temperature and elevation.

The geostatistical techniques, KED and OK, include spatial dependence as part of their interpolation. This may be a reason why OK performs so poorly compared to KED and RR in the interpolation of temperature. OK relies primarily on the spatial dependence of temperature, known to be weak, particularly compared to precipitation (Gomez et al., 2008). This was observed in Gomez et al. (2008) where in regions of sparse climatologically stations and complex terrain, temperature was best interpolated using altitude as the sole predictor, and ignoring the spatial relationship.

Precipitation

Annual precipitation averaged 1311 mm across the SAR ranging from 932 mm to 2205 mm. Monthly precipitation ranged from 37 mm to 303 mm with an average of 109 mm. Averaged across stations, minimum monthly precipitation occurred in October and maximum monthly precipitation occurred in July. Daily precipitation averaged 3.77 mm ranging from 0 mm to 419 mm.

Precipitation generally increased as elevation increased ($P<0.001$, F-test; Figure 4). Mean annual precipitation and elevation had a weak positive relationship with a correlation of 0.44. There was a seasonal relationship between monthly precipitation and elevation, where stronger relationships were found in the summer months, with correlations ranging from a minimum of 0.06 in October to a maximum of 0.59 in September (Figure 6). There was also a spatial relationship for the correlations between elevation and precipitation with stronger correlations for southern sites that increased during the summer months (Figure 5). Annual and monthly correlations were analyzed for three latitudinal groups (LatGroup 1: Latitude < 35.26, LatGroup 2: 35.26 < Latitude < 36.03, LatGroup 3: Latitude > 36.03). For the most southern group, elevation and annual precipitation had a moderately strong relationship with a correlation of 0.63 (F-test, $P<0.001$). LatGroup 2 had a slightly weaker relationship with a correlation of 0.57 (F-test, $P<0.001$), and the LatGroup 3 relationship was the weakest with a correlation of 0.44, not different than when all stations were grouped together (F-test, $P<0.05$). The relationship between monthly precipitation and elevation was impacted by season. Correlations were higher in summer months for the southern 2 groups, with correlations of 0.85 for LatGroup 1 and 0.71 for LatGroup 2 (F-test, $P<0.001$; Figure 5a). In winter, LatGroup 1 had a strong relationship with a correlation of 0.79, but no relationship existed in the remaining groups (F-test, $P<0.001$; Figure 5b). No differences were found when stations were grouped by longitude.

Overall KED and OK outperformed RR when estimating annual, monthly and daily precipitation. Often KED was more accurate than OK, such as during the summer

and in the lower latitudes, but not significantly so. KED was only significantly better (smaller RMSE) than OK at daily estimates, most likely due to the large sample size. All methods performed worst in the summer months, except for KED and RR in the southern most group.

Annual precipitation estimates were biased for all methods, although much more so for RR (25.5 mm $year^{-1}$) than OK (2.5 mm $year^{-1}$) and KED (2.8 mm $year^{-1}$) (Table 2). OK and KED had very similar results across the study period. The RMSE for RR estimating annual precipitation was on average 19.4% above OK and KED RMSE. KED had a lower RMSE compared to OK for 9 of the 21 years and OK had a lower RMSE for 12 of the 21 years. RR was outperformed for all years except for 2000 when it had the lowest RMSE, and 2001 when it had a lower RMSE than OK. All precipitation interpolation methods were analyzed using TOST, and all models were found to be reasonable estimates of daily precipitation at the 36% of the standard deviation, though both KED and OK were acceptable at the 15% of the standard deviation. When analyzed for monthly estimates, the results did not change. However, annual estimates of precipitation were not significant and only passed at 70%, considered a very liberal test (Wellek, 2003). Though we do have reasonable estimates of precipitation, we only examined 20 years for annual precipitation, data that varies greatly from year to year.

Models performed differently by season. OK performed worse in the summer months compared to winter, where the performance of KED and RR was not significantly different during the summer. Additional differences were found when analyzed by

season and latitudinal groups. Both models performed worst in the summer months, however for the two southern most groups, KED and OK, RMSE decreased during the summer months.

Prediction error increased as elevation increased with KED mean error impacted the least by changes in elevation. Elevations above 600 m showed an increase in bias, with RR derived annual precipitation mean error jumping from -19 mm $year^{-1}$ below 600 m to an average of -55 mm $year^{-1}$ above 600 m. OK estimated annual precipitation had a bias of -10 mm $year^{-1}$ for sites below 600 m and 41 mm $year^{-1}$ for sites above 600 m. KED derived annual precipitation had the smallest increase in bias with a mean error of -0.7 mm $year^{-1}$ for sites below 600 m and an increase to -12 mm $year^{-1}$ for sites above 600 m.

A moderately strong, decreasing linear trend with time existed for OK mean error (ρ=0.72; F-test, P<0.05), trends for KED and RR did not exist. RMSE of annual precipitation estimates increased over time for OK and KED, with a strong linear trend for OK (ρ=0.78; P<0.05) and a moderate linear trend for KED (ρ=0.58; P<0.001). OK RMSE increased more rapidly through time, showing an increase in RMSE of 4.0 mm $year^{-1}$ compared with KED's RMSE trend of 2.6 mm $year^{-1}$. RMSE for all methods followed a similar pattern to that of measured precipitation, as precipitation increased, RMSE increased (Figure 7). Though measured precipitation slightly increased over our study period, the change was not significant (F-test, P<0.05). Both RR and KED RMSE

from estimating annual precipitation had the strongest relationships with annual precipitation (ρ=0.87; ρ=0.79), OK had a moderate relationship (ρ=0.59).

RR consistently overestimated monthly precipitation, leading to a mean monthly error of 2.33 mm month^{-1}, where KED and OK were much lower (Table 2). KED slightly overestimated monthly precipitation on average with a mean error of 0.30 mm month^{-1} and OK slightly underestimated monthly precipitation on average with a mean error of -0.26 mm month^{-1} with one month of overestimation. RMSE of monthly precipitation from cross validation was lowest for KED. RR RMSE was on average 23% higher compared to both OK and KED for all months. The monthly pattern for RMSE was similar across all methods peaking in the summer months and March and decreasing in the fall and winter months including April and May. There was a moderate relationship between average monthly precipitation and mean error from KED derived monthly precipitation (ρ=0.63) and weak relationships for OK (ρ=0.50) and RR (ρ=0.45) derived monthly precipitation and measured monthly precipitation.

Results for interpolating daily precipitation showed mean error for RR had a positive bias, consistent with both the monthly and annual results (Table 2). KED and OK mean error remained near zero, though RMSE for KED was smaller than OK RMSE. The standard deviation of mean error increased throughout the study period, from 1985 to 2005, for KED and OK derived daily precipitation, but not significantly (F-test, P>0.05).

The best methods for interpolating precipitation in the southern Appalachian Mountains are KED and OK most likely due to the strong spatial dependence of precipitation and the weak relationship between precipitation and elevation in our study region. As opposed to temperature, where we found earlier in this chapter models that included elevation performed the best, for precipitation, elevation did not improve the estimates. The relationship between precipitation and elevation across the SAR is weak, consequently, elevation does not improve the interpolation of precipitation, as demonstrated by the high RMSE for RR. Goovaerts (2000) found elevation increased predictive power in interpolation as long as the correlation between the climate variable and elevation was above 0.75. Our overall correlation between precipitation and elevation was 0.44, well below Goovaerts (2000) minimum, confirming their result. Carrera-Hernandez and Gaskin (2007), however, found that adding elevation to the interpolation of precipitation improved results over ordinary kriging even with low correlations with elevation. Their correlations ranged from 0 to 0.25 for precipitation and elevation, much lower than our correlation with precipitation. Differences between our studies that may be potential explanations include gauge density and time scale. Their study had nearly 10 times more gauges per square kilometer than our study. Increased gauge density, most likely lead to more accurate climate interpolation results, particularly in a mountainous region. Further, their study included only two months of data, both from June, making comparisons between our results difficult.

Though the strength of the precipitation and elevation relationship was weak overall, it was stronger in the southern regions and during the summer. This supports our

explanation, of model performance dependent on elevation and precipitation relationship. OK performed significantly worse in the summer months compared to winter, where the performance of KED and RR was not significantly different during the summer. OK performed worse than KED and RR in the summer because the relationship between precipitation and elevation strengthened.

Another possible explanation for the weak results of RR in estimating precipitation could be the strength of spatial dependence. Since precipitation shows greater spatial variation than temperature in the SAR, methods incorporating spatial dependence, OK and KED, may improve estimates over those that ignore it, RR. This was observed in Gomez et al. (2008) where in regions of sparse climatologically stations and complex terrain, temperature was best interpolated using altitude, and precipitation was best interpolated using averages of similar neighboring stations due to the differences in spatial variation. The unique spatial variation in precipitation, compared to temperature, is a result of the complex processes involved in generating cloud formation, adverse storm trajectories, and ultimately precipitation (Singh, 1997; Gomez et al., 2008).

VPD

Mean annual VPD varied considerably across time with a high of 0.82 kPa reached in 2001 and a low of 0.52 kPa in 2003. VPD also varied considerably by season and site with higher values in the summer months and at the higher elevation site, CS77, compared to the lower elevation site, CS21 (t-test, $P<0.01$; Table 3).

VPD model validation using TOST showed M_{temp} was significant at 36% of the standard deviation, but M_{RH} was not significant until 50% of the standard deviation. M_{RH} performed better at CS21, while M_{temp} performed better at CS77 according to RMSE and bias (Table 3). M_{temp} VPD had biases of 0.15 kPa and -0.08 kPa for CS21 and CS77 respectively, whereas M_{RH} VPD had biases of -0.09 kPa and 0.40 kPa, for CS21 and CS77 respectively (Table 3). RMSE was 0.29 kPa and 0.21 kPa for M_{temp} VPD at CS21 and CS77 respectively and was 0.13 and 0.46 for M_{RH} VPD at CS21 and CS77 respectively.

M_{temp} VPD were significantly higher than those estimated from M_{RH} for both sites (t-test, $P<0.01$; Table 3). Maximum measured VPD were significantly higher than maximum estimated VPD for both methods and both sites (t-test, $P<0.05$). The variance of VPD estimates from both methods was lower than the measured VPD variances for both sites. Seasonally averaged error showed a distinctive pattern of increases in the spring and summer months for both methods and decreases in the fall and winter months (Figure 8).

Another important result is the impact of interpolated temperatures on estimating M_{temp}. In most studies, temperature is not continually measured across the landscape, but rather interpolated from sparse climate stations. As a result, temperatures usually contain error. Since temperature is the main input into M_{temp}, inaccurately estimated temperature will impact the accuracy of M_{temp} VPD estimates. Using our interpolated temperature layers from the first part of this study, estimated temperatures were replaced in the

estimation of VPD using M_{temp} at CS21 and CS77. VPD accuracy did not change significantly for CS77. However, when using estimated temperatures, RMSE and mean error at CS21 were significantly greater than M_{temp} and M_{RH} calculated from measured temperatures.

Measured VPD was in the expected range for the humid SA. VPD was larger at the high elevation site and during the summer (Carter et al., 1987; Kubota, 2005; Zhang et al., 2005). Errors associated with estimating VPD averaged 0.22 kPa, well within the expected range found from Glassy and Running (1994) of 0.11 kPa to 0.43 kPa.

One possible explanation for M_{RH} having smaller errors than M_{Temp} at CS21 is the greater amount of information found in M_{RH}. M_{Temp} estimates both saturation vapor pressure and ambient vapor pressure with no vapor pressure information other then temperature and the assumed relationship between temperature and vapor pressure. On the other hand, M_{RH} estimates ambient vapor pressure using relative humidity, which is strongly related to ambient vapor pressure as long as there is an acceptable estimation of saturation vapor pressure. Consequently, M_{RH} includes more information in the estimation of VPD compared to M_{Temp} and this difference may explain the increased predictive power.

Positive biases in M_{Temp} VPD in the summer months may be related to the differences between daily dew point temperature and minimum temperature, which are greater during the summer months (Kimball et al., 1997). According to Kimball et al.,

(1997) differences between dew point temperatures and minimum temperatures are not expected to be large in humid environments. Their study found differences between dew point and minimum temperature derived VPD should be lower than 0.3 kPa. Our results are comparable, as we found summer biases between 0.1 kPa and 0.15 kPa from M_{Temp} VPD.

Increased bias of M_{Temp} VPD may also be a result of the non-linear relationship between temperature and VPD (Hashimoto et al., 2008). Consequently, as VPD increases, the error associated with measuring VPD with temperature would increase exponentially. Hence, error would increase from the winter months to the summer months, and since bias in the winter months started as negative and ended as positive, mean errors would be closer to zero for M_{Temp} derived VPD than the positive M_{RH} derived VPD bias.

The positive bias in M_{RH} VPD is primarily due to errors in summer. Winter estimates had a relatively small bias. Positive biases associated with M_{RH} VPD may be a result of RH measurement error. RH sensors are prone to error and degradation over time, resulting in measurement error according to Glassy and Running (1994). Increases in RH in the summer months might magnify this error resulting in larger errors during the summer. In contrast, M_{Temp} estimates had a smaller positive bias in the summer months and small negative bias in the winter months, resulting in a more accurate mean monthly and annual VPD compared to M_{RH} derived VPD (Figure 8).

Large positive summer biases from M_{RH} VPD also may be a result of how average daily RH is computed, resulting in an overestimation during the summer months. Instead of measuring 15-min or hourly RH values to compute VPD and averaging VPD throughout the day, mean daily RH was used to compute average daily VPD directly. This process has the potential to underestimate RH for the day and therefore overestimate VPD. Since hourly RH varies more during the summer than winter, mean RH and therefore VPD will be more influenced during the summer months (Court and Waco, 1965)

PAR

Daily PAR measurements (PAR_m) had similar distributions at S2 and S4 for all years, with ranges from 0 to 1875.8 $\mu mol\ m^{-2}\ s^{-1}$ at S2 and 24.25 to 1917.8 $\mu mol\ m^{-2}\ s^{-1}$ at S4, though mean annual PAR_m was significantly higher at S2 compared to S4 (t-test, $P<0.01$). Deviations from the mean among annual PAR_m were consistent between sites with no significant difference, although overall S2 had a slightly lower standard deviation. Monthly variation in PAR_m peaked in May and June for S2 and S4, respectively, and reached a minimum in December. Monthly deviation in PAR_m was largest in the summer months when PAR_m maximums were reached.

The M_{BC} model performed better than M_{HS} for both sites in terms of RMSE, however M_{HS} had a smaller bias at S2 (Figure 9). Overall, M_{HS} estimated PAR had a mean error of 91.24 $\mu mol\ m^{-2}\ s^{-1}$, a 13% overestimation, whereas M_{BC} estimated PAR

had a mean error of -49.2 $\mu mol\ m^{-2}\ s^{-1}$, a 6% underestimation. When separated by site, at S2, mean error was 98 $\mu mol\ m^{-2}\ s^{-1}$ for M_{HS} and 0.53 $\mu mol\ m^{-2}\ s^{-1}$ for M_{BC}. Yet for S4, mean error for M_{BC} PAR was -108.5 $\mu mol\ m^{-2}\ s^{-1}$ and for M_{HS} PAR was 83 $\mu mol\ m^{-2}\ s^{-1}$.

PAR model validation using TOST found both models were reasonable estimates of daily PAR at the 36% of the standard deviation. M_{HS} estimated PAR had an RMSE of 324 $\mu mol\ m^{-2}\ s^{-1}$ whereas M_{BC} estimated PAR was slightly lower with an RMSE of 302 $\mu mol\ m^{-2}\ s^{-1}$. M_{BC} PAR had a lower RMSE compared to M_{HS} PAR for both S2 and S4. Daily mean error averaged annually were primarily negative from 2003 though 2005, with a larger bias from 2006 through 2009 for both methods at both sites. For M_{HS} and M_{BC} at S2, there was a strong positive relationship with mean annual PAR error and mean annual maximum temperature but no relationship at S4. No other relationships with climate were found.

Mean monthly error in estimated PAR was negative in winter and positive in summer months for both sites and methods (Figure 10 a and b). The largest mean errors for both methods occurred in the summer months and peaked in July at S2, as well as for M_{HS} mean error at S4. M_{BC} mean error was largest in the winter months and reached a maximum in October. Variation was also another important feature to note. PAR_M values varied considerably with standard deviations near 300 $\mu mol\ m^{-2}\ s^{-1}$ for both sites. Both methods result with standard deviations near the anticipated 300 $\mu mol\ m^{-2}\ s^{-1}$.

M_{BC} and M_{HS} predicted PAR and associated error showed clear seasonal variations that varied by elevation. Overall, M_{BC} overestimated PAR_m in the summer and underestimated PAR_m in the winter. At S4, the high elevation site, M_{BC} had a more extreme negative bias during winter compared to S2, the low elevation site. In the summer months M_{BC} estimates had a more extreme positive bias at S2 compared to S4. M_{HS} estimates demonstrated a similar pattern for the summer months, with more extreme positive biases at S2 compared to S4. In the winter, M_{HS} estimates had relatively little bias at either site, leading to an overall overestimation.

The best method for estimating PAR in SA is M_{BC}, though bias performance differed by site. Predicting PAR is difficult in the complex terrain of the SA. The results of our PAR analysis demonstrate that change in daily temperature and elevation is significant in models that predict PAR. Ranking the models according to RMSE reveals that M_{BC} is the better model, even though M_{HS} includes elevation as an additional predictor. M_{BC} also has lower overall bias and smaller deviations in error compared to M_{HS}. Though M_{BC} was the better model overall, both M_{HS} and M_{BC} had strengths and weaknesses.

Mean PAR_m significantly differed between our two sites, S2 and S4, as did model error. This may be in part due to differences in terrain. Terrain or canopy shading, a result of steep slopes and the position of the sensor, potentially blocks sun. Comparing midday, morning or evening PAR across different seasons, shows us if sun angle impacts

PAR at different times of the day. However, this analysis found no differences, confirming terrain shading was not a factor. Beyond terrain and canopy shading, miscalibration of equipment may be responsible for the differences in PAR_m across sites.

One possible explanation for the increased error associated with S2 for both models is the larger standard deviation at the site. Increased variation often leads to increased error (Clinton, 2003).

Previous studies confirmed the seasonal and elevation patterns in PAR. Abraha and Savage (2008) used M_{BC} to estimate solar radiation across a variety of global sites and found it performed best at higher elevations compared to lower elevation sites. They also found that M_{BC} performed better than the original Hargreaves-Samani model. Diodato and Bellocchi (2007) found radiation was generally overestimated by M_{HS}, and bias decreased slightly in summer months when averaged over 13 study sites in Italy. Ball et al. (2004) also observed a slight over estimation when using M_{HS}.

Seasonality, in monthly PAR, might be a result of increased precipitation in the summer months, particularly for M_{HS}. Abraha and Savage (2008) found poorer performance during the rainy season, most likely due to increased cloud cover. Bois et al. (2008) and Udo and Aro (2000) also found underestimates more pronounced during rainy seasons than dry seasons.

Underestimates in the winter, primarily from M_{BC}, are not likely a result of snow cover as described by Thornton and Running (1999). They found snow reflection to increase measured solar radiation inappropriately resulting in underestimates during the winter. Although snow cover increases with elevation, and average snow depth and frequency are likely larger for S4 than S2, snow is infrequent at CHL. Snow cover averages a few days per year at the highest elevations, with a long yearly time series of no snow, leading to doubt this reasoning as an explanation for our observed differences.

Conclusion

In this research we determined the best methods for interpolating temperature and precipitation and the best methods for estimating VPD and PAR in the SA. Temperature was best interpolated using methods dependent on elevation and precipitation was best interpolated using methods dependent on spatial location. PAR was best estimated using the Bristow and Campbell model and VPD was best estimated using the temperature-based method. Future studies are needed to examine the impact from climate station density and location on model performance.

Temperature Prediction Method	Bias (^{o}C)	RMSE (^{o}C)
Maximum Temperature		
Regional Regression	0.0046	2.1767
Kriging External Drift	-0.0039	2.1475
Ordinary Kriging	0.0503	2.7981
Minimum Temperature		
Regional Regression	-0.0027	2.1839
Kriging External Drift	0.0010	2.1768
Ordinary Kriging	0.0096	2.4320

Table 1: Error in estimating daily temperature by prediction method from data collected from 1992-2008 from two climate stations CS21, CS77. Bias is mean error measured as temperature minus observed temperature. RMSE is root mean squared error. Error was computed using leave-one-out cross validation.

Time Step	Prediction Method	Estimate	Bias	RMSE	MAE	Standard deviation
Daily	Regional Regression	3.0125	0.0648	6.83	2.92	0.6142
	Kriging External Drift	2.9441	0.0020	6.37	2.78	0.4977
	Ordinary Kriging	2.9366	0.0020	6.38	2.85	0.4973
Monthly	Regional Regression	111.52	2.33	17.63	13.23	17.52
	Kriging External Drift	109.11	0.30	13.45	10.03	13.49
	Ordinary Kriging	108.92	-0.26	13.90	9.67	13.94
Annual	Regional Regression	1336.70	25.45	215.39	163.67	214.66
	Kriging External Drift	1314.06	2.81	171.54	127.68	172.17
	Ordinary Kriging	1313.74	2.49	172.03	127.44	172.66

Table 2: Precipitation prediction errors based on daily (mm day^{-1}), monthly (mm $month^{-1}$) and annual (mm $year^{-1}$) precipitation from 1985-2005 at 134 climate stations. Bias is mean error measured as precipitation minus observed precipitation, RMSE is root mean squared error. MAE is mean error after values are made positive. Error was computed using leave-one-out cross validation.

			Temperature Method (kPa)		*Relative Humidity Method (kPa)*	
		Measured VPD (kPa)	*Estimated VPD*	*Error*	*Estimated VPD*	*Error*
Combined	*Mean*	0.57	0.61	0.04	0.42	0.15
	RMSE			0.25		0.34
	Standard deviation	0.39	0.30	0.25	0.29	0.30
	Maximum	2.26	1.85	0.77	1.99	1.91
	Minimum	0.00	0.04	-1.65	0.00	-0.49
CS21	*Mean*	0.36	0.51	0.15	0.45	-0.09
	RMSE			0.29		0.13
	Standard deviation	0.27	0.23	0.25	0.25	0.10
	Maximum	1.93	1.27	0.77	1.75	1.91
	Minimum	0.00	0.04	-1.65	0.00	-0.49
CS77	*Mean*	0.78	0.70	-0.08	0.38	0.40
	RMSE			0.21		0.46
	Standard deviation	0.37	0.33	0.19	0.31	0.24
	Maximum	2.26	1.85	0.57	1.99	1.32
	Minimum	0.01	0.09	-1.10	0.00	-0.33

Table 3: Statistics of measured and predicted daily VPD for two sites, CS21 and CS77 at CHL, from 1992-2008. Prediction methods are a temperature-based method and a relative humidity-based method. RMSE is root mean squared error. All units are in kPa.

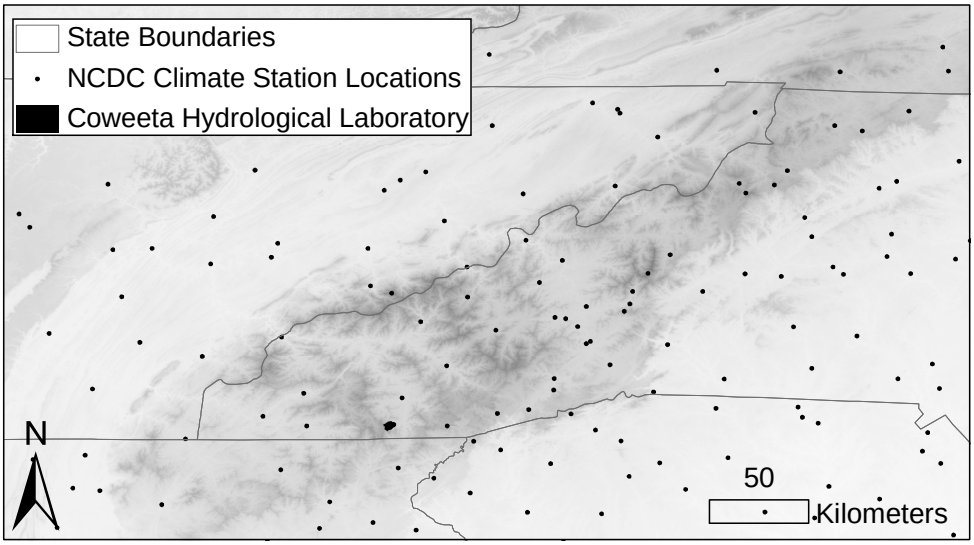

Figure 1: Southern Appalachian study area with locations of 134 NCDC climate stations and the Coweeta Hydrological Laboratory.

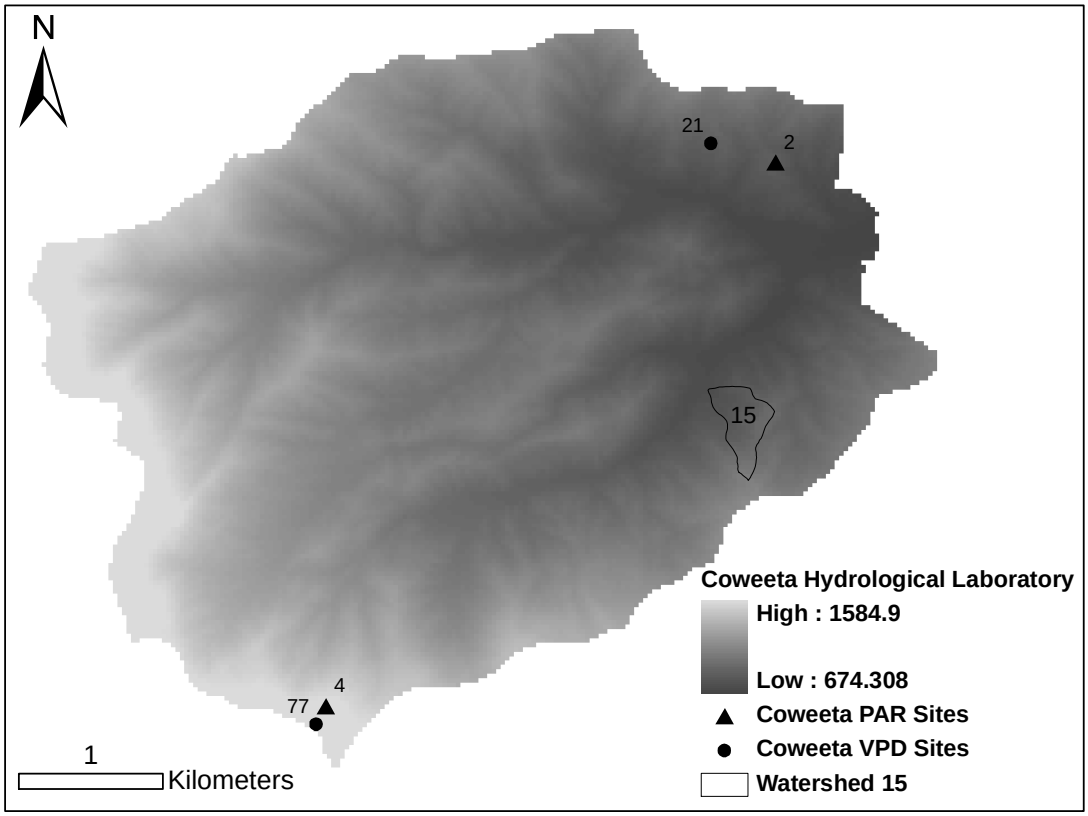

Figure 2: Coweeta Hydrological Laboratory digital elevation model with WS15, VPD climate station locations CS21 and CS77, and PAR locations S2 and S4.

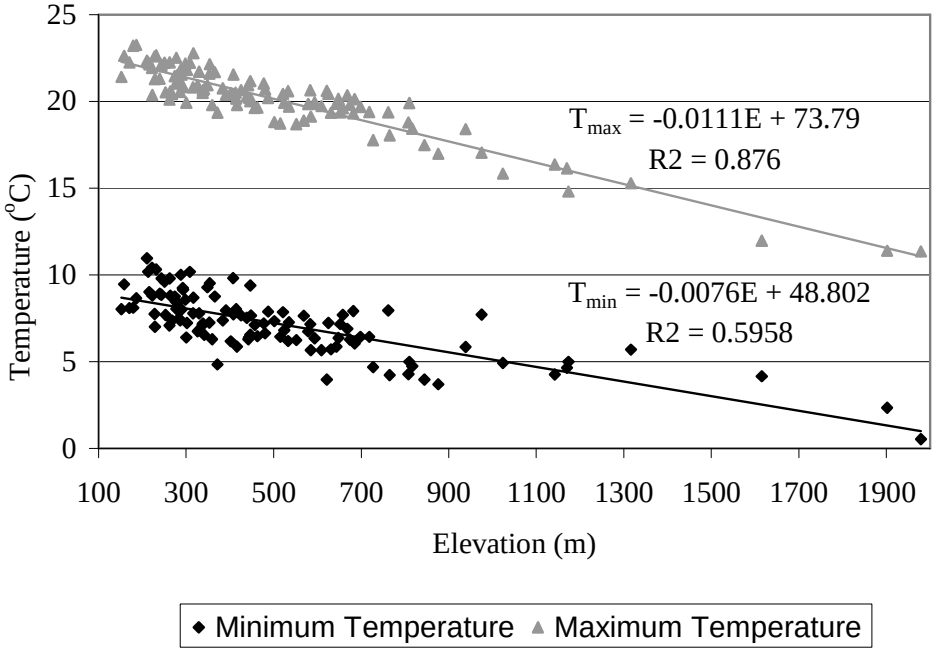

Figure 3: Relationship between elevation and measured mean annual minimum and maximum temperature (^{o}C) from 134 climate stations across the SA from 1985-2005.

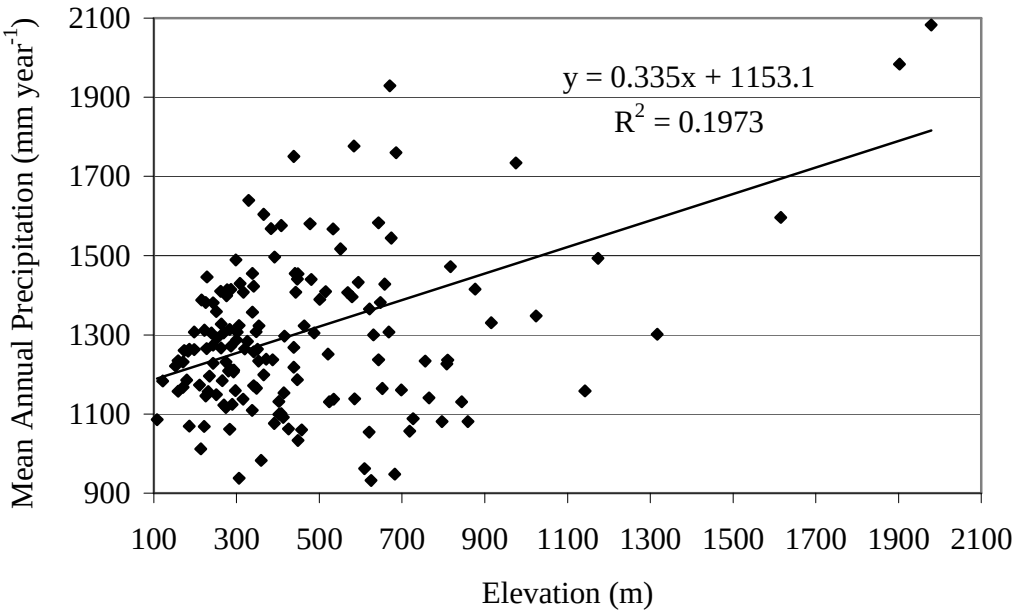

Figure 4: Relationship between elevation and mean annual precipitation from 134 climate stations across the SA from 1985-2005.

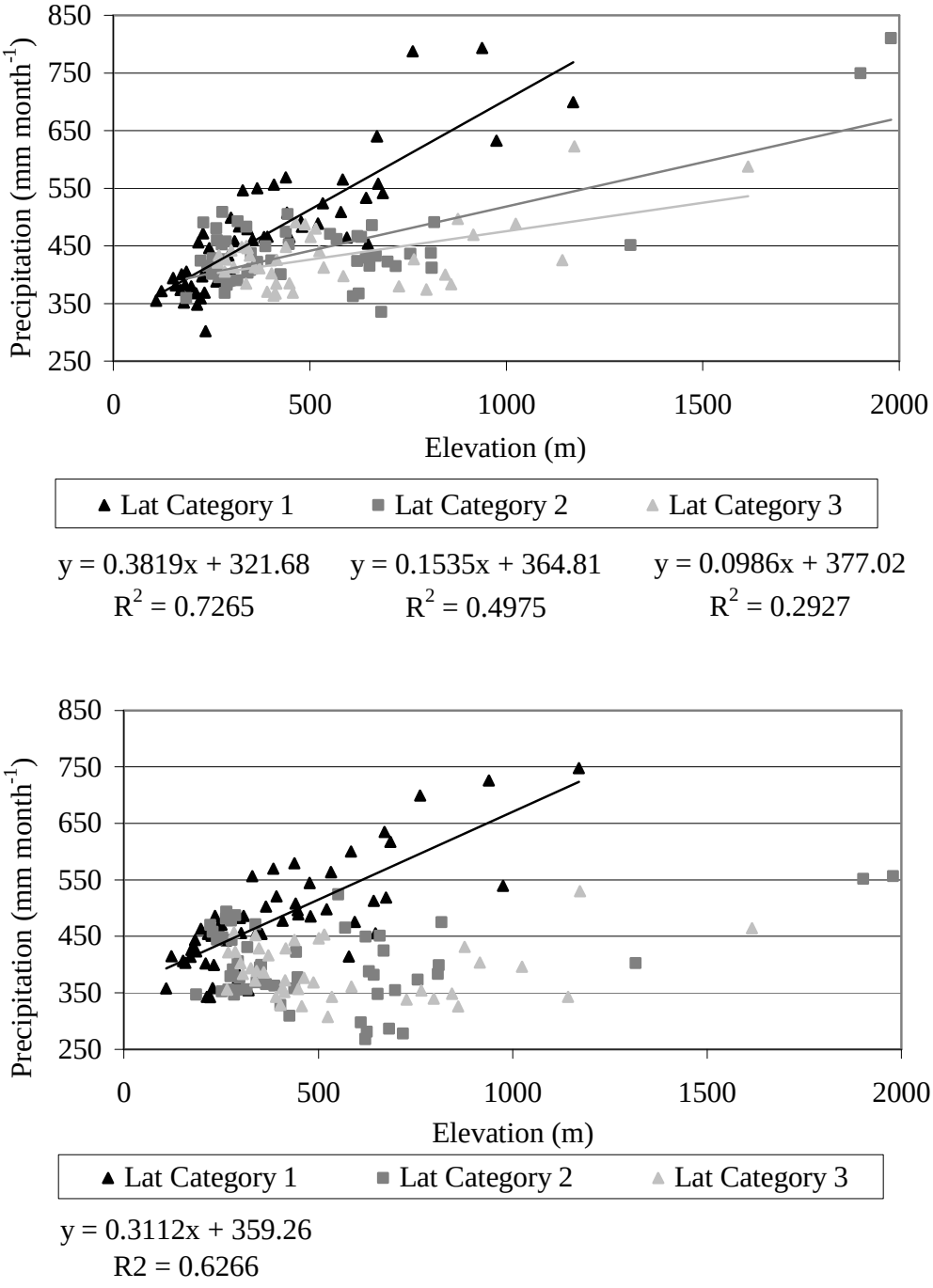

Figure 5: (a) (Top) Relationship between elevation and summer precipitation and (b) (Bottom) relationship between elevation and winter precipitation. Data was from 134 climate stations across the SA from 1985-2005. Significant relationships identified with line and listed equation.

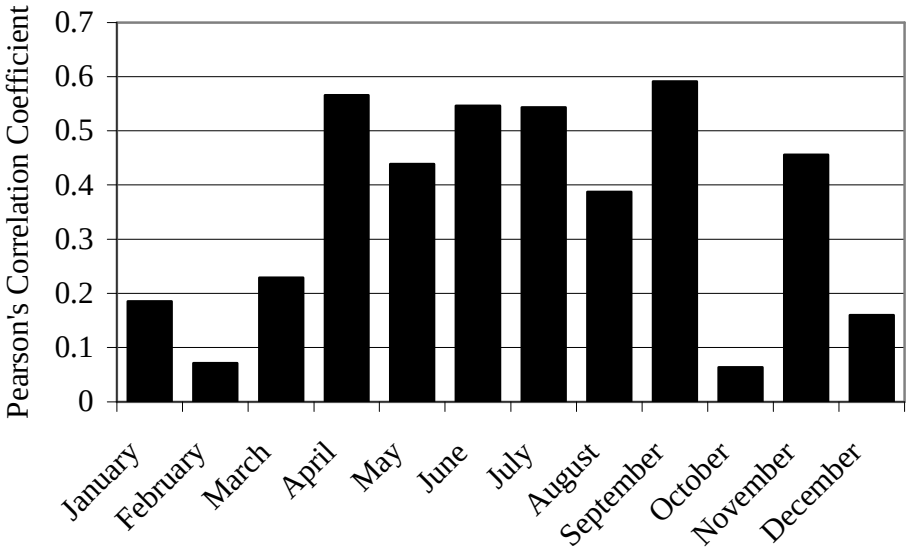

Figure 6: Monthly correlation for elevation and mean monthly precipitation from 134 climate stations across the SA from 1985-2005.

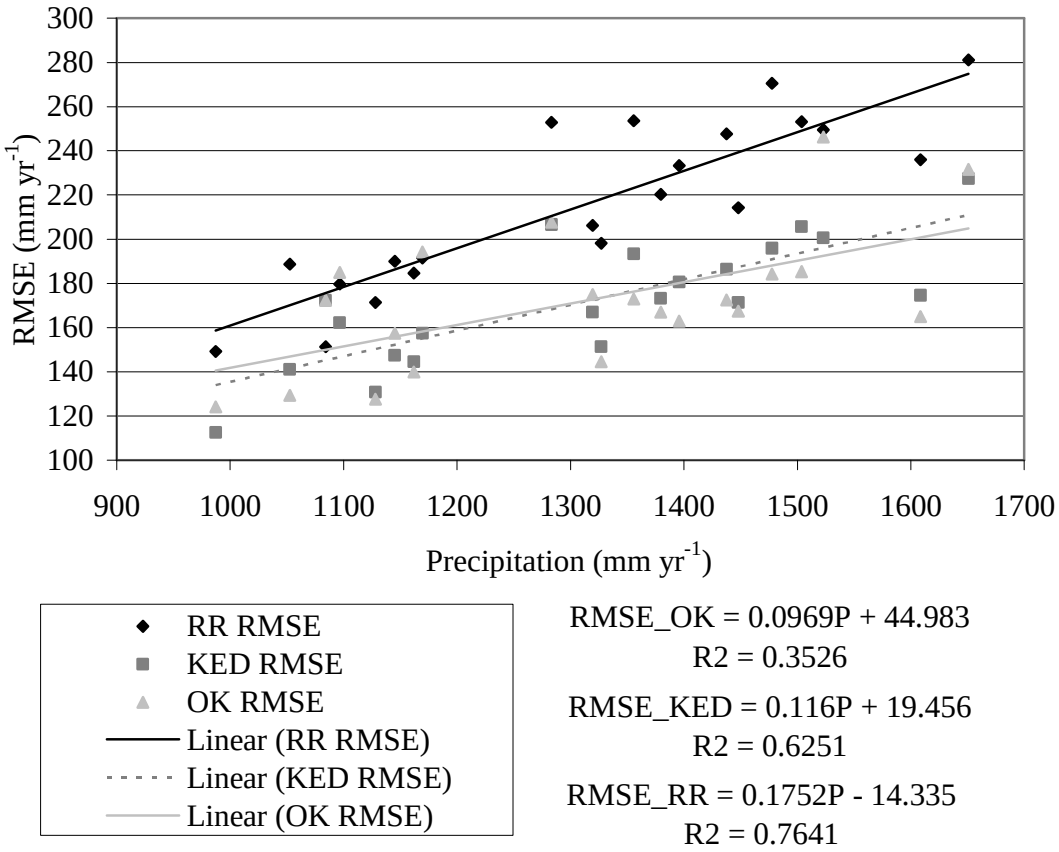

Figure 7: Comparison of precipitation prediction methods and the relationship between total annual precipitation and annual precipitation RMSE. Data was from 134 climate stations in the SA from 1985-2005. Showing linear regression equations and R-squared values.

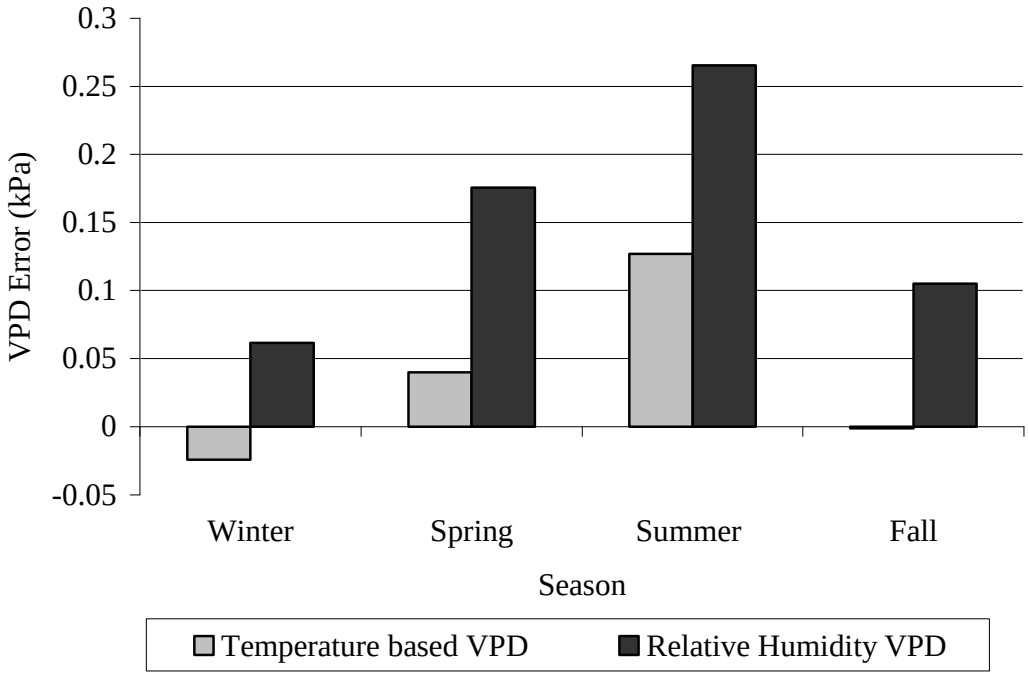

Figure 8: Mean seasonal error from daily VPD predictions using the temperature and relative humidity methods. Data used was the combined data set from two climate stations, CS21 and CS77, at the Coweeta Hydrological Laboratory and was collected from 1992-2008.

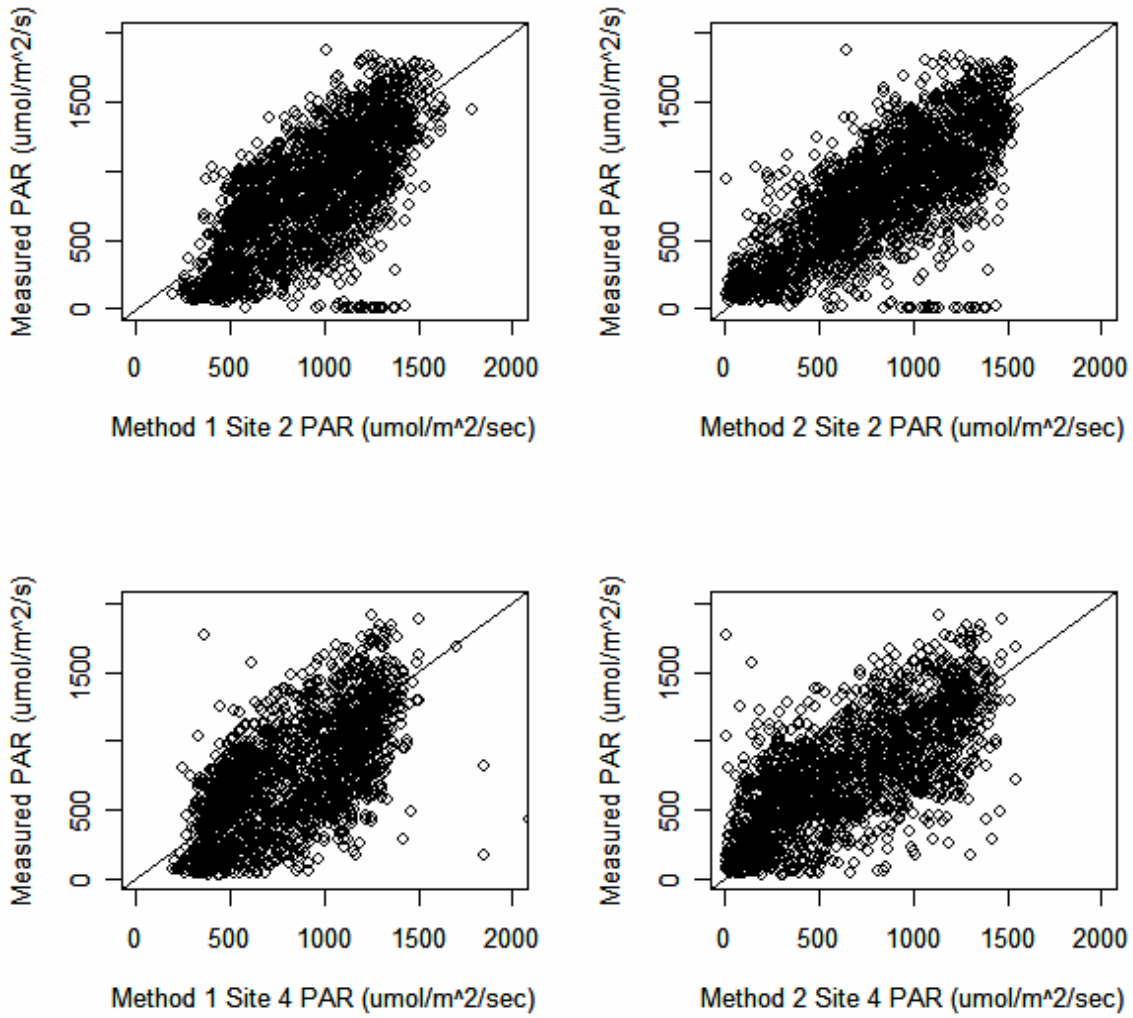

Figure 9: Predicted versus measured PAR for two methods, the Hargreaves-Samani method and the Bristow-Campbell method. Data used was collected on two sites, S2 and S4 in the Coweeta Hydrological Laboratory from 2003-2009. Method 1 represents Hargreaves-Samani estimated PAR, Method 2 represents Bristow-Campbell estimated PAR.

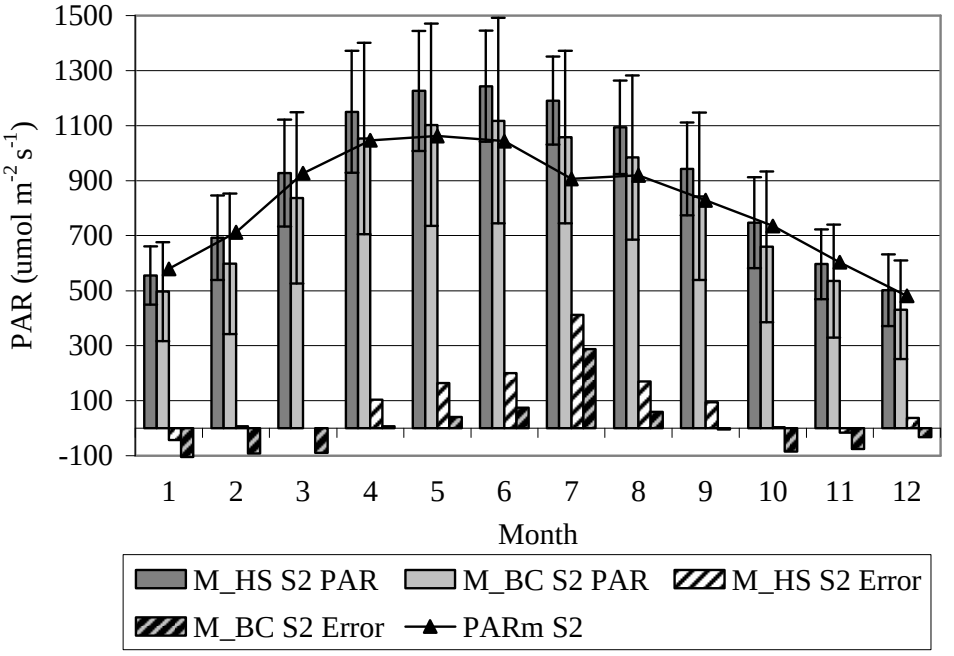

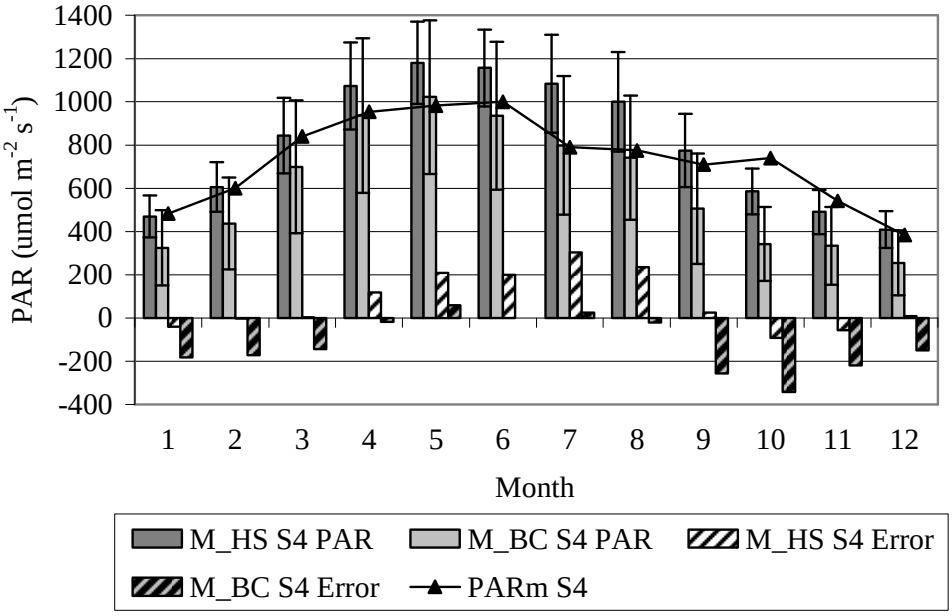

Figure 10: (a) (top) Mean monthly estimated PAR, error, and PARm for S2 and (b) (bottom) Mean monthly estimated PAR, error, and PARm for S4. Data was collected from 2003-2009. (M_HS = Hargreaves-Samani method estimated PAR, M_BC = Bristow-Campbell method estimated PAR, PARm = measured PAR) Error bars represent +/- 2 standard deviations.

Chapter 2: Scaling up species-specific sap flow models to the watershed and a comparison to local models.

Evapotranspiration (ET), the combination of plant transpiration and surface evaporation, can vary across space and time, and is a significant component of the hydrological cycle in densely forested regions. Quantifying ET is critical to understanding the available water resource, especially in the southern Appalachians (SA). In the SA, ET averages 50% of annual precipitation in forested watersheds and can climb to 85%. However, ET is among the most difficult and complex component of the water cycle to measure and model. Of the studies that estimate ET, few use scaled sap flow models and none have examined larger watersheds over long time scales with a variety of methods in the SA. This lack of robust comparisons shows a need for further research, and a broader comparison among catchment ET derived from sap flow and other ET estimation methods. Our general approach compared four ET estimation methods to the catchment water balance estimates of ET (ET_{CWB}) on 15 catchments in the SA. Estimates were based on catchment properties and interpolated climate variables and used regional historic data sets to estimate climate fields, measurements of forest structure, and estimates of leaf phenologies. Error propagation was performed on LAI, precipitation, and sap flow and focused on the model parameters for LAI and sap flow to determine relative impacts from estimation error. Our results show that all models performed reasonably well. ET_{SAP} underestimated ET_{CWB} by -11% and ET_{LU}, ET_{Precip}, and ET_{HAM} overestimated ET_{CWB} by 6.1%, 6.4%, and 18%, respectively. Although ET_{SAP} had a slightly larger mean error and RMSE compared to our other ET models, ET_{SAP} has advantages for some classes of application. Mainly, sap flow models offer increased

flexibility by allowing us to look at interacting species composition and changes in future forests with only a 4% absolute difference in mean error compared to our best model. Error propagation found that estimated ET was more sensitive to LAI, than sap flow or precipitation. Precipitation had the lowest sensitivity, most likely due to its relatively small coefficient of variation.

Introduction

The hydrological cycle encompasses precipitation, evaporation, plant transpiration, subsurface storage, subsurface flow and surface flow (Eisenbies et al., 2007). Evapotranspiration (ET), the combination of plant transpiration and surface evaporation, can vary across space and time, and is a significant component of the hydrological cycle in densely forested regions. Mountainous regions, such as the southern Appalachian Mountains (SA) have been described as “water towers” for the surrounding area, because precipitation exceeds ET (Feldman, 2001). However, water balance varies through time with changes in climate and plant water use. Quantifying ET is critical to understanding the available water resource in this region. In the SA, ET averages 50% of annual precipitation in forested watersheds and can climb to 85% (Lu et al., 2003). Due to high annual rainfall from this region, this results in over 1000 mm of water returning to the atmosphere annually (Zhang et al., 2001). Recent droughts across the southeast US attest to the potential impacts of changes in water availability, underscoring the need to better quantify the water cycle, and improve ET estimates (Moorhead, 2003).

ET is among the most difficult and complex component of the water cycle to measure and model (Morton, 1983). ET measurements are especially difficult in natural systems due to the presence of large trees and heterogeneous cover types. In addition, difficulties arise due to variations in environmental conditions across small spatial and temporal distances. Currently, the most accurate ET measurement method uses lysimeters, creating a closed system below-ground and measuring ET via weight loss (Vaughan, 2007). This method is difficult to replicate for a forest stand, so alternate methods have been developed (Stein et al., 1995; Riekerk, 1985). These include eddy covariance, tent enclosure, and sap flow techniques (De Rocher and Tausch, 1994; Kjelgaard, 1997; Stoy et al., 2006). Most of these, however, are also limited to small, homogenous systems.

ET is both spatially and temporally variable due to climate heterogeneity (Douglass, 1967; Murakami, 2007; Ford and Vose 2007; Kosa and Pongput, 2007). Spatial variation of climate is well documented, with temperature and precipitation changing with elevation and latitude. Climate also varies seasonally and annually. Future climates may change forested ecosystems and impact water cycles (Ellison et al., 2005). Climate change projections show increases in temperature and shifts in precipitation; both increases and decreases depending on location and season (Rowntree, 1988; Mitchell, 1989; Kattenberg et al., 1996; Houghton et al., 2001; IPCC, 2001). The resulting impacts on ET may be complex and not well defined for the SA (Arnell, 1992; Najjar, 1999; Stone et al., 2001; Guo et al., 2002). Globally, climate change has been shown to change transpiration at the tree level and thus ET and runoff at the catchment

level (Arnell, 1992; Gardenas and Jansson 1994; Kremer et al., 1996; Kellomaki and Vaisanen, 1997; Najjar, 1999; Stone et al., 2001; Guo et al., 2002; Sabate, 2002; Shenbin et al., 2006). Annual increases in temperature may increase ET totals given adequate water, although the magnitude and pattern of increases are unclear due to feedbacks and interactions among multiple factors. Increases in precipitation may have the potential to decrease ET with fewer days of low humidity, but may not severely impact ET for the SA given their current high levels of annual precipitation (Garbrecht et al., 2004). Decreases in precipitation would most likely lower ET due to less water availability. However, less precipitation may also decrease humidity, increasing ET rates. Uncertainty in climate change impacts on water yield call for further study.

ET is also difficult to quantify due to variations caused by landscape heterogeneity, in particular the variation of species across the landscape. Species composition and structure are vulnerable to both changes in climate and introduced species. Species ranges may shift both north and up elevation given increases in annual temperature (Iverson et al., 1999; Lesica and McCune, 2004; Parmesan and Yohe, 2003; Parmesan, 2006; Foden et al., 2007). This may lead to species extinction (Thomas et al., 2004, Thuiller et al., 2008). Changes in species composition may also be amplified by invasive insects and pathogens. In North Carolina alone, the National Forest Service estimates 1,673,000 acres at risk from at least 31 invasive insects, pathogens and disease (FHM report, 2006). That places over 7% of the state's forest cover at risk, with threats expected to increase (Simberloff, 2000; Stachowicz et al., 2002). Historically, introduced species have altered forest composition and structure, diminished biodiversity, decreased

biomass and have led to species extinction. Introduced pests in the eastern US include insects, such as the gypsy moth (*Lymantria dispar),* hemlock wooly adelgid (*Adelges tsugae*), balsam wooly adelgid (*A. piceae*), Asian longhorned beetle (*Anoplophora glabripennis*) and the emerald ash borer (*Agrilus planipennis*), and pathogens, including chestnut blight (*Cryphonectria parasitica*), Dutch elm disease (*Ophiostoma novo-ulmi*), butternut canker (*Sirococcus clavigignenti-juglandacearum*), dogwood anthracnose (*Discula* spp.), and sudden oak death (*Phytophthora ramorum*).

Forest impacts from these pests have been substantial. American chestnut (*Castanea dentata*), for example, was a dominant SA species comprising up to 35% of the forests in the SA but is now depleted due to the chestnut blight. Such impacts from introduced species in addition to changes in climate have the potential to alter forest composition and therefore watershed ET (Simberloff, 2000; Stachowicz et al., 2002).

Developing models to estimate the impacts from these changes on ET will help us to better understand the future implications of forest compositional changes on our water resource. This may be accomplished using sap flow models. Because of their unique species-specific development, ET may be estimated using the relationship between species composition, climate and water use. However, we must first determine the capability of sap flow models to estimate catchment ET.

Our broad goal is to compare ET estimation methods to estimate changes in water availability due to changes in climate and species. The inability to accurately measure

ET across forested ecosystems has led to the development of various estimation methods, including catchment water balance, energy balance, process-based, and hydrometeorological models (Rana and Katerji, 2000). Each estimation method can be useful but also has limitations. The catchment water-balance method deduces ET from the difference in watershed inputs, precipitation and inflow, and outputs, evaporation, transpiration, and outflow (Ponce and Shetty, 1995). Error can be difficult to quantify in catchment-based estimates of ET given that the accuracy is largely dependent on measurement and estimation error.

Energy balance methods, most often the Bowen ratio, use the ratio of latent and sensible heat to determine the flow of energy at the leaf surface. Sensible heat is heat energy transferred between a surface and the air when there is a temperature difference. Latent heat is the energy transferred when water changes state. Energy balanced methods require detailed measurements of both latent and sensible heat at small scales for the greatest accuracy (Spittlehouse and Black, 1980; Cellier and Olioso, 1993; Malek and Bingham, 1993). Using energy balance equations to estimate ET may be highly accurate over small areas (Perez et al., 1990; Nie et al., 1992; Prueger et al., 1997; Gowda et al., 2007), however, the high variability of climate across space leads to inaccurate estimates when up scaling (Malek and Bingham, 1993). In addition, Bowen ratio based energy balance algorithms do not close, leading to potential errors.

In an alternative approach, ET models are developed to mathematically represent the physiological process of ET. These models generally attempt to describe

transpiration by means of the stomatal conductance, canopy structure, and climate. Often, process-based models lead to accurate estimates of ET over a variety of landscapes. However, due to the complex nature of catchment ET, these models can become complex with long compute times (Beven, 1989; Battaglia and Sands, 1998; Sivapalan, 2005). Additionally, input variables are difficult to model across space. Examples include the Penman-Monteith and Hargreaves-Samani models (Hargreaves-Samani, 1982; Biftu and Gan, 2000; Samani, 2000; Oudin et. al., 2005; Yoder et al., 2005). Both use relationships between climate variables and ET to develop equations for different types of vegetation. These models are accurate in homogenous conditions, however, parameters required for these equations are often difficult to obtain (Lu et al., 2005).

Hydrometeorlogical models are an alternate approach that requires relatively few measured variables and parameters. Some models, particularly climate driven models, estimate ET as a single quantity. Models predict potential evapotranspiration (PET), the maximum amount of ET given unlimited water availability, and then define the relationship between actual ET and PET (Kay and Davies, 2008). There are numerous PET models that differ based on input variables, from temperature-based to those including radiation, wind, and soil characteristics (Priestley and Taylor, 1972).

Schreiber (1904), Budyko (1958), and Pike (1964) were three of the first to develop predominantly empirical models relating PET and actual catchment ET (Donohue et al., 2007). Each found a non-linear relationship predicting ET using

precipitation, PET, and often an energy variant. More recently, modifications including soil moisture (Calder and Newson, 1979; Milly, 1994) and vegetation parameters (Turner, 1991; Zhang et al., 2001, Lu et al., 2003, Zhou et al., 2008) have improved models. In a recent study, Lu et al. (2005) compared 6 PET models for the SA and determined that the top two models were Hamon (1963) and Turc (1961). Coefficients specific to the SA for Hamon (1963) were developed by Federer and Lash (1978), making Hamon (1963) a particularly good option for this region. A recent model developed for the southeastern U.S. from Zhang et al. (2001, 2004), converts PET to ET using precipitation and a vegetation coefficient.

Regression models have also been developed to estimate catchment ET using watershed characteristics as the explanatory variables. Recently, Lu et al. (2003) developed a multivariate linear regression equation for the SA based on annual rainfall, mean catchment elevation, latitude and percent forest cover. Results from Lu et al. (2003) show strong predictive ability for this region with model R^2= 0.79.

Most current ET models have not incorporated forest composition and structure, attributes that directly impact ET. Given potential changes of forest stands from climate and introduced species, described earlier, including these attributes in ET models is imperative for estimating future conditions. Consequently, ignoring these stand characteristics will lead to error when estimating ET, because additionally, models that include such attributes can be used to study the impacts from changes in climate and species composition on ET. Component-based models are one approach to address these

issues. Instead of estimating ET as a single quantity, as described above, these models estimate the three primary components of ET: transpiration, interception, and soil evaporation.

In one approach, sap flow models estimate transpiration and are combined with models of interception and soil evaporation. Specifically for the SA, soil evaporation is considered to be small due to a closed canopy and high humidity levels (Ford, 2005). Interception, however, can be high in this region. One model developed from Helvey (1964) shows rates as high as 50% of annual precipitation. These rates are dependent on a number of factors, primarily leaf surface area and frequency and intensity of precipitation, with higher leaf surface area in conifer stands compared to deciduous stands and in dense stands compared to sparse stands. Helvey's interception model uses both total annual precipitation and number of storms above 1.5 mm to compute annual interception. Storm number was used because interception is relatively small for both very large and very small storms (Helvey, 1964). More popular models including Gash (1979) and Rutter et al. (1971) were developed for areas of lower precipitation and less varied species composition, and thus may not be appropriate for the SA.

Sap flow models are based on xylem thermal measurements (Granier, 1985). These methods use heat pulse/heat dissipation techniques with either compensation or non-compensation (Closs, 1958; Cohen et al., 1981; Green and Clothier, 1988). Two sensors are inserted into the sapwood, one above another, approximately 10 cm apart. The upper sensor is heated and the difference in temperature between the upper and lower

sensors is used to calculate the sap flow velocity. The sap flow velocity along with stand height is used with empirically derived equations to calculate the sap flow density, which is used to calculate whole plant water use.

Sap flow measurements allow us to estimate differences in transpiration among species, and how this transpiration responds to climatic conditions. Studies have shown that transpiration varies among tree taxa on a leaf and tree basis, e.g., consistent differences in rates have been measured between conifers and hardwoods (Ewers et al., 2002). Transpiration rates have also been measured across a variety of species, including red and silver birch (*Betula lenta and B. pendula*) (Kelliher et al., 1992), willow (*Salix spp.*) (Lindroth et al., 1995), oak (*Quercus spp.*) (Granier et al., 1996), beech (*Fagus spp.*) (Granier et al., 2000), cottonwood (*Populus spp.*) (Schaeffer et al., 2000) red maple (*Acer rubrum*), loblolly pine (*Pinus taeda*), chestnut oak (*Q. prinus*), white oak (*Q. alba*), red oak (*Q. rubra*), yellow-poplar (*Liriodendron tulipifera*) (Wilson et al., 2001), black gum (*Nyssa sylvatica*) (Wullschleger et al., 2001), Japanese cedar (*Cupressus japonica*) (Kumagai et al., 2005), apricot (*Prunus armeniaca*) (Nicolas et al., 2005) and white pine (*Pinus strobus*) (Ford et al., 2007). This variation between species results from differences in physiological factors, including stomatal conductance and responsiveness to climate, and in structural characteristics such as rooting depth, leaf area, canopy architecture, and the amount and permeability of sapwood (Ewers et al., 2002; Vose et al., 2003; Kumagai et al., 2005; Ford et al., 2007). Differences in transpiration rates among woody species may impact total catchment transpiration and alter streamflow. Previous studies have shown that changes in species composition can impact stand ET

and total catchment yield (Bosch and Hewlett, 1982; Ford and Vose, 2007, Wattenbach et al., 2007).

Although tree-level models developed from sap flow are useful for studying plant and species responses, estimating the impact of species composition at the catchment level requires scaling from trees to stands (Oishi et al., 2008). Such upscaling has been attempted, generally on managed plantations (Breda et al., 1993, Nicolas et al., 2005), with few species (Cermak et al., 1995; Ford et al., 2007), on small areas, over short time periods, and in the catchments used to develop the sap flow equations (Wilson et al., 2001; Wullschleger et al., 2001; Ford et al., 2007). Ford et al. (2007) scaled sap flow equations on a 13.5 ha eastern white pine stand for annual estimates over one and a half years. Wilson et al. (2001) scaled annual estimates on a hardwood stand of 6 species to a 97.5 ha watershed over two years. Wullschleger et al. (2001) used hourly estimates for 8 species across a 1.92 ha watershed. Wilson et al. (2001) compared annual estimates of ET, composed of scaled up transpiration and an estimate of interception, to catchment water balance estimates of ET, ET_{CWB}, and found annual errors of -16% and -28% from two years of data. Ford et al. (2007) performed the same procedure on a white pine stand for two years with errors of -7% and -14% of ET_{CWB}.

Scaling sap flow to the watershed requires a variety of interpolated and estimated inputs creating additional and unknown variability. To further understand the impact of such variation on ET_{CWB}, ET_{SAP} and any associated error, sensitivity analysis should be

performed on the more variable inputs including precipitation, LAI, and sap flow equations.

There is no consensus on the best methods of scaling sap flow from trees to catchment, particularly at broader areas over a range of conditions. Few people have scaled sap flow models to larger watersheds over longer time scales, and each has used different methods. This lack of robust comparisons shows a need for further research, and a broader comparison among catchment ET derived from sap flow and other ET estimation methods.

This paper addresses four questions. First, how well does scaled, sap flow ET (ET_{SAP}) estimate ET_{CWB} across a variety of catchment sizes, species distributions, and mean elevations in the SA? Second, how do ET_{CWB} and ET_{SAP} differ spatially and temporally and how do they relate to climate variables? Third, using a sensitivity analysis, how do variation in ET_{CWB} inputs, including interpolated precipitation, estimated LAI and sap flow equation parameters, contribute to ET_{CWB} and associated errors? And finally, to what extent does ET_{SAP} compare to three established ET estimation methods for the region? These methods include a regionally developed multivariate linear regression model for the SA (Lu et al. 2003), a regionally recommended PET model (Hamon 1963) used along with a recently proposed actual ET and PET relationship (Zhang et al. 2001), and a regression model using precipitation as the sole predictor.

Methods
Study Area

Our study area, herein called the southern Appalachian region (SAR), encompassed western North Carolina, northern Georgia, and eastern Tennessee (Figure 1). Climate across the SAR is temperate, moist, and humid. Average annual temperatures range from 10 ^{o}C in the north to 18 ^{o}C in the south, with average annual precipitation ranging from 850 mm to over 2500 mm. The region is composed of Paleozoic and Precambrian bedrock deposited approximately 800 million years ago (Sankovski and Pridnia, 1995). Overstory composition and forest communities vary strongly with terrain and elevation across the SA (Whittaker, 1956; Bolstad et al., 1998a), and communities include mixed-deciduous (*Q. alba*, *Q. rubra*, *R. psuedoaccacia*, and *Carya* spp.), northern hardwoods (*A. saccharum*, *Tilia spp*., *B. aleghaniensis*, *A. octandra*), xeric oak-pine (*Q. coccinea*, *Q. prinus*, *O. arboretum*, and *P. rigida*), and cove (*L. tulipifera*, *B. lenta*, *Magnolia* spp.). Understory most commonly includes *Rhododendron* spp. and *Kalmia* spp (Bolstad et al., 2001). Soils in this region vary considerably even at small scales and are most often represented by the orders ultisol and inceptisol where ultisols are found in basins, ridges, and areas of gentle topography, and inceptisols are found on steeper slopes (Swank and Crossley, 1988).

Approach

Our general approach compared five methods for estimating annual ET on 15 catchments in the SAR. Estimates were based on catchment properties and interpolated climate variables. This approach included a regional historic data set to estimate climate

fields, measurements of forest structure, and estimates of leaf phenologies to drive models of ET.

Data Collection

Data including streamflow, climate, and watershed properties were compiled for 15 watersheds located in the SAR (Figure 1). Study watersheds (WS1-WS14) were selected upstream from a USGS streamflow gauge site with at least 15 years of data, with the exceptions of watersheds WS11 (5 years) and WS13 (6 years), included for more complete distributions of watershed sizes and locations. Watersheds were selected for their location (within the SA), size (less than 140 km^2), and percent forest cover (at least 90%). Fourteen watersheds were above USGS gauging stations, and one in the USDA Forest Service's Coweeta Hydrological Laboratory (CHL) situated near the southern edge of our study region (Figure 2). CHL is a 2185 ha watershed composed of a variety of gauged watersheds, with over 80 years of continuous hydrological and climatologically data. Coweeta watershed 18 (WS15) was selected in part because the tested sap flow model was developed there.

Watersheds ranged in size from 0.13 sq km to 134.4 sq km and in elevation from 329 m to 2038 m (Table 1). Precipitation and discharge increased with elevation, with up to 2100 mm $year^{-1}$ of precipitation and 1350 mm $year^{-1}$ of discharge at higher elevations, and an average 1300 mm $year^{-1}$ precipitation and 600 mm $year^{-1}$ discharge at lower elevations (USGS, 2006; NCDC, 2006).

Watershed characteristics for our 14 USGS watersheds, including size, gauge elevation, and gauge locations were downloaded from a USGS website (USGS, 2006). WS15 watershed data were provided by CHL. Daily averaged instantaneous runoff was downloaded from the USGS and CHL, summed annually and divided by watershed size to find total annual runoff per unit area (R_t). All watersheds were delineated using ArcGIS 9.0 and data from the USGS. A depressionless elevation layer was created from USGS 30 m digital elevation models and flow direction and flow accumulation were computed in turn. Finally, pour points and flow accumulation layers determined watershed boundaries. Final watershed areas were compared to the USGS reported watershed areas.

Relevant climate variables for the SAR were downloaded from the National Climatic Data Center (NCDC) and interpolated across each watershed. Daily precipitation, minimum temperature and maximum temperature were obtained from the NCDC for 134 climate stations across the SAR from 1985-2005 (NCDC, 2006; Figure 1). The NCDC used a variety of instruments to measure temperature, including glass thermometers, thermistors and thermocouples. Daily maximum temperature and minimum temperature were recorded in degrees Fahrenheit and converted to degrees Celsius. Precipitation was recorded at 15-min intervals and summed over 24 hour periods by the NCDC. Precipitation measurements were most commonly made using either tipping bucket or standard weighing gauges and were presented by NCDC in hundredths of inches and converted to millimeters (NCDC, 2009). Gauge sites ranged in

elevation from 100 m to 1980 m and range in annual precipitation from 854 mm $year^{-1}$ to 2418 mm $year^{-1}$.

Our general approach consisted of estimating spatial fields of climate variables across each study watershed, and applying those estimates to the ET models to estimate water flux. First, spatial estimation was required to determine precipitation and temperature across each watershed. Several techniques were examined and compared for our region to determine the best method for interpolation. Numerous studies have shown the advantages to using kriging with external drift to interpolate both precipitation and maximum and minimum temperature (Phillips et al., 1992; Skirvin et al., 2003; Carrera-Hernandez and Gaskin, 2007; Haberlandt, 2007). Other studies have found regional regression (Bolstad et al., 1998b) and ordinary kriging (Goovaerts, 2000) provide better estimates. To identify the best method for our study region, regional regression, kriging, and kriging with external drift estimates were compared to point based daily estimates across the study area for precipitation, minimum temperature, and maximum temperature. Leave-one-out cross validation was implemented using all available climate stations for each day (Kove and Bolstad, in prep). Kriging with external drift was used because it provided the best daily interpolations of precipitation, minimum temperature, and maximum temperature.

Annual precipitation (P) for each catchment was calculated using the estimated daily total precipitation, interpolated for each cell, summed annually and divided by

catchment size. Daily maximum and minimum temperature were used in calculating VPD and PAR for use in our ET models.

Photosynthetically active radiation (PAR) is not measured consistently across the SA, and was estimated. Most commonly, PAR is estimated from temperature, latitude, and day of year (DOY). To estimate PAR, daily extraterrestrial solar radiation, R_e (MJ m^{-2} s^{-1}), was calculated from Bristow and Campbell (1984) using latitude and DOY. Global solar radiation, R_g (MJ m^{-2} s^{-1}) was found by calculating the transmittance, T_t, using the difference between maximum and minimum temperature, ΔT , and multiplying by R_e, where:

$$T_t = 0.7 \cdot \left(1 - \exp\left(-0.004 \cdot \Delta T^{2.4}\right)\right)$$

The Bristow and Campbell (1984) transmittance model was used because it was found to be superior over Hargreaves-Samani (Annandale et al., 2002) when compared to daily measured PAR data on CHL, particularly during the summer months (Kove and Bolstad, in prep). PAR was converted from R_g assuming 4.608 µmol quanta J^{-1} (Campbell and Norman, 1998) and that 50% of global solar radiation fell in the range of 400-700 nm (Landsberg and Waring, 1997; Ford et al., 2007).

Additional meteorological variables and fluxes were estimated using the best available models. Vapor pressure deficit (VPD) was also not measured sufficiently across our study area and was estimated from temperature using the temperature based method of Yoder et al. (2005). Soil evaporation was assumed to be zero due to the closed

canopy and thick forest floor (Essery, 1992; Ford et al., 2007). Forest interception, $\sum I$, however is very high in the SA relative to precipitation (Helvey, 1967) and was estimated using the equation derived for mature hardwoods in the CHL Basin from Helvey and Patric (1965) based on total annual precipitation, $\sum P$ and number of storms over 1.5 mm, *n*:

$$\sum I = 0.083\left(\sum P\right) + 0.036(n).$$

Sap flow models require that we estimate LAI and composition cell by cell across each watershed, though there are no good estimates of LAI or agreements on the best methods to use. Optical methods used to estimate LAI and species composition saturate in high LAI areas, making them not good for the SAR. Allometric methods, generally considered one of the most accurate methods, require site specific measurements that were not available in the SAR. Instead, we applied a regression approach estimating LAI from elevation. Leaf area in deciduous taxa has been reported to be strongly correlated with elevation and to a lesser extent with terrain shape in the SA (Bolstad et al., 2001). A linear relationship developed from Bolstad et al., (2001) was developed to estimate LAI for each grid cell across the catchments using elevation, where as elevation increased LAI generally decreased.

Forest community composition varies spatially and can affect sap flow estimates of ET. Estimating forest composition is difficult at the resolution required, particularly in areas we never visit. Remote sensing methods are applicable for the region, but can not

estimate composition down to species and densities. Instead, remote sensing would designate stands as deciduous or coniferous, not detailed enough for our sap flow models. Instead, we collected community composition from county level forest inventory and analysis data (FIA) downloaded from the USDA forest service website (USDA, 2007), and applied a single composition to each watershed. If a watershed covered more than one county, area-based weighted averages were used.

Annual ET was calculated five different ways. First, annual ET was calculated as described above using $ET_{CWB} = P - R_o$. ET_{CWB} was used as our estimate for the "true" ET in all subsequent comparisons. Ground water storage and losses due to deep flow were assumed insignificant over annual time scales due to steep slopes and impenetrable bedrock (Ford et al., 2007). We also assume that the net ground water storage change over our annual time step was negligible (Essery, 1992). Interannual storage may result in errors in individual years, but because we are averaging over 20 years of data, we expect errors to balance over the entire study period (Winter, 1981).

Second, annual ET was calculated from scaled sap flow equations (ET_{SAP}) developed by Ford et al. (in prep). ET_{SAP} was found by multiplying El_{sp} by our species-specific LAI totals, described earlier. Daily values were summed across the watershed and across the year to compute annual catchment ET_{SAP}. Ford measured sap flow on eight species (*A. rubrum, B. lenta, Tsuga Canadensis, P. strobus, Q. prinus, Q. rubra, L. tulipifera and Carya spp*.) within CHL. Transpiration was estimated at 15 second intervals and averaged every 30 minutes (Granier, 1985). Daily totals were then used to

find species-specific transpiration equations based on VPD, PAR and day of year (DOY). Detailed methods are described in Ford et al. (2007) with EL_{sp} equations defined as follows:

$$EL_{chestnut\_oak} = \left(1 - e^{(-0.3055 \times VPD)}\right) - 0.00015 \times PAR + e^{(-0.00954 \times DOY)}$$

$$EL_{red\_oak} = \left(1 - e^{(-0.07728 \times VPD)}\right) + 0.000009264 \times PAR + e^{(-0.015151 \times DOY)}$$

$$EL_{hickory} = \left(1 - e^{(-0.49504 \times VPD)}\right) - 0.00031 \times PAR + e^{(-0.006435 \times DOY)}$$

$$EL_{tulip\_tree} = \left(1 - e^{(-0.2538 \times VPD)}\right) + 0.000136 \times PAR + e^{(-0.007702 \times DOY)}$$

$$EL_{white\_pine} = 0.21677 \times \left(1 - e^{(-0.79411 \times VPD)}\right) + 0.000179 \times PAR$$

$$EL_{birch} = 0.5943 \times \left(1 - e^{(-3.4558 \times VPD)}\right)$$

$$EL_{hemlock} = 0.1698 \times \left(1 - e^{(-2.9216 \times VPD)}\right)$$

$$EL_{red\_maple} = 0.3978 \times \left(1 - e^{(-2.0029 \times VPD)}\right)$$

The third method uses Lu et al's (2003) empirical relationship developed for the southeast U.S. to calculate mean annual watershed ET (ET_{LU}). Lu et al.'s (2003) model is defined by

$$ET_{LU} = 1098.786 + 0.309P - 0.289E - 21.840L + 1.96F$$

where P is annual precipitation (mm), L is the watershed latitude at the outlet (decimal degrees), E is the mean watershed elevation (m), and F is the percentage of watershed covered by forests multiplied by 100. ET_{LU} is calculated for each watershed every year.

The fourth method to estimate catchment ET is based on the Hamon (1963) method:

$$PET_{HAM} = 0.1651 \cdot D \cdot \rho_{sat} \cdot C$$

where PET_{HAM} = potential forest ET (mm day^{-1}), D = daylight hours (hr), C = locally derived correction coefficient of 1.2 (Federer and Lash, 1978), and ρ_{sat} = saturation vapor density (g m^{-3}) at the mean daily temperature (^{o}C) defined as:

$$\rho_{sat} = 216.7 \cdot \frac{e_s}{T_a + 273.3}$$

Where T_a = average temperature (^{o}C), e_s = saturation vapor pressure (mb) and where:

$$e_s = \frac{e^o(T_{\max}) + e^o(T_{\min})}{2}$$

$$e^o(T) = 6.108 \cdot \exp\left[\frac{17.26939 \cdot T_a}{T_a + 237.3}\right]$$

PET_{HAM} is calculated for each watershed cell, summed annually and averaged for each watershed each year. Then annual PET_{HAM} is converted to annual ET_{HAM} following Zhang et al. (2001):

$$ET_{HAM} = P\frac{\left(1 + w\left(PET_{HAM} / P\right)\right)}{\left(1 + w\left(PET_{HAM} / P\right) + P / PET_{HAM}\right)}$$

Where P =annual precipitation (mm $year^{-1}$) and w = vegetation coefficient for forests = 1.

The final method used to estimate ET, ET_{Precip}, was a simple regression model. Due to the generally strong relationship between precipitation and ET, we included this

model for comparison. Annual catchment precipitation was used as the sole predictor in a linear regression model estimating annual catchment ET_{CWB}. An estimate of annual ET_{CWB} for each catchment was then computed using each catchments annual precipitation and the linear regression model.

Each estimate of ET was compared to ET_{CWB}. Mean error and root mean squared error (RMSE) were calculated annually to compare accuracy in estimating annual ET compared with ET_{CWB}. Error was calculated by subtracting estimated ET by ET_{CWB}. Percent error was calculated by dividing error by ET_{CWB} and subtracting from 1. Pearson's correlation coefficient (ρ) was estimated and residual plots examined, including residuals versus time and residuals versus predicted values.

Monte Carlo simulations were used to propagate randomly generated errors for each model, using 1000 simulations for 1986-2005 for precipitation and LAI on all watersheds. Only one watershed selected at random, and 100 simulations were analyzed for sap flow due to computational load. Precipitation was interpolated across the entire study area, so all watersheds were included in each simulation. However, LAI was estimated on each watershed separately, resulting in 1000 simulations per watershed. Sensitivity analysis of LAI and sap flow focused on the model parameters, however sensitivity analysis for precipitation focused on propagating daily error calculated from the interpolated daily precipitation and the measured daily precipitation at the climate stations.

ET sensitivities to LAI estimates and sap flow equation parameters were examined by generating values from normal distributions. Mean and standard deviations for theses were from the best available sources, either from statistical fits reported in the sap flow models or LAI models, or from estimates in literature reported values.

LAI sensitivity analysis was performed on one parameter, the intercept, from the linear equation based on elevation: $LAI = 10.3 - 0.00447 \cdot Elevation$ (Bolstad et al., 2001). The intercept, 10.3, was varied based on a normal distribution spanning the 95% confidence interval ranging from 7.75 to 12.85. New LAI values were calculated from the propagated interception parameters for the elevation of each cell on each watershed. We also looked at the impacts of LAI variation on ET estimation. The newly generated LAI values from the Monte Carlo simulation were used to calculate ET estimates by multiplying the daily transpirations estimates by the new LAI value and summing across the watershed and year. The new ET estimates are then compared to our original ET_{SAP} values.

Sensitivity analysis of sap flow models examined each species individually. Annual sap flow was calculated for four species on WS 5 for 1986, assuming each species model was 100% of the LAI of the watershed. WS 5 was used because it was an average elevation watershed. Only four species models were analyzed (tulip poplar (*L. tulipifera*), red oak (*Q. rubra*), chestnut oak (*Q. prinus*), and hickory (*Carya spp*.)) because there was not data available for the remaining equations, including the parameter statistics. Each model contained three parameters used in the analysis following the form

$\text{Transpiration}=\left(1-e^{(-b1\times VPD)}\right)+b2\times PAR+e^{(-b3\times DOY)}$. Parameters b1, b2 and b3 were varied assuming a uniform distribution spanning the 95% confidence intervals (Table 3). The randomly generated parameters from the Monte Carlo simulation were used to calculate new daily estimates of sap flow and summed annually. Annual sap flow estimates of ET were compared to the original ET_{SAP} estimates.

Sensitivity analysis was also performed for daily precipitation. Daily precipitation models were created and cross-validation analysis was performed by Kove et al. (in prep). Daily variation from the cross validation analysis was used in the sensitivity analysis. This is beneficial since we are using the specific daily errors estimated from the network of precipitation observations each day. Total daily error was summarized into a probability distribution from which randomly generated errors were selected. We summed the original daily estimate of precipitation along with the randomly generated deviation to calculate a new estimate of daily precipitation, and summed this annually. New annual precipitation totals were compared to the original estimates of precipitation and were also used to calculate new ET_{CWB}. The difference between the original ET_{CWB} and the new ET_{CWB} was examined.

Results

Catchment Water Balance ET

Annual ET_{CWB} averaged 745 mm yr^{-1} with a standard deviation of 178 mm yr^{-1}. Annually averaged ET_{CWB} increased slightly from 1986 to 2005 (F-test; <0.05) where

ET_{CWB} was a minimum of 592 mm year^{-1} in 1986 and a maximum of 873 mm year^{-1} in 1993. This increase was largely due to the lowest value, occurring near the start of the study period, so this may be a result of the period sampled. However, removing the minimum year (1986) also removed the significant increase. The standard deviation of ET_{CWB} calculated for each watershed averaged 121 mm year^{-1}. ET_{CWB} variation between watersheds was similar to ET_{CWB} variation within watersheds.

The proportion yield averaged 56% for our study watersheds but ranged from 43%-68% for watershed averages, with extreme annual minima and maxima of 20% and 91% respectively. Variation in proportion yield was more due to discharge variation than changes in precipitation. Proportion yield varied with a mean standard deviation of 9% and a range of 4% to 14%.

Interception estimates varied predominantly by mean annual precipitation, with an average interception of 325 mm year^{-1}, a minimum of 166 mm year^{-1}, and a maximum of 743 mm year^{-1}. Variability was also related to mean annual precipitation, as precipitation increased, the standard deviation of interception decreased (F-test, $P<0.001$). Interception was not related to watershed characteristics, including mean elevation or mean annual temperature.

General Overview

Model performance was comparable across methods, with no model substantially better than the others by all criteria, although there were statistically significant

differences for some summary measures (Figure 4). According to mean error, ET_{Precip} performed the best and ET_{SAP} performed the worst, with a mean error range of nearly 200 mm $year^{-1}$ between the different ET estimation methods. RMSE showed a much smaller range with only a 35 mm $year^{-1}$ difference (Table 2; Figure 7).

Performance by watershed varied. For some watersheds, all methods performed poorly, notably on watershed 13, where errors averaged nearly twice as large as in other watersheds for most methods. Watershed 13 is not significantly different in any known way including elevation, percent forest, latitude, or species composition. Temporal variation was similar across all models (Figure 3). For all models, variation year to year was less than the variation from one watershed to the next.

ET_{SAP}

ET_{SAP} estimates averaged 630 mm $year^{-1}$ with a standard deviation of 122 mm $year^{-1}$. On average, across all years and watersheds, ET_{SAP} underestimated ET_{CWB} by 11%, with a mean error of -113 mm $year^{-1}$ and a standard deviation of 126 mm $year^{-1}$. Performance varied significantly within years and watersheds, from a 48% underestimate to a 192% overestimate. When averaged by watershed, ET_{SAP} was positively correlated to mean annual precipitation and mean annual runoff (ρ= 0.94 and 0.91 respectively, F-test; $P<0.001$). In addition, average watershed ET_{SAP} underestimated ET_{CWB} for higher elevation sites and overestimated ET_{CWB} for lower elevation sites, with a correlation of 0.54 (F-test, $P<0.05$; Figure 5). ET_{SAP} was also positively correlated with mean LAI and percent *L. tulipifera* (F-test, $P<0.05$), though LAI and percent *L. tulipifera* were also

strongly correlated with elevation. When averaged annually, there was a significant relationship between ET_{SAP} and mean annual temperature, with a correlation coefficient of 0.65 (F-test; $P<0.05$). Annually averaged mean error increased significantly with proportion yield (runoff/precipitation), with correlations of 0.65 and 0.70 respectively (F-test, $P<0.001$).

ET_{HAM}

ET_{HAM} predominantly overestimated ET_{CWB}, with an average of 18%, and ranged from -25% to 361%. Mean error was 85 mm $year^{-1}$ with a standard deviation of 168 mm $year^{-1}$ and an RMSE of 188 mm $year^{-1}$. ET_{HAM} averaged 829 mm $year^{-1}$ with a standard deviation of 110 mm $year^{-1}$ and when averaged annually, ET_{HAM} was related to mean annual precipitation and mean annual temperature with correlations of 0.95 and 0.64 respectively (F-test; $P<0.05$). Averaged annually, ET_{HAM} mean error significantly decreased from 1986 through 2005 with a correlation coefficient of 0.41 (F-test, $P<0.001$).

ET_{LU}

On average, ET_{LU} overestimated ET_{CWB} by 6.1%, the lowest mean percentage error of all methods. ET_{LU} had the second smallest bias of all models with a mean error of 1.6 mm $year^{-1}$ but the largest mean error standard deviation of 182 mm $year^{-1}$. ET_{LU} had the most extreme overestimation of 642 mm $year^{-1}$. ET_{LU} also had the second lowest RMSE of 182 mm $year^{-1}$. On average, ET_{LU} overestimated 8 of the 15 watersheds ranging from a mean watershed underestimation of -26% to a maximum overestimation

of 80%. As expected, ET_{LU} had a strong positive relationship to mean annual precipitation with a correlation of 0.997 (F-test; P<0.001). When errors were averaged annually, both mean error and RMSE for ET_{LU} increased with increasing precipitation, indicating a nonlinear relationship may exist (F-test, P<0.05).

ET_{Precip}

ET_{Precip} had the lowest mean error and RMSE of all models, with -0.04 mm $year^{-1}$ and 168 mm $year^{-1}$ respectively, though ET_{Precip} mean error varied more than all other models (Table 2). ET_{Precip} overestimated ET_{CWB} by 6.4%, the second lowest value of all models. When averaged by watershed, ET_{Precip} mean error significantly increased with increasing proportion yield and runoff, with correlation coefficients of 0.83 and 0.51 respectively (F-test, P<0.05).

Sensitivity Analysis

Estimated ET was more sensitive to LAI, followed by sap flow equation parameter estimates, and then precipitation. Precipitation had the lowest sensitivity, most likely due to its relatively small CV compared to LAI and sap flow. LAI and sap flow had larger variation in model parameters leading to a greater impact on ET estimation.

The analysis of LAI uncertainty showed that LAI model variation has the potential to contribute significantly to ET_{SAP} variation (Figure 6). There was a slight negative bias in the resulting ET estimates and the variation was large relative to average ET_{SAP}. The mean change in ET_{SAP} from LAI uncertainty was -16.8 mm $year^{-1}$. The

changes to annual ET_{SAP} ranged from -935.4 mm year^{-1} to 1122.5 mm year^{-1} with a standard deviation of 222.3 mm year^{-1}. Results varied by watershed, higher elevation watersheds differed more from baseline values than lower elevation watersheds (F-test, $P<0.05$).

Sap flow model uncertainty resulted in significant changes to annual estimates of ET_{SAP} (Figure 3). There was a mean change of 5.2 mm year^{-1} and an overall standard deviation of 71.9 mm year^{-1}, with a minimum of -265.3 mm year^{-1} and a maximum of 239.7 mm year^{-1}. Results varied by species, with greater uncertainty in the parameter estimation for *Carya* spp., resulting in a mean error of 10.4 mm year^{-1} and a standard deviation of 96.0 mm year^{-1}. The species model with the least uncertainty was *Q. rubra* with a mean error change of 2.4 mm year^{-1} and a standard deviation of 25.3 mm year^{-1}. Tulip tree had a mean change of -4.7 mm year^{-1} and a standard deviation of 87.9 mm year^{-1} and chestnut oak had a mean change of 12.8 mm year^{-1} and a standard deviation of 55.0 mm year^{-1}.

The uncertainty analysis found daily precipitation error resulted in minor changes to annual catchment water balance estimates of ET (Figure 1). There was no significant bias, with a mean error change of 0.0195 mm year^{-1}. There was a standard deviation of 4.02 mm year^{-1} and a maximum change of 18 mm year^{-1} and a minimum change of -17 mm year^{-1}.

Discussion

Model Comparison

On average, all models performed reasonably well with mean percentage errors ranging from -11% to 18%. The model with the lowest mean percentage error was ET_{LU}, though at a 6.4% overestimation all models were relatively close. RMSE was also practically similar across models, with a range of 36 mm $year^{-1}$, from 168 mm $year^{-1}$ to 204 mm $year^{-1}$. Though the difference among models is statistically significant, 36 mm $year^{-1}$, it is 4.8% of the average ET_{CWB}, a relatively small amount ($P<0.05$). ET_{SAP} was the only model to on average underestimate ET_{CWB}. ET_{LU}, ET_{Precip}, and ET_{HAM} used annual precipitation in varying forms as their driving explanatory variable and overestimated ET_{CWB} by 6.1%, 6.4%, and 18%, respectively.

Although ET_{SAP} had a slightly larger mean error and RMSE compared to our other ET models, the model has advantages for some classes of application. The main advantage is the ability to examine the interactions between species composition and ET. Sap flow models offer increased flexibility by allowing us to look at interacting species composition and changes in future forests with only a 4% absolute difference in mean error compared to our best model. As discussed earlier, climate change and invasive species will alter forest composition and hence ET. Sap flow models allow us to examine these impacts to plan for future changes.

An additional advantage of sap flow models is the lower variation in ET error compared with the other ET methods. Even with an overall underestimation, having smaller extreme errors allows the sap flow models to have less extreme errors and more likely to have a smaller bias when averaging over shorter time periods.

Our other ET methods had lower mean error and RMSE than ET_{SAP}. However, when watershed RMSE was averaged, ET_{SAP} had a lower RMSE than ET_{HAM} and ET_{LU}. This signifies that ET_{SAP} RMSE was greater for watersheds with a longer period of record compared to ET_{HAM} and ET_{LU}. However, no significant relationships were found with period of record and RMSE or mean error by model.

Previous studies show that Hamon et al. (1963) had a correlation coefficient of 0.63 with ET_{CWB} (Lu et al., 2005), where our study showed a much lower correlation of 0.34. Lu et al.'s (2005) study did not use a conversion from PET to ET, so one would expect their estimates to be worse than one that used a conversion. When our ET values were averaged annually the correlation coefficients between ET_{CWB} and ET_{HAM} rose to 0.62. Zhang et al. (2004) found an even higher correlation with ET_{CWB} of 0.89, though they used Fu's PET model instead of Hamon's PET model. Another study using Zhang et al. (2001) to estimate catchment ET and comparing to ET_{CWB} found mean errors from -16.5% to 1.6% with an average of a 2.5% overestimation (Amatya and Trettin, 2007). Our mean average ranged form -12% to 100% with an average of 23% error for ET_{HAM}, an order of magnitude larger. One major difference was the calculation of PET, Amatya and Trettin (2007) used the Thornthwaite (1948) method. The Thornthwaite PET method

was rejected for this study because it was found inferior to the Hamon method by Lu et al. (2005).

Lu et al.'s (2003) ET model was originally developed for determining the mean annual watershed ET, not individual year ET values. Performance shows, however, it is also capable of estimating annual ET for the SA with results comparable to other leading models. In Lu's original study, they found an RMSE of 62.13 mm $year^{-1}$. In our study, using annually averaged ET values, RMSE was 181.9. This could be a result of the differences in study area. All of our study watersheds were nearly completely forested, but Lu et al. had a wide range of forest covers representing their percent forest term. Amatya and Trettin (2007) also used Lu et al.'s (2003) model to determine catchment ET and found errors ranged from -0.5% to 16% with an average of 0.5%. Our mean average ranged from -26.3% to 79.8% and an average of 11%. Differences may have been a result of the difference in location of the studies and precipitation regimes. The Amatya and Trettin (2007) study was performed outside of the SA in South Carolina.

Error Sources

On average, our calculated ET_{SAP} underestimated ET_{CWB} by 11% and was well within the range of those observed by others. This is notable given we're estimating across a larger area and for more years than similar studies. Ford et al. (2007) averaged -11% as well, with errors ranging from -7% to -14% for a white pine watershed at CHL in 2004 and 2005. Wilson et al. (2001) underestimated a deciduous stand using species-specific sap flow equations by 16% and 28% for two different years. Additionally, Oishi

et al. (2008) compared sap flow derived ET estimates to eddy-covariance ET estimates and resulted in either a 3% underestimation or a 10% overestimation, depending on the plot.

Underestimation of ET_{CWB} from sap flow could result from a number of causes. First, ET_{CWB} may not accurately estimate ET. A catchment water balance does not accuretly estimate ET when there are annual net changes in ground water storage. Any bias should diminish over time, because the longer time periods average the net change over many years. When averaging results over the 20 year period, overall error statistics are significantly decreased for a majority of the watersheds and years than compared to individual years on individual watersheds. Extreme maxima and minima range between -48% error and 192% error. Ground water storage changes over the annual water year are most likely not zero, as commonly assumed (Wilson et al., 2001; Ford et al., 2007; Oishi et al., 2008), although in most years in the SA, winter rainfall brings soils to near saturation. One study examined the relationship between catchment water balance error and soil water storage level and found that at the monthly and seasonal time scale, there was a significant relationship between error and soil moisture (Essery, 1992). However, at the annual time scale and for all study watersheds, there were no significant relationships between catchment water balance error and ground water storage level, suggesting that at the annual time scale, the assumption of negligible net storage differences is valid.

Since ET_{CWB} is calculated directly from precipitation and streamflow, any error in these measurements or from the spatial and temporal scaling of these values will impact ET_{CWB}. Rain gauge measurement error is most often caused from turbulence and increased winds around the gauges (Stellman, 2001). One study by Stellman (2001) quantified this error for Georgia at approximately +/- 2% of annual precipitation totals. Rain gauge error substantially increases in windy conditions with one study finding errors of up to -25% (Frei and Schar, 1998). On average for the SA, mean annual wind speed is near 0.5 m s^{-1} with the higher rates from January through April (Hursh, 1948). According to Yang et al. (1998), precipitation at or below 1 m s^{-1} led to rain gauge measurement error near zero. Wind speed, however, is higher near the northern North Carolina and Tennessee boarder and on ridges with maximum speeds of up to 7.4 m s^{-1} (Raichle and Carson, 2009). Further, if rain gauges underestimate precipitation, our estimates of ET_{CWB} would also be underestimated increases the discrepancy between ET_{CWB} and ET_{SAP}.

Scaling precipitation from point based measurements to the watershed also leads to error in precipitation estimates. A recent study examined interpolation error in the SA and found annual error averaged 3 mm $year^{-1}$, 0.2%, when using geostatistical techniques that include elevation (Kove and Bolstad, in prep). A minimal bias is important, however, the error magnitude is better described by mean absolute error (MAE). MAE was estimated at 172 mm $year^{-1}$, approximately 13% of mean annual precipitation, a potentially significant source of error in ET_{CWB}.

Runoff, also used in the estimation of ET_{CWB}, is an unlikely source of error. Runoff measurement error is not well documented, though Hoover (1944) did find discrepancies between neighboring watersheds of identical size and slope at CHL and implied the cause could be measurement error. Also, other studies have documented cases of extreme runoff leading to underestimates in runoff from water washing over the weir (Zhou et al., 2008). Though this may occur during a rare tropical storm, it is very unlikely to make a significant impact on annual runoff. Additionally, subsurface flow would decrease runoff, however it is unlikely in the SA due to steep slopes and impenetrable bedrock (Ford et al., 2007).

Evaporation Model Error

We were not able to test the accuracy of Helvey and Patric's (1965) model, used to estimate canopy interception and evaporation. However, in Helvey and Patric, measured error rates of 5% annual interception were found, an average of 12 mm $year^{-1}$. For our results, a 5% interception error rate would result in an average error of 16 mm $year^{-1}$ across our study watersheds. Helvey and Patric did not find an underestimation, so interception error would not help explain our bias.

Sap flow Measurement Error

The underestimation from ET_{SAP} of ET_{CWB} may also be a result of sap flow measurement error. This error could be caused from sensor error or the measurement of unrepresentative trees. Wilson et al. (2001) considered the possibility of sap flow sensor error as a cause of their 28% underestimation of ET_{CWB} from sap flow ET estimates. Lu

et al. (2004) confirmed the underestimation in Wilson et al. (2001) may have been a result of the modified probes used.

Variability in sap flow due to ring porosity could also attribute to the underestimation of ET_{CWB}. According to Wilson et al. (2001) and Clearwater et al., (1999) sap flow estimated transpiration in ring porous trees can underestimate actual transpiration by up to 45%, theoretically, due to radial variation. However, Wilson et al. (2001) did not find the radial variation significant in their study to require additional inquiry. Further, in the SA, ring porous species make up less than 35% of the overstory LAI (Woodcock, 1989).

There also may be spatial sampling error in model development versus application. Most studies model sap flow on the same stands measured when developing the models. However, our study developed sap flow on stands in CHL, and applied these models over much of the SA, potentially adding variability due to sampling. Variability in sap flow among the same species has been documented across space (Engel et al., 2002; Mackay et al. 2002; Ewers et al., 2008). Studies have estimated from 12 to 20 trees should be measured per stand when estimating via sap flow derived ET (Kostner et al., 1996 and 1998; Kumagai et al., 2005; Ford et al., 2007). The ET_{SAP} equations used here were developed on WS15 and bias and RMSE was among the lowest observed for our watersheds, at -2.9% this difference is not notable.

Ford et al. (2007) discussed variability when scaling sap flow estimates from trees to stands and determined that the greatest scaling error resulted from omitting plot to plot variability, as opposed to within-tree variability. Plot to plot variability means the variability in measurements between plots that is not accounted for by species composition. Our study assumes that there is no variability among plots, and that watershed ET from a single species will react similarly across the SA. This assumption could explain the variability of our estimates.

ET_{SAP} both over- and under-estimated ET_{CWB}, suggesting there is a small measurement bias. If there were a systematic bias in our models due to measurement errors, we would expect this bias to be reflected across all watersheds, and we did not. Watershed-averaged error ranged from -38.6% to 62.8%, with similar number both above and below the overall mean of -11%. There could have been other errors that mask a bias, but given this range, measurement errors are likely small relative to other factors.

Model Input Error

Another potential explanation for our underestimation of ET_{CWB} by ET_{SAP} is the accuracy of our input data. Sap flow model inputs including VPD, PAR, LAI and species composition were all estimated and therefore come with error. It is likely that data plays a role in the underestimation of sap flow models, though it is difficult to quantify. Temperature is measured at climate stations and interpolated across the landscape, leading to estimation error, but the estimation appears unbiased. Variables in our sap flow models, including VPD and PAR, are based on interpolated temperatures.

Interpolated temperatures resulted in mean errors of 0.0010 ^{o}C for minimum temperature and -0.004 ^{o}C for maximum temperature for the SA, according to Kove and Bolstad (in prep). Though these small errors are relatively insignificant, RMSE reached 3 ^{o}C, potentially leading to larger errors, especially for higher elevations during the summer months (Kove and Bolstad, in prep). Errors of 3 ^{o}C in temperature do not correspond to a constant VPD error because VPD is nonlinear, so the impact depends on the minimum and the maximum temperature and the daily temperature range. Impacts from a temperature error of 3 ^{o}C on VPD range from 0.08 to 0.36. PAR is also nonlinear and dependent on elevation and temperature range with impacts from a 3 ^{o}C temperature error ranging from 100 to 155 µmol quanta J^{-1}.

Species composition and distribution may also affect ET estimates from sap flow models. We used the most accurate, current data on species composition, though accuracy of species compositions was not analyzed. Our observed differences in transpiration from the species sap flow models, run individually and in our MCMC tests shows a change in composition may result in larges changes in ET. For example, daily *L. tulipifera* transpiration estimated with our sap flow models was nearly three times larger than all other species under equal climate conditions and LAI. Shifts in species composition could possibly impact ET_{SAP} significantly.

Sap flow derived ET estimates are strongly driven by LAI (Scanlon and Albertson, 2003). Both differences in LAI duration, phenologies, and LAI maximums will impact sap flow ET estimates. Dates used for the initiation of budburst, full leaf, and

leaf senescence in this study were estimated using regionally developed relationships with climate variables and elevation (Kove and Bolstad, in prep). Our models were developed at CHL with data from 2003 through 2009 using 8 species at two different locations. Though the RMSE of the models on CHL averaged around 3 days, error may be larger for our study due to higher species diversity, wider ranges of elevation, and wider ranges of latitude. Therefore, variation in watershed error may be a result of the differences in phenological dates across the SAR unexplained by our phenological models.

LAI maximums will also impact ET estimates. Bolstad et al's (2001) terrain driven LAI model was developed in the region with R^2=0.58. Error in estimates of LAI may explain the differences in RMSE among watersheds. The Monte Carlo analysis shows increased error in ET_{SAP} due to LAI parameter variability. ET_{SAP} mean error and mean LAI were significantly correlated, though most likely due to their relationships with elevation.

Missing Components

Finally, sap flow underestimates may be due to missing components in our sap flow ET models, potentially the exclusion of understory transpiration, soil evaporation, nocturnal fluxes and winter transpiration. Ford et al. (2007) noted the underestimates were possibly a result of the exclusion of soil evaporation for the water balance equation and from the exclusion of hardwood LAI that made up ~3% of their total watershed LAI. Additionally, Oishi et al. (2008) claim that soil evaporation is a major component of

water loss, and is often ignored in current studies using sap flow and a potential explanation for a portion of our underestimation.

Further, the exclusion of understory LAI may contribute to our underestimation. Most studies have been conducted on extremely small watersheds where a large percentage of the trees are measured, including understory trees and shrubs. Understory transpiration was ignored in our models since the only accessible estimate of LAI was that of the canopy. A closed canopy should result in low understory transpiration. However Wullschleger et al. (2001) found, in a deciduous stand at Oak Ridge, Tennessee understory transpiration was 17% of the total stand transpiration, potentially explaining a portion of our underestimation. However, since most sap flow studies did include measurements of understory transpiration and still underestimated ET_{CWB}, this is unlikely to be a significant cause of ET_{SAP} error.

Nocturnal fluxes in addition to winter fluxes may also be responsible for the lost transpiration in our estimates. Oishi et al. (2008) claimed current study underestimates from sap flow derived ET may be a result of ignored nocturnal fluxes. They state that including this variable could increase sap flow ET by 22%, much larger than our 11% mean underestimation. During the night, trees recharge upper trunks and branches in addition to general nocturnal water loss often ignored in sap flow studies (Oishi et al., 2008). Additionally, winter transpiration is often ignored. Though most of our study watersheds are deciduous, a small percentage is evergreen leading to potential winter ET. Ford and Vose (2007) found high winter transpiration in hemlock stands during the

winter months, confirmed by other studies (Martin, 2000; Ellsworth, 2000). However, other studies confirmed low winter transpiration (Catovsky et al., 2002). Ford et al. (2007) claims the difference in these results may be due to lower temperatures, where coniferous trees have substantially less winter ET. If this reasoning were true, our study watersheds with more coniferous cover would have larger error. However, our data show no relationship between error and species composition.

Conclusion

ET_{SAP} underestimated catchment water balance ET on average by 11%, similar to findings by Ford et al. (2007), -7% to -14% yet smaller than those found by Wilson et al. (2001), -16% to -28%. Possible explanations for the underestimate include excluded components such as soil evaporation, nocturnal fluxes, and understory transpiration, and inaccurate inputs such as, LAI, PAR and species composition. Such complexities demonstrate the difficulty in applying sap flow models to heterogeneous terrain and the need to improve models. Potential improvements include the improvement of spatial estimates of LAI, PAR and species composition particularly for mountainous terrain. Further, sap flow models might be improved with the addition of precipitation since there is a strong relationship with annual ET and annual precipitation. Other beneficial additions could include nocturnal fluxes and an elevation term.

Using sap flow models to estimate ET is becoming more common, due, in part, to an increased desire to understand the relationships between species composition, climate, and ET. Our central interest was to determine the ability of sap flow models, derived off

site, in estimating ET compared to the catchment balance method and three other methods. ET_{SAP} performed comparatively to other ET estimation methods. Though errors were slightly larger, the benefits from using sap flow models to estimate ET, including the ability to examine climate and species effects, outweigh the slight increase in error. Our results indicate that sap flow models are a beneficial way to estimate ET even if the models are derived off site. Further, inputs can be estimated through geostatistical techniques and do not require onsite measurement for comparable accuracy to similar studies.

Further studies are needed to examine the potential for improving our sap flow models. First, developing models with a larger dataset, more than the two years used here, would benefit the models. Also, expanding the species set used would enhance these models. Finally, model limitations including the absence of precipitation, understory ET and soil evaporation should be analyzed further.

Watershed ID	County(s)	Area (sq km)	Avg Temp (^{o}C)	Mean Elevation (m)	Elevation Range (m)	Percent Forested	Rainfall (mm yr^{-1})	Runoff (mm yr^{-1})	Percent Yield	Study Period (years)
1	Caldwell and Watauga	74.6	12.7	658	(368, 1183)	100	1332	596	43%	20
2	Clay and Macon	134.4	10.3	1212	(932, 1667)	100	2115	1347	63%	20
3	Burke	66.6	13.6	550	(343, 880)	99	1365	627	44%	20
4	Transylvania	104.6	11.5	975	(628, 1820)	98	1702	1068	61%	16
5	Buncombe	37.8	9.8	1287	(805, 1950)	100	1689	1010	59%	16
6	Buncombe	14.1	10.0	1243	(837, 1724)	100	1573	695	43%	19
7	Haywood	71.5	8.9	1458	(902, 1942)	100	1988	1249	62%	20
8	Haywood	86.8	9.3	1406	(864, 1942)	100	2010	1266	62%	17
9	Haywood	127.4	9.9	1213	(751, 1848)	100	1713	793	46%	20
10	Yancey	112.1	10.1	1192	(812, 2028)	100	1626	1099	66%	20
11	Macon	48.6	10.7	1190	(985, 1499)	98	2165	1486	68%	4
12	Transylvania	30.3	11.7	948	(687, 1230)	99	1781	1039	57%	17
13	Transylvania and Henderson	69.4	12.4	880	(767, 1151)	98	1637	1171	70%	5
14	Wilkes and Watauga	124.6	12.7	632	(329, 1248)	100	1299	673	50%	20
15	Macon	0.1	13.2	860	(726, 993)	100	2007	1001	49%	20

Table 1: Watershed characteristics from 1986-2005 from the USGS streamflow gauges, 10m digital elevation model, and from the NCDC climate station data. Where percent yield = runoff/rainfall x 100 averaged for each watershed.

			Mean Error (mm yr^{-1})				RMSE (mm yr^{-1})				Percent Difference			
WS	Helvey I	ET_{CWB}	ET_{SAP}	ET_{HAM}	ET_{Lu}	ET_{Precip}	ET_{SAP}	ET_{HAM}	ET_{Lu}	ET_{Precip}	ET_{SAP}	ET_{HAM}	ET_{Lu}	ET_{Precip}
1	246	736	-65.0	82.9	-5.7	-41.6	125.6	142.0	116.0	116.3	-9.5%	13.4%	1.1%	-3.6%
2	387	769	-108.6	82.4	62.2	29.7	149.5	128.8	138.9	103.2	-14.3%	12.9%	9.5%	5.8%
3	251	738	-32.8	113.3	42.6	-38.9	98.4	150.5	108.7	100.7	-5.6%	17.0%	7.2%	-3.7%
4	312	633	34.9	219.5	135.1	110.2	111.9	242.3	196.3	148.2	5.2%	37.2%	23.7%	19.8%
5	310	678	-108.5	108.5	-13.1	63.4	141.2	139.7	114.7	111.9	-16.3%	18.0%	-0.4%	11.4%
6	289	878	-316.7	-99.7	-234.7	-151.2	329.7	135.1	252.6	179.2	-36.8%	-10.2%	-26.3%	-16.1%
7	364	739	-194.5	47.7	-24.0	42.9	215.8	106.9	118.3	105.7	-26.5%	8.5%	-2.4%	7.7%
8	368	744	-178.7	56.7	-8.0	40.6	203.8	108.1	126.8	105.1	-24.2%	9.2%	0.1%	7.0%
9	314	920	-347.1	-118.6	-225.1	-174.6	354.8	140.3	235.2	191.3	-38.6%	-12.2%	-24.3%	-18.3%
10	298	527	-40.0	266.5	143.3	206.7	147.1	301.8	222.4	249.7	0.8%	66.4%	41.8%	54.0%
11	396	679	3.5	189.6	175.0	126.2	63.4	207.6	187.3	142.9	0.1%	30.5%	26.4%	20.4%
12	326	742	-22.9	128.0	60.3	12.3	120.3	172.7	154.8	114.5	-3.5%	19.6%	10.1%	3.7%
13	300	466	250.8	398.6	311.5	268.8	303.4	428.5	366.7	302.9	62.8%	100.3%	79.8%	69.9%
14	240	625	56.3	185.9	100.2	64.6	148.1	238.3	179.7	147.2	12.0%	37.0%	22.6%	16.5%
15	522	1006	-78.0	-46.8	-105.0	-221.9	196.3	196.7	219.1	296.0	-2.9%	1.0%	-5.8%	-17.4%
Mean	326	745	-112.5	84.7	1.6	-0.04	204.1	187.6	181.9	168.2	-10.7%	18.4%	6.1%	6.4%

Table 2: Mean watershed error statistics including ET_{CWB}, and ET estimate mean error, RMSE and percent error for ET_{SAP}, ET_{HAM}, ET_{LU}. Where percent difference = (ET estimate/ ET_{CWB} – 1) x 100. Averages were computed using 15 watersheds and all years (1986-2005) instead of averaging columns in this table since some watersheds had more years of data than others.

Species	*Parameter*	*Mean*	*Standard Error*	*Lower 95% CI*	*Upper 95% CI*
Quercus rubra	b1	0.0773	0.0404	-0.00303	0.1576
	b2	9.264×10^{-6}	0.000032	-0.00006	0.000074
	b3	0.0152	0.00117	0.0128	0.0175
Quercus prinus	b1	0.3055	0.1182	0.0704	0.5406
	b2	-0.00015	0.000077	-0.00030	3.429×10^{-6}
	b3	0.00954	0.00129	0.00699	0.0121
Liriodendron tulipifera	b1	0.2538	0.1587	-0.0655	0.5731
	b2	0.000136	0.000113	-0.00009	0.000363
	b3	0.00770	0.00166	0.00435	0.0111
Carya Spp.	b1	0.4950	0.2644	-0.0307	1.0208
	b2	-0.00031	0.000131	-0.00057	-0.00005
	b3	0.00644	0.00157	0.00331	0.00956

Table 3: Parameter estimates, standard errors and 95% confidence intervals for the sensitivity analysis of the sap flow transpiration equations.

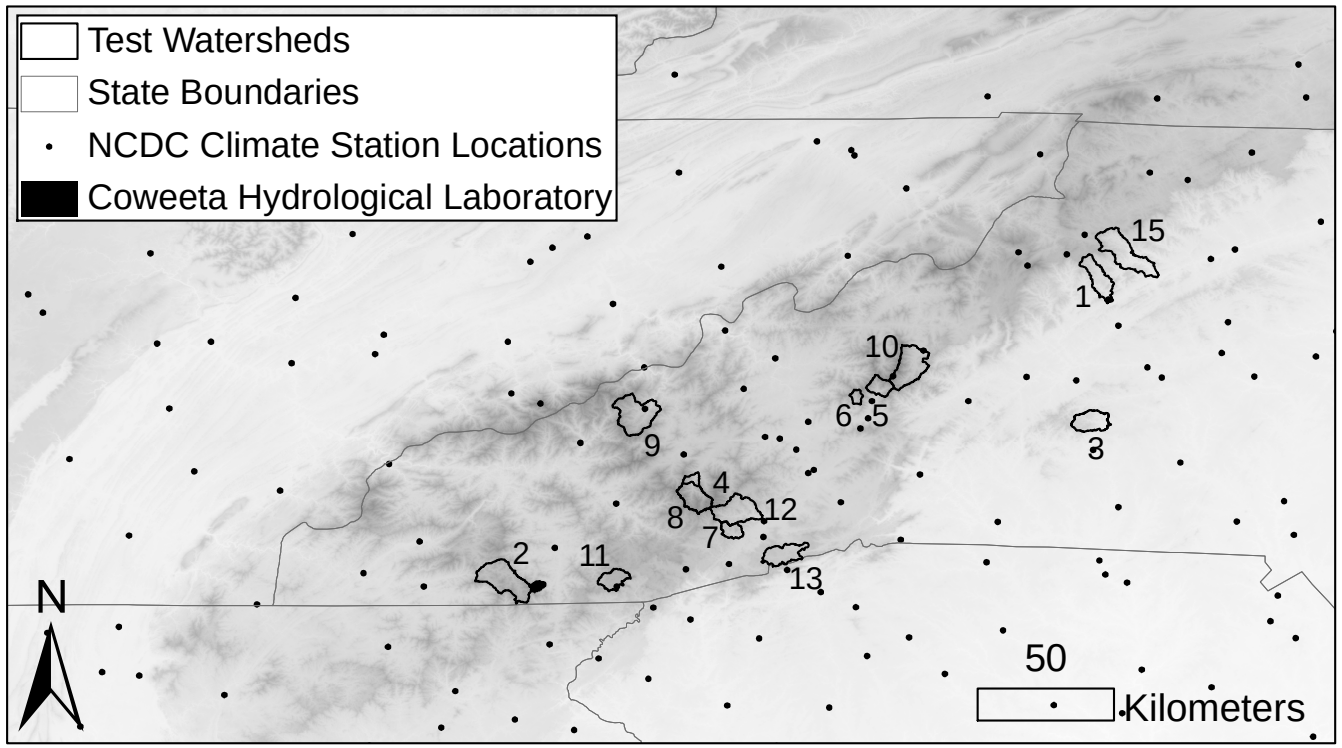

Figure 1: Study area including western North Carolina, northern Georgia and South Carolina, eastern Tennessee and southern Virginia. Fifteen test watersheds, including the Coweeta Hydrological Laboratory. NCDC climate station locations, including precipitation gauge stations and temperature stations.

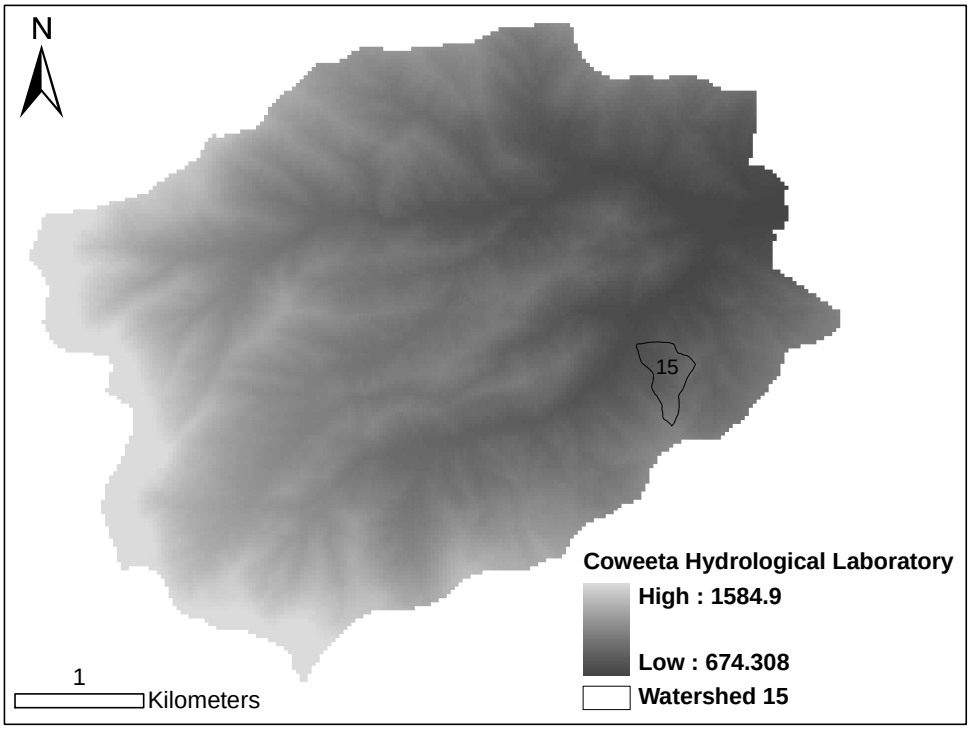

Figure 2: Coweeta Hydrological Laboratory digital elevation model with WS15.

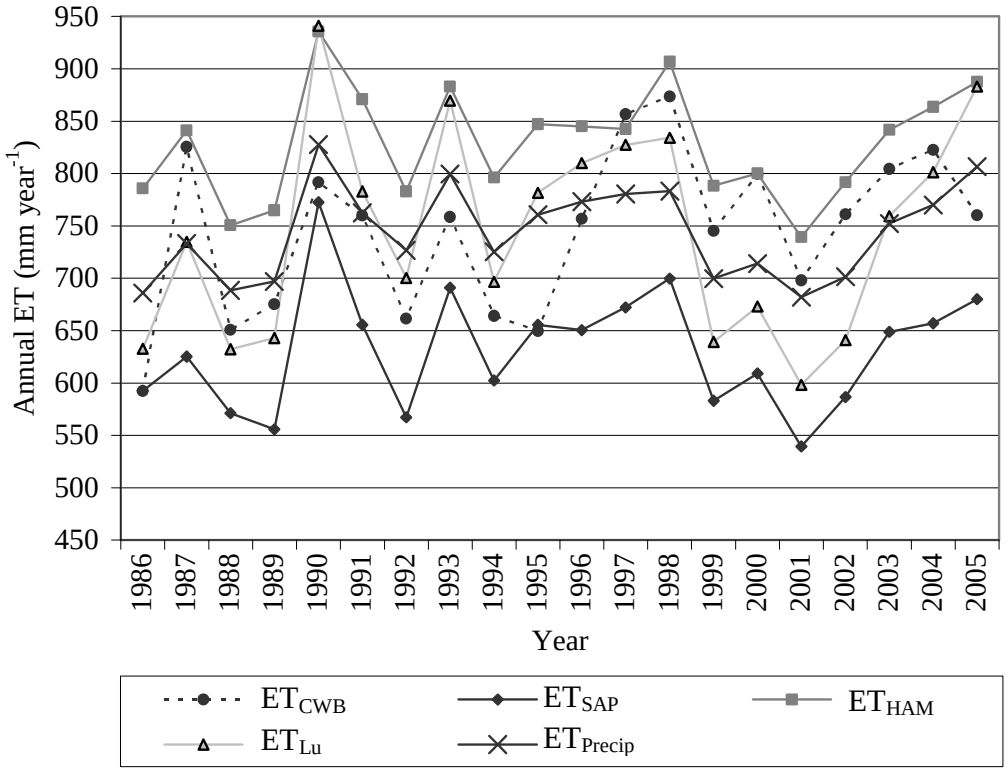

Figure 3: Annually averaged ET estimates for 5 estimation methods on 15 watersheds (WS1-WS15) from 1986-2005, except for missing data (WS 4 for 1991-1994, WS 5 for 1986-1989, WS 6 for 1986, WS 8 for 1986-1988, WS 11 for 1986-2001, WS 12 for 1986-1987 and 2005, WS 13 for 1991-2005).

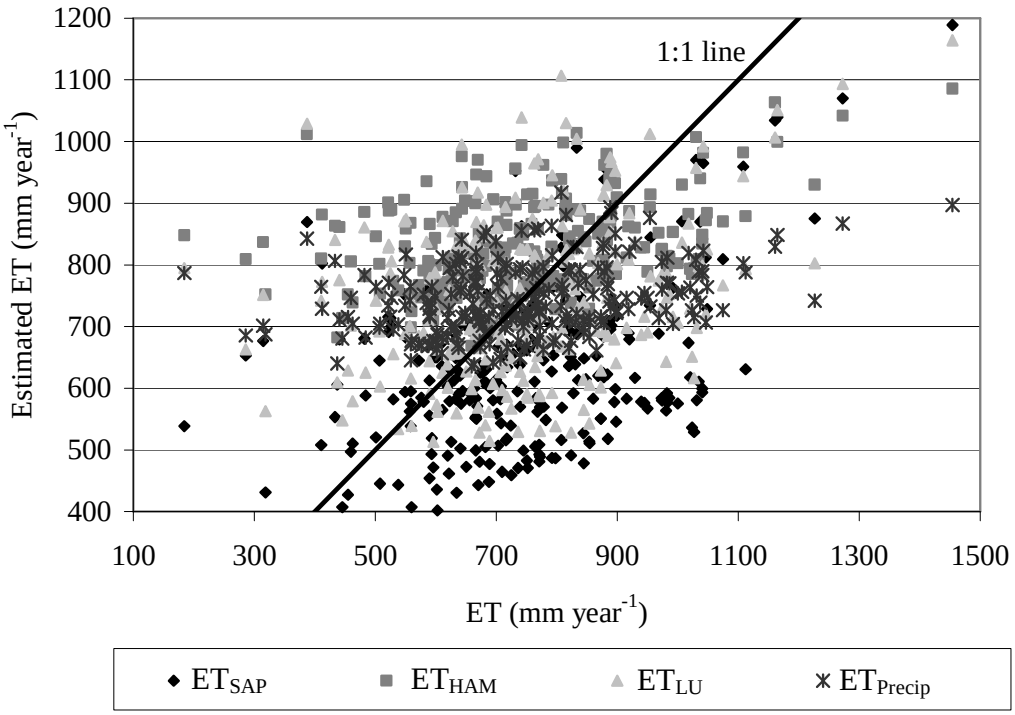

Figure 4: Annual ET_{CWB} versus estimated ET, showing results from four ET estimation methods, ET_{SAP}, ET_{Ham}, ET_{Lu}, ET_{Precip} for 15 watersheds (WS1-WS15) from 1986-2005.

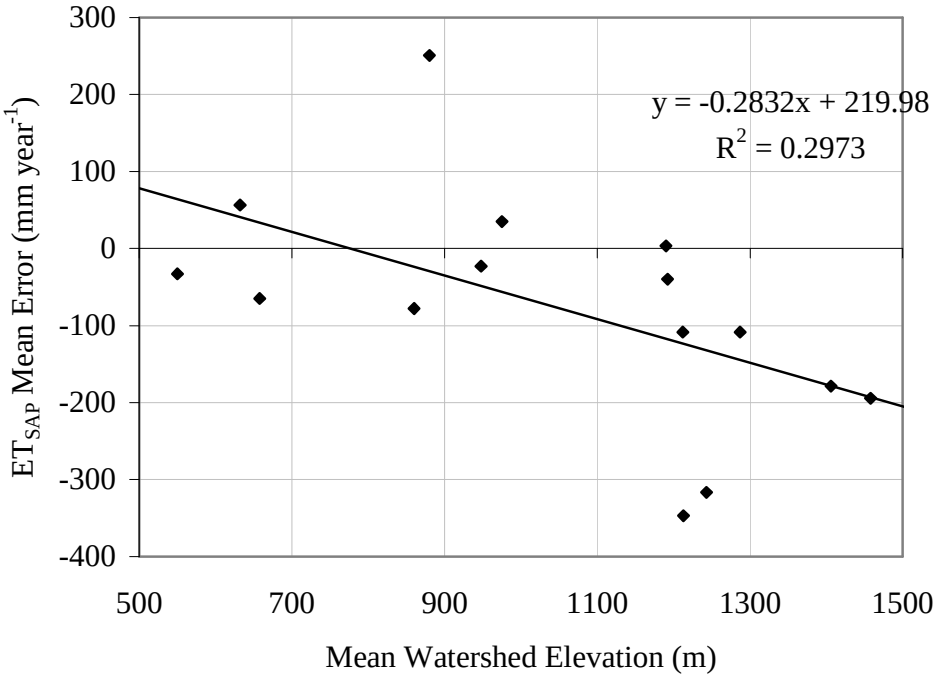

Figure 5: ET_{SAP} mean error (compared to ET_{CWB}) versus mean watershed elevation from 15 watersheds (WS1-WS15) from 1986-2005. Data was fit with a linear regression equation and shown with model R^2.

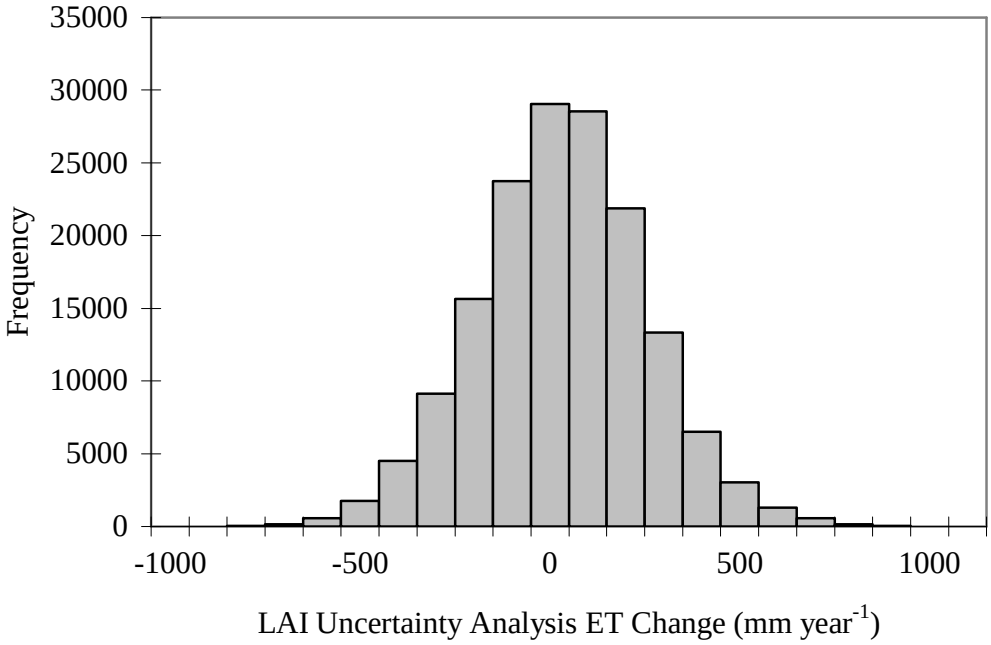

Figure 6: Annual change of ET_{SAP} resulting from LAI model error propagation generated using LAI from the Monte Carlo simulations across 15 watersheds (WS1-WS15) from 1986-2005, with 1000 simulations each.

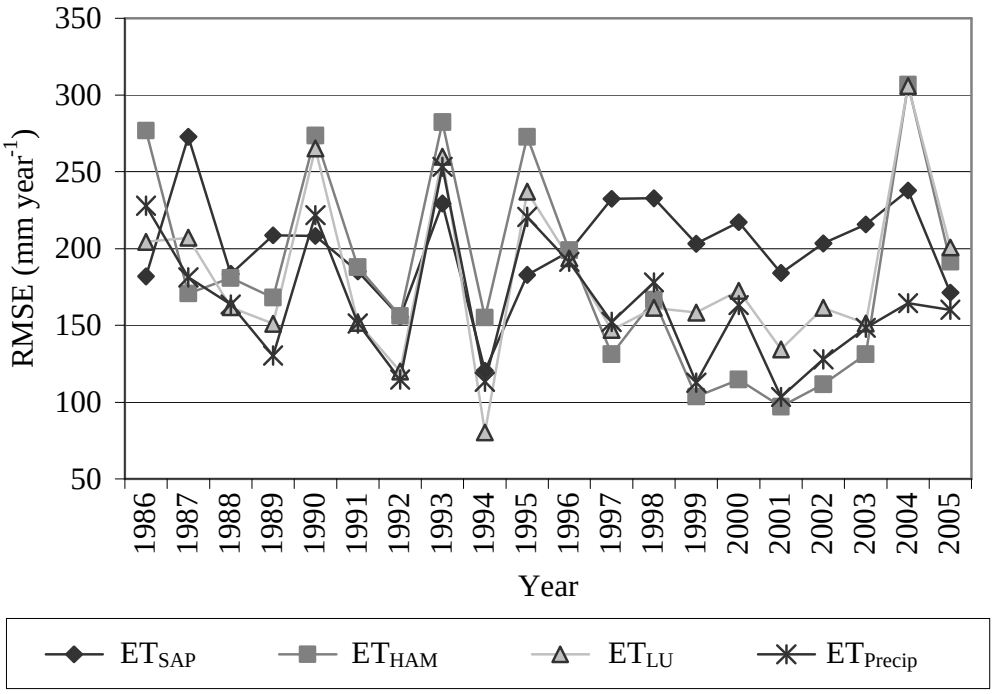

Figure 7: Annual RMSE for four ET estimation methods, ET_{SAP}, ET_{Ham}, ET_{Lu}, and ET_{Precip} when compared to ET_{CWB} and averaged across 15 watersheds (WS1-WS15) from 1986-2005.

Chapter 3: Impacts from estimating phenology and leaf area index on modeled evapotranspiration of the southern Appalachians.

Tree phenology and leaf area index (LAI) are key structural characteristics related to forest mass and energy cycles. Phenology and maximum LAI drive ecosystem processes by defining the length of the growing season during which leaves produce energy through photosynthesis, thereby impacting total annual productivity and plant water use. Despite their importance, both phenology and LAI are poorly quantified in time and space with sparse observations and data collections. Many models of forest water use and productivity use regionally fixed values for phenology and LAI or the average of historically observed values, ignoring spatial and temporal variation. Little research has been done on the impacts that these estimates might have on estimates of evapotranspiration (ET). Further, phenological studies are lacking for the southern Appalachians (SA). Our goal for this study was to examine the phenology of the SA, determine the best phenological and LAI estimates, and examine the impact various models might have on estimates of ET. Additionally, we examined the relationship between canopy PAR and spring and fall phenologies. We found the optimal growing degree day model for bud burst used a 2 ^{o}C threshold and a starting date of DOY 65 resulting in an RMSE of 3 days. For full leaf, a 5 ^{o}C threshold and a starting date of DOY 95 produced an RMSE of 5.34 days. For the fall, mean dates were best.

Phenology of the SA was best estimated by locally fixed dates varying with elevation. Canopy PAR was a good predictor of our phenologies including the proportion of bud burst, color change and leaf fall. Models fit better for the lower

elevation site than the higher elevation site, and elevation improved the estimation for color change and leaf fall. Finally, error results show the best phenological model is not as important as the best LAI model when estimating sap flow derived ET. Mean ET estimates varied on average by 3.1% among our three phenological methods, while ET estimates varied by more than 11.5% between the two LAI methods. A 3.1% error is still large enough to be a consideration in the modeling process given that many published errors from sap flow derived ET is near 10%.

Introduction

Phenology is the study of the timing of recurring biological events (Lieth, 1974). A long history of research in northern temperate forests has shown springtime phenologies to be almost universally related to temperature. Autumn phenologies are less well understood but have been shown to relate to temperature, daylength, and at times water balance (Hunter and Lechowicz, 1992; Schaber and Badeck, 2003; Fracheboud et al., 2009). Tree phenology represents the timing of bud burst and leaf development in the spring and leaf senescence in the autumn. Leaf area index (LAI), the total one-sided area of leaf tissue per unit ground area, is an important parameter in ecophysiology, for scaling up gas exchange from leaf to canopy. Both LAI and phenology drive ecosystem processes by defining the energy potential and growing season length during which leaves produce energy through photosynthesis and lose water through transpiration, thereby impacting total annual productivity and plant water use (Kramer et al., 2000; Linderholm, 2006).

Despite its importance, phenology is poorly quantified in time and space. Phenology data are sparse, with only a few recent observations available across the United States annually and even fewer historic observations (except across Europe and Asia) (Richardson et al., 2006). The National Phenology Network, initiated in 2007 in the U.S., aims to rectify the paucity of phenological data by using citizen-scientists to collect data and record their observations online (http://www.usanpn.org). Although this will develop a useful dataset, there is a current need to model phenological events, especially for areas not frequented by the general public, and for modeling historical phenologies. While phenologies are often observed by humans, they may be measured in forests through above and below canopy photosynthetically active radiation (PAR) (Menzel, 2002). Above/below canopy PAR, hereafter referred to as canopy PAR (PAR_C), may show the progression of leaf development through the decrease in the proportion of above canopy PAR that reaches the forest floor. Such models may allow PAR sensors to collect canopy phenology data, improving frequency, scope, consistency, and quality of phenological observations (Menzel, 2002).

The main drivers of tree phenology are temperature and photo period (Menzel, 2002). Phenological events do not occur on the same calendar day each year because of trade-offs between the need to grow and store nutrients and the need to avoid damage from freezing temperatures (Lopez et al., 2008). Early-season warming initiates development, but enough warming has to occur for bud burst and leaf growth. Consequently, inter-annual variation in leaf phenology is primarily a result of climate variation (Lechowicz, 1984). Spring leaf development is mainly estimated using growing

degree-days (GDD), so that the difference in phenology due to a cool or warm spring may be predicted. GDDs are a measurement of heat accumulation above a threshold temperature and from a given starting date (Hunter and Lechowicz, 1992). The threshold temperature in thermal sums is the point at which growth occurs in a plant, and varies among species. Many developmental events in plants depend on GDD and can therefore be predicted using these thermal sums (Hunter and Lechowicz, 1992).

Phenology also differs among and within species as well as climate (Lechowicz, 1984), and phenological variations exist between some populations (Chmura and Rozkowski, 2002; Chmura, 2006), but not universally (Chuine et al., 2000; Vitasse et al., 2009). Differences between these studies might be attributable to inter- and intra-species genetic differences (Nienstaedt, 1974; Flint, 1974). Variations between elevations also influence leaf phenology, but are most likely due to differences in temperature and precipitation (von Wuehlisch et al., 1995; Badeck et al., 2004; Vitasse et al., 2009).

Leaf development often requires a cooling period during which the bud lies dormant. Dormancy is released by a subsequent heating period (Perry, 1971), although the physiological mechanism behind these processes is still not fully understood (Linkosalo et al., 2006). Some argue that this cooling period can decrease required thermal sums, thereby impacting spring phenology (Falusi and Calamassi, 1990; Heide, 1993; Raulier and Bernier, 2000). However, other studies show that winter chilling does not improve upon models of spring phenology that use GDDs (Hunter and Lechowicz,

1992; Heide, 1993; Schaber and Badeck, 2003). Uncertainty regarding the inclusion of winter chilling in modeling spring phenology still exists (Vitasse et al., 2009).

Spring phenology models used in the literature vary considerably. Some studies use average phenology dates from regional phenology observations, where others use models from the literature or fit local models (Kergoat, 1998; Zierl, 2001; Gerten et al., 2004; Kucharik et al., 2006). Spring phenological models vary from simple linear regressions to more complicated process-based models, however some argue that adding complexity, overall, does not improve model performance (Chuine et al., 1999; Hunter and Lechowicz, 1992; Heide, 1993; Schaber and Badeck, 2003).

Autumn phenology has not been studied as extensively as spring phenology (Menzel, 2002), and as a result, the complexities of senescence confound models of autumn phenology (Fracheboud et al., 2009). Autumn phenological controls may include temperature through cooling sums, or soil moisture, drought, leaf age, photoperiod, or carbohydrate accumulation (Fracheboud et al., 2009). Photoperiod may predict autumn phenology in aspen (*Populus tremuloides*), although not other species (Keskitalo et al., 2005). Fracheboud et al. (2009) also found aspen fall phenologies were primarily controlled by photoperiod, but also suggested that low temperatures, water availability and nutrient availability may also play a role. Consequently, there is no consensus on the best modeling approaches (Schaber and Badeck, 2003), probably due to the weak relationships between simple meteorological factors and autumn senescence (Menzel, 2002). Cooling degree days has also been used in modeling autumn phenology (Cannell

and Smith, 1983). A study by Vitasse et al. (2009) looked at autumn phenology in oak (*Quercus petraea)*, beech (*Fagus sylvatica)*, sycamore (*Acer pseudoplatanus)* and ash (*Fraxinus excelsior)*. They found temperature to be strong predictors of autumn phenology for both *Q. petraea* and *F. sylvatica*, but no relationship for *F. excelsior* and *A. pseudoplatanus*. Further, altitudinal differences in autumn phenology were found for all species except for *A. pseudoplatanus*. Further studies are needed to validate potential controls of spring and autumn phenology.

Phenologies are important for productivity and evapotranspiration (ET) because they affect the length of photosynthesis and corresponding leaf water flux. ET, the combination of plant transpiration and surface evaporation, can vary across space and time, and is a significant component of the hydrological cycle in densely forested regions (Murakami et al., 2000). Mountainous regions, such as the southern Appalachian Mountains have been described as "water towers" for the surrounding area, because precipitation exceeds ET (Feldman, 2001). However, water balance varies through time with changes in climate and plant water use. Quantifying ET is critical to understanding the available water resource in this region. In the SA, ET averages 50% of annual precipitation in forested watersheds and can climb to 85% (Lu et al., 2003). Due to high annual rainfall in the SA, this results in over 1000 mm of water returning to the atmosphere annually (Zhang et al., 2001). Recent droughts across the southeast US attest to the potential impacts of changes in water availability, underscoring the need to better quantify the water cycle, and improve ET estimates (Moorhead, 2003).

Phenology defines growing season length, the period during which plants are photosynthesizing and using water. Models of forest water use and productivity should incorporate phenologies, but many use average observed values or fixed dates estimated based on the region (Ford et al., 2007). Using fixed phenologies in ET models leads to a uniform growing season length, and does not account for annual changes in temperature. Little research has been done on the impacts that variations in growing season initiation and duration have on annual ET estimates. In addition, the variability of different phenological estimates and the impacts on annual ET estimates should be examined. Determining these impacts would allow modelers to know the extent to which deviations in phenology may impact their results.

Due to the importance of LAI in regulating ecosystem processes such as water and carbon cycling, we hypothesize that improvements in quantifying leaf phenology will increase our ability to accurately model ET. To test this hypothesis we (1) examined the phenology of forest tree species in the SA and (2) quantified the impacts of various phenological and LAI values on estimates of annual ET. The first section examines measured phenology from Coweeta Hydrological Laboratory (CHL), examining temporal and elevational impacts by looking at differences in spring and fall phenologies on two different elevation sites across 7 years. Additionally, we investigated the predictive ability of climate variables in estimating spring bud burst, fall color change, and leaf fall phenology. Finally we examined the relationship between canopy PAR and spring and fall phenologies.

The second section compared the impacts of phenology models and LAI estimates on predicted annual ET. We compare ET estimates computed using three phenology models at two levels of maximum LAI for a total of six ET estimation methods. The three methods used to estimate phenological dates included a fixed, elevation invariant date, average dates from our regional dataset that varied by elevation, and phenological dates using the optimal climate models developed in section one of this paper. The two methods used to estimate LAI were a terrain-based method that varied by elevation, and a constant LAI based on the regional literature. We will compare the predictive ability of the six ET estimation methods with catchment water balance ET (ET_{CWB}), considered the true value of ET. We will also compare each methods result to ET_{C_T}, the model using the most ecologically sound estimation of LAI (terrain based model) and phenology (climate driven model).

Methods

Study areas

Two study areas were used in this paper, one for the phenological analysis and a second for the ET estimates. The phenological analysis was based on a 7-year data set (2003-2009) from the USDA Forest Service's Coweeta Hydrological Laboratory (CHL) located in western North Carolina (Figure 1). Data included spring and fall phenology observations, and were collected at two locations, a high elevation site 4 (S4) at 1380 m above sea level and a low elevation site 2 (S2) at 810 m above sea level (Figure 2). Climate is moist, humid temperate with average annual precipitation of 1978 mm (Swank and Crossley, 1988). Average minimum annual temperature was 6.5 ^{o}C and average

maximum annual temperature was 20 ^{o}C (Swank, 1988). The ET estimates were performed on our second study area, herein called the southern Appalachian region (SAR). The SAR encompasses western North Carolina, northern Georgia, and eastern Tennessee and includes CHL (Figure 1). Average annual temperatures range from 10 ^{o}C in the north and 18 ^{o}C in the south, with average annual precipitation ranging from 850 to over 2500 mm (NCDC, 2006).

Soils in CHL and the SAR vary considerably at small scales and are most often represented by the orders ultisol and inceptisol (Swank and Crossley, 1988) where ultisols are found in basins, ridges and points of gentle topography and inceptisols are found on steeper slopes. Overstory composition and forest communities include mixed-deciduous (*Q. alba*, *Q. rubra*, *R. psuedoaccacia*, and *Carya* spp.), northern hardwoods (*A. saccharum*, *Tilia spp*., *B. aleghaniensis*, *A. octandra*), xeric oak-pine (*Q. coccinea*, *Q. prinus*, *O. arboretum*, and *P. rigida*), and cove (*L. tulipifera*, *B. lenta*, *Magnolia* spp.) (Bolstad et al., 2001). Understory most commonly includes *Rhododendron* spp. and *Kalmia* spp (Bolstad et al., 2001).

CHL climate data, including temperature, soil moisture and precipitation, were used to estimate spring phenologies. Climate data were collected from stations near S2 (CS21) and S4 (CS77) (Figure 2). CS77 was located on a ridge at 1439 m with 18% slope and an aspect of N 2^{o} W. CS21 was located on a sideslope at 848 m with 21% slope and an aspect of S 2 ^{o} E (Bolstad et al., 1998). Both climate stations measured precipitation and temperature every minute and logged 15 minutes totals or averages

respectively. Daily sums of precipitation and maximum and minimum temperatures were computed. PAR was measured using a Licor LI-190SZ at S2 and S4 both above and below canopy every 1 minute and logged 1 hour averages. Negative PAR values were corrected to zero. Daily PAR was calculated by averaging the midday PAR from 1000 to 1400 hours.

Phenological observations

The phenologies of eight species were monitored on a weekly basis at both S2 and S4 throughout the spring and autumn of each year 2003-2008, except for spring 2005. Species monitored included red maple (*Acer rubrum),* blackgum (*Nyssa sylcatica),* Northern red oak *(Quercus rubra),* chestnut oak (*Q. prinus),* American witchhazel (*Hamamelis virginiana),* sorrel tree (*Oxydendrum arboretum),* serviceberry (*Amelanchier arborea),* and flame azalea *(Rhododendron calcendulaceum).* Ten branches were flagged on each tree and a visual estimation of the phenological stage was made and recorded for each branch. Spring leaf phenology was categorized on a scale of 0-5, with stage 0 representing a sealed winter bud, stage 1 representing bud burst, and stage 5 representing a fully expanded leaf. Bud stage ratio was computed by dividing the value by 5. This brought the spring phenology to a scale from zero to one. In autumn, a visual estimation was made on the percent 1) of leaves that have changed from their original color and 2) of leaf loss relative to the original coverage on each branch. Both a color change ratio and a leaf fall ratio were computed by dividing by 100 and subtracting from 1. This brought the color change and leaf fall phenology values to a scale from 0 to 1 and also allowed for a more intuitive decreasing trend in the fall. Phenological event day of year

(DOY) was averaged for each site across years, including bud burst, full leaf, color change and leaf fall initiation and completion.

Leaf Phenology Methods

We modeled bud burst, color change and leaf fall phenologies using climate variables and soil moisture. First, thermal sums including heating degree days and cooling degree days were used to estimate phenologies. Second, various temperature variables and for fall phenology, soil moisture was included. In addition, the relationship between phenology ratios and canopy PAR was examined.

Three methods were used to estimate phenological dates. The first method employed globally fixed phenological dates, $PHEN_{GF}$, selected from regional literature and constant across elevation. These literature-based dates were determined by averaging values based on published phenology from Mowbray and Oosting (1968), Day et al. (1977), Norby et al. (2003), Chason et al. (1991), and Lopez et al. (2008). $PHEN_{GF}$ phenologies were fixed annually as well as spatially resulting in a date of bud burst initiation of DOY 96, full leaf at DOY 134, color change initiation at DOY 269, and leaf off at DOY 314. The second method, $PHEN_{LF}$, used elevation dependent phenological dates based on a locally measured elevation and phenology dataset at CHL. They are defined as follows where Elev = elevation in m and phenology units are in DOY:

$$\text{Bud burst} = 0.0186 \cdot \text{Elev} + 70.006$$

$$\text{Full Leaf} = 0.0277 \cdot \text{Elev} + 107.41$$

$$\text{Color Change} = -0.0037 \cdot \text{Elev} + 276.53$$

$$\text{Full Leaf} = -0.0058 \cdot \text{Elev} + 317.44$$

The third method, $PHEN_C$, used phenological dates estimated from our best climatological driven model ($PHEN_C$).

Phenological dates were modeled using climate variables for two purposes. First, we were interested in determining which variables best predicted phenological dates, giving the lowest RMSE. In addition, models were applied to estimate phenology for application in estimating ET. Climate variables used included thermal sums, mean temperatures and soil moisture averaged over the year, summer, fall and September, number of summer days above 17 ^{o}C and number of fall days below 12 ^{o}C. We also used all possible combinations of these variables.

Thermal sums including GDD's and cooling degree days (CDD) were used as predictors for spring and fall phenologies. GDD's were calculated according to McMaster and Wilhelm (1997) where: $GDD = \left(\frac{T_{\max} + T_{\min}}{2} \right) - T_{base}$ and where T_{max} is the daily maximum air temperature, T_{min} is the daily minimum air temperature, and T_{base} is the threshold temperature below which the process of interest does not progress. GDD's were accumulated from a starting date. Also, when the mean temperature was below the base temperature, no degree days were accrued: $\left(\frac{T_{\max} + T_{\min}}{2} \right) < T_{base}$, then

$\left(\frac{T_{\max}+T_{\min}}{2}\right)=T_{base}$. CDD's were computed using: $CDD=-\left(T_{base}-\left(\frac{T_{\max}+T_{\min}}{2}\right)\right)$,

when $\left(\frac{T_{\max}+T_{\min}}{2}\right)>T_{base}$, then $\left(\frac{T_{\max}+T_{\min}}{2}\right)=T_{base}$.

Thermal sums were calculated for 10 phenological events. Spring events include leaf cessation and full leaf both defined as the date in which 25% of branches reached each event. Leaf expansion for 5 springs at each of 2 elevations, and the mean GDD was calculated for a range of start dates and temperature threshold combinations. Error was calculated when using these combinations for each year and elevation as the difference between observed and modeled phenological event. RMSE was calculated from this list of errors. The thermal sums producing the best phenology estimates were determined by RMSE values. We calculated the RMSE by first finding the difference between the observed and predicted starting dates, squaring the values, calculating the mean and taking the square root. Threshold temperatures used ranged from 0 ^{o}C to 20 ^{o}C increasing by 1 ^{o}C (Richardson et al., 2006) and starting dates included ranged from DOY 1 to DOY 105 increasing in increments of 5 days. The starting date and threshold temperature giving the smallest RMSE was assumed the best model for the phenology.

Fall phenologies were modeled based on a number of variables, but thermal sums were not included because they provided little predictive value. Simple linear regressions were developed with each climate variable and the phenological dates. These variables include mean summaries of annual soil moisture (January 1 – October 17), summer soil

moisture (June 21 – September 21), late summer soil moisture (August 1 – October 17), September soil moisture (September 1 – September 30), annual mean temperature (January 1 – October 17), summer mean temperature (June 21 – September 21), late summer mean temperature (August 1 – October 17), September mean temperature (September 1 – September 30), late summer mean minimum temperature (August 1 – October 17), late summer mean maximum temperature (August 1 – October 17), number of late summer days below 12 ^{o}C (August 1 – October 17), number of summer days above 17 ^{o}C (June 21 – September 21). All possible combinations of these variables were also used. Using each linear regression model, phenologies were predicted for each year at each elevation, and errors were calculated. From each list of errors, RMSE was calculated, and the lowest RMSE was compared to the lowest RMSE from using an average date per elevation site. The lowest RMSE was assumed the best fall phenological predictor.

PAR_C was computed by dividing daily below canopy PAR by above canopy PAR and subtracting from 1. PAR_C was then used as a predictor in estimating both spring and autumn phenological ratios. Relationships between PAR_C and bud burst, color change and leaf fall were computed using linear regressions. Models were compared by examining Pearson's correlation coefficient (ρ), and RMSE.

Leaf Area Index

Maximum LAI was estimated using two methods. The first was a fixed mean LAI, 5 m^2 m^{-2} (LAI_M), selected form the regional literature by averaging values obtained

from Wullschleger et al. (2001), Chason et al. (1991), Scarlock et al. (2001), and Hutchinson et al. (1986). The second method, LAI_T, was a terrain based approach developed by Bolstad et al. (2001). This method was based on the understanding that leaf area is correlated across the SA with elevation and to a lesser extent with terrain shape (Whittaker, 1956; Bolstad, 2001). LAI_T was calculated using a linear relationship with elevation and was applied to each grid cell across the catchments based on elevation.

Forest community composition varies spatially and can affect sap flow estimates of ET. Estimating forest composition and LAI is difficult at the resolution required, particularly in areas we never field verify. Remote sensing methods are applicable for the region, but can not estimate species-specific LAI well. Instead, remote sensing would designate stands as deciduous or coniferous, not detailed enough for our sap flow models. Additionally, broad satellite estimated LAI values saturate in areas of high LAI, common in the SAR, leading to inaccurate values. Testing satellite LAI techniques were beyond the scope of this work. Instead, we collected community composition from county level forest inventory and analysis data (FIA) downloaded from the USDA forest service website (USDA, 2007), and applied a single composition to each watershed. If a watershed covered more than one county, area-based weighted averages were used. LAI values were calculated using the terrain based method described above.

For both methods, LAI was set to zero until the date of budburst initiation and was proportionally increased until reaching maximum LAI at the date of full leaf expansion. Maximum LAI lasted from the date of full leaf to the date of color change

initiation and proportionally decreased to zero through at the date of complete leaf color change.

Watersheds ranged in size from 30.3 to 134.4 km^2 and in elevation from 329 to 2038 m (Table 1). Precipitation and discharge varied based on elevation with higher elevation watersheds receiving up to 2100 mm $year^{-1}$ of precipitation and 1350 mm $year^{-1}$ of discharge, whereas lower elevation sites received precipitation on average of 1300 mm $year^{-1}$ with discharge of 600 mm $year^{-1}$ (NCDC, 2006; USGS, 2006). Watershed characteristics for our 14 USGS watersheds, including size, gauge elevation, and gauge locations were downloaded from a USGS website (USGS, 2006). Watershed characteristics for our CHL watershed were compiled at CHL.

Meteorological measurements

Climate variables were used to compute precipitation used in the calculation of the catchment water balance and temperature used in the calculation for VPD and thermal sums. Climate variables for the SAR were downloaded from the National Climatic Data Center (NCDC) and interpolated across each watershed using kriging with external drift following Kove and Bolstad (in prep). Daily precipitation, minimum temperature and maximum temperature were obtained from the NCDC for 134 climate stations across the SAR from 1985-2005 (NCDC, 2006). NCDC used a variety of instruments to measure temperature, including glass thermometers, thermistors and thermocouples. Daily maximum temperature and minimum temperature were recorded in degrees Fahrenheit and converted to degrees Celsius. Precipitation was recorded at 15-min intervals and

summed over 24 hour periods by NCDC. Precipitation measurements were most commonly made using either tipping bucket or standard weighing gauges and were presented by NCDC in hundredths of inches and converted to millimeters (NCDC, 2009). Gauge sites range in elevation from 100 m to 1980 m and range in annual precipitation from 854 mm $year^{-1}$ to 2418 mm $year^{-1}$.

Our sap flow models required VPD and PAR as inputs. PAR was not measured consistently across the SA, and thus had to be estimated from temperature, latitude, and DOY. To estimate PAR, daily extraterrestrial solar radiation, R_e (MJ m^{-2} s^{-1}), was calculated from Bristow and Campbell (1984) using latitude and DOY. Global solar radiation, R_g (MJ m^{-2} s^{-1}) was found by calculating the transmittance, T_t, using difference between maximum and minimum temperature, ΔT, and multiplying by R_e, where:

$$T_t = 0.7 \cdot \left(1 - \exp\left(-0.004 \cdot \Delta T^{2.4}\right)\right)$$

The Bristow and Campbell (1984) transmittance model was used because it was found to be superior over the modified Hargreaves-Samani (Annandale et al., 2002) when compared to daily measured PAR data on CHL, particularly during the summer months (Kove and Bolstad, in prep). PAR was converted from R_g assuming 4.608 μmol quanta J^{-1} (Campbell and Norman, 1998) and that 50% of global solar radiation fell in the range of 400-700 nm (Landsberg and Waring, 1997; Ford et al., 2007).

In addition to PAR, vapor pressure deficit (VPD) was not measured sufficiently across our study area and was estimated using the temperature-based method of Yoder et

al. (2005). Soil evaporation was assumed to be zero due to the closed canopy and thick forest floor (Ford et al., 2007). Forest interception, $\sum I$, however is high in the SA relative to precipitation (Helvey, 1967) and was estimated using the equation derived for mature hardwoods in the CHL Basin from Helvey and Patric (1965) based on total annual precipitation, $\sum P$ and number of storms over 1.5 mm, *n*:

$$\sum I = 0.083\left(\sum P\right) + 0.036(n).$$

ET Estimation

Our general approach was to estimate ET while using a variety of phenological and LAI estimates. Sap flow models were used to predict annual ET across 15 watersheds using three different phenological scenarios and two maximum LAI scenarios from 1985-2005. Annual ET estimates were compared across phenology and LAI estimates to determine the impacts of each method relative to the catchment water balance method of estimating annual ET, here considered actual ET (Ford et al., 2007).

We estimated ET on 15 watersheds following the methods of Kove and Bolstad (in prep) using three estimates of phenology dates and two estimates of maximum LAI. Annual ET was calculated from scaled sap flow equations (ET_{SAP}) developed by Ford (In prep). ET_{SAP} was found by multiplying transpiration by our species-specific LAI totals, calculated using the two methods described earlier. Daily values were summed across the watershed and across the year to compute annual catchment ET_{SAP}. Ford measured sap flow on eight species (*A. rubrum, B. lenta, Tsuga Canadensis, P. strobus, Q. prinus,*

Q. rubra, L. tulipifera and Carya spp.) within CHL. Transpiration was estimated at 15 second intervals and averaged every 30 minutes (Granier, 1985). Daily totals were then used to find species-specific transpiration equations based on VPD, PAR and DOY. Detailed methods are described in Ford et al. (2007).

Annual ET error was computed as the difference between each ET estimate and the catchment water balance ET estimates (ET_{CWB}) defined as: $ET_{CWB}=P- R_o$, where P = annual precipitation and R_o = annual runoff. Mean error was calculated as the average error for each simulation across each watershed and year. RMSE and standard deviation were also computed for each simulation. Simulations were compared using mean error, RMSE, maximum error, minimum error, and standard deviation of error. Models were also compared to the ET estimate that used $PHEN_C$ and LAI_T, ET_{C_T}, because of the assumption that these estimates are the most ecologically accurate, showing the relative impact of LAI and phenological estimates on the estimates of ET developed in Chapter 2. In addition, model results were averaged by watershed and by year to determine if annual or watershed characteristics were related to model estimates of ET and the error associated.

Catchment water balance estimates required annual precipitation and runoff for each watershed. Annual precipitation for each catchment was calculated using the average daily total precipitation from our interpolated surface, summed annually. Daily averaged instantaneous runoff was downloaded from the USGS and CHL and were

summed annually and divided by watershed size to find total annual runoff per unit area (R_o).

Results and Discussion

Phenology

Average bud burst occurred on DOY 91 and full leaf occurred on DOY 139, averaged across sites and years. For S2, average date of bud burst was on DOY 86 and full leaf was on DOY 131 (Table 2). For S4, average date of bud burst was on DOY 97 and full leaf was on DOY 147. The earliest date of bud burst on S2 was DOY 75 and the latest was 17 days later. The earliest date of full leaf on S2 was DOY 124 and the latest was 14 days later. For S4, the earliest bud burst was DOY 91 and the latest was 12 days later, and the earliest full leaf was DOY 141 with the latest following 13 days later. The average interval between initiation and cessation of leaf expansion was 48 days, with 45 days for S2 and 50 days for S4. The longest interval was 63 and the shortest was 34 days, both at S2.

Mean initiation of color change was DOY 272 and mean initiation of leaf fall was DOY 287. Mean cessation of color change was DOY 305 and mean cessation of leaf fall was DOY 311. For S2 and S4, the mean initiation of color change was DOY 273 and DOY 271, respectively (Table 2). The mean cessation of color change was DOY 303 for both S2 and S4. For leaf fall at S2 and S4, the mean initiation was DOY 293 and DOY 276, respectively, and the mean cessation was DOY 313 and DOY 309, respectively. The earliest and latest initiation of color change occurred on S4 at DOY 259 and DOY

282 respectively. The earliest and latest cessation of color change occurred on S4 and was DOY 299 and DOY 313, respectively. The earliest initiation of leaf fall occurred at S4 on DOY 273 and the latest occurred at S2 on DOY 297. The earliest completion of leaf fall occurred at S4 on DOY 303 and the latest occurred at S2 on DOY 316. The average interval between color change initiation and leaf fall cessation was 38 days, 39 days for S2 and 37 days for S4. The longest interval was 47 days, and the shortest was 28 days, both at S2.

Growing season length, from initiation of bud burst to the cessation of leaf fall, averaged 217 days, with 225 days for S2 and 210 days for S4. The shortest growing season length was 200 days on S4 and the longest was 240 days on S2. Standard deviation, variation in growing season length between years, was approximately 10 days for both sites. The difference between growing season lengths at S2 and S4 averaged 15 days with a standard deviation of 5 days.

Dates of bud burst, full leaf, and leaf fall varied significantly more among years than dates of color change between elevations. At the low elevation site, bud burst initiation occurred on average 11 days sooner than the high elevation site, and full leaf occurred on average 16 days sooner than the high elevation site. Color change initiation on the low elevation site occurred 2 days sooner on average compared to the high elevation site, and mean DOY for color change cessation did not differ by elevation. Leaf fall initiation occurred 17 days sooner at the low elevation site and leaf fall cessation occurred 4 days sooner at the low elevation site.

Bud burst proportion increased linearly with DOY for both the high and the low elevation site during the active period, with correlation coefficients of 0.86 and 0.89 respectively (Figure 3). Bud burst varied by species where red maple was the earliest species to flush and Northern red oak the latest (Figure 4). Mean DOY for the initiation and cessation of color change were strongly related to mean DOY for the initiation and cessation of leaf fall with a correlation coefficient of 0.90. The cessation of fall phenologies, color change and leaf fall, were more correlated with each other than the initiation of fall phenologies (Figure 5).

Spring and fall phenological dates measured at CHL are consistent with observations from other regional studies. Mowbray and Oosting (1968) studied phenological events in the Thompson Gorge in the Blueridge Mountains (near 800 m) and found an average leaf expanding date of DOY 113, similar to our date of DOY 108 for the low elevation site. Day et al. (1977) studied CHL phenology and documented mean bud burst at DOY 95.5, mean leaf color change at DOY 283 and mean leaf fall at DOY 309. Our phenological dates were similar for bud burst (DOY 97) and leaf fall (DOY 309), but not for color change (DOY 271), with our results 12 days sooner, potentially a result of species differences. Lopez et al. (2008) documented a 24 day differences in bud burst dates between species, and Raulier and Bernier (2000) documented a 41 day range for full leaf dates between species. Alternatively, site conditions may also have influenced our results, Lopez et al. (2008) found bud burst dates varied by up to 18 days when comparing xeric and mesic sites of the same species.

A study by Norby et al. (2003) examined phenological dates at Oak Ridge near 230 m and found 50% leaf out at DOY 134 and 50% leaf fall at DOY 279. Our 50% leaf out (DOY 109) was significantly earlier and 50% leaf fall (DOY 294) was significantly later than Norby et al. (2003). Earlier spring and later fall phenologies are indicative of lower elevation site, however our site was 600 m higher. Other possible explanations could include species differences, or climate differences between our study years.

Chason et al., (1991) also studied phenological dates at Oak Ridge and found leaf fall started near DOY 265 and ended around DOY 334. Though a lower elevation site should have both a later leaf fall start and finish, our mean leaf fall finish occurred 25 days sooner than Chason et al. (1991). Other possible explanations include differences in species, climate due to elevation or adjacency to mountains.

The relationship between elevation and phenological dates has been documented extensively. Hopkin's Law states that there is a 3.3 day delay for every 100 m increase in elevation for spring onset (Fitzjarrald et al., 2001). Though our results were lower than Hopkin's Law, particularly for bud burst, they were more similar to recent literature. Vitasse et al. (2009) found that leaf unfolding dates decreased with increasing elevation at a rate of 1.1 to 3.4 days for every 100 m increase in elevation, and varied by species. Our results show a delay of 1.8 days 100 m^{-1} for bud burst and 2.7 days 100 m^{-1} for full leaf, within the range found by Vitasse et al., (2009). Similar studies found results between 2-3 days 100 m^{-1} including Richardson et al. (2006) with 2.7 days 100 m^{-1} for

spring onset, Rotzer and Chmielewski (2001) found a 2.8 day advance with 100 m increase for downy birch, and Dittman and Elling (2006) found a ratio of 2 days 100 m^{-1} for beech., all confirming our results.

Phenology Models

Overall, $PHEN_{LF}$ provided the most accurate phenology for leaf expansion, when tested at CHL, followed by $PHEN_C$ and $PHEN_{GF}$. $PHEN_{LF}$ was better at estimating bud burst compared to $PHEN_{GF}$, and $PHEN_C$, but for full leaf it was only better than $PHEN_{GF}$. For fall phenologies at CHL, $PHEN_{LF}$ was better at predicting both color change and leaf off compared to $PHEN_{GF}$.

Our optimally calculated GDD models, $PHEN_C$, performed well at estimating CHL spring phenology dates, the initiation of bud burst and cessation of full leaf. The optimal GDD for the initiation of bud burst used a start date of DOY 65 and a threshold temperature of 2 ^oC and resulted in an RMSE of 3 days. The optimal GDD for full leaf cessation used 5 ^oC for the threshold temperature and a start date of DOY 95 resulting in an RMSE of 5.34 days. For the fall, mean soil moisture in September best modeled color change with an RMSE of 5.34 days and leaf fall was best modeled by the number of summer days above 17 ^oC, with an RMSE of 5.24 days (Table 3). However, they were not practically different than the RMSE from using the average DOY as a predictor of color change and leaf fall fitted to elevation, with an RMSE of 5.6 days.

Across our test watersheds, $PHEN_C$ estimated dates of spring phenology averaged DOY 100 for bud burst and DOY 149 for full leaf. Mean watershed bud burst and full leaf DOY primarily vary by elevation, with lower elevation watersheds having earlier estimates of bud burst and full leaf DOYs than higher elevation watersheds. Mean watershed bud burst DOY ranged by 17 days from DOY 92 to DOY 109. Mean watershed full leaf DOY ranged from 138 to 159, a difference of 21 days.

$PHEN_C$ estimated dates were significantly later than $PHEN_{LF}$ estimated dates when averaged by watershed. Both methods varied primarily by elevation, with higher elevation watersheds starting later in the spring. Locally fixed spring phenologies, $PHEN_{LF}$, were significantly sooner than $PHEN_C$ (t-test, $P<0.05$). Minimum and maximum mean bud burst DOY occurred at the same watersheds for $PHEN_{LF}$ and $PHEN_C$. Averaged across watersheds, bud burst $PHEN_{LF}$ was DOY 89, 11 days sooner than $PHEN_C$, and ranged from 80 to 97. Full leaf $PHEN_{LF}$ averaged DOY 136, 13 days sooner than $PHEN_C$. Since $PHEN_{GF}$ did not vary by watershed, comparisons were made using overall averages. Bud burst $PHEN_{GF}$ happened between $PHEN_C$ and $PHEN_{LF}$, but full leaf $PHEN_{GF}$ was sooner than both other methods.

Fall phenologies were estimated using two methods, $PHEN_{LF}$ and $PHEN_{GF}$. $PHEN_{LF}$ was very similar to $PHEN_{GF}$, where averages across our study watersheds for color change were DOY 273 and 268 respectively and averages for leaf fall were DOY 311 and 314 respectively. Color change and leaf fall $PHEN_{LF}$ estimated dates varied little across watersheds ranging by only 3 days for color change and 5 days for leaf fall

between the high and low elevation watersheds. Higher elevation watersheds reached color change and leaf fall sooner than low elevation watersheds.

Growing season length was on average 10 days shorter for $PHEN_C$ estimated dates and 4 days shorter for $PHEN_{GF}$ estimated dates compared to $PHEN_{LF}$ estimated dates. Watersheds with the lowest mean elevation had the longest growing seasons and those with the highest elevation had the shortest growing seasons. Annual variation existed for $PHEN_C$ estimated bud burst and full leaf with some years reaching budburst 16 days sooner than other years and some years reaching full leaf 13 days sooner. Mean annual temperature was not strongly correlated with annually averaged bud burst DOY but was with full leaf DOY (ρ=0.79).

Predicting phenological dates using climate variables is well documented in the literature, particularly for spring phenology, though the best methods are still site specific. Our results confirm that GDD predicted phenological events better than any other climate variables tested (Hunter and Lechowicz, 1992). The optimal threshold temperatures were close to those found in the literature. Threshold temperatures ranged from 0 ^{o}C in Nizinski and Saugier (1988) to 10 ^{o}C in Raulier and Bernier (2000), though most were closer to 5 ^{o}C, which was our threshold for full leaf (Valentine, 1983; Lechowicz, 1984; Hunter and Lechowicz, 1992). The optimal bud burst threshold for our study was 2 ^{o}C, similar to Thomson and Moncrieff (1982).

Predicted starting date depended strongly on the GDD accumulation start date. This is in contrast to other studies. Optimal starting dates were much more varied, from January 1st through 10 days before the reported bud burst DOY (Nizinski and Saugier, 1988; von Wuehlisch et al., 1995). Our best starting date for bud burst was DOY 65, nearly 25 days before mean measured bud burst for our low elevation site. The best starting date for full leaf was DOY 95, nearly 40 days prior to mean full leaf DOY. Though some studies found little variation in RMSE when changing starting date (Thomson and Moncrieff, 1982), our study showed differences in RMSE of up to 10 days depending on the starting date. Using our best model, 2 ^{o}C and DOY 65 for the calculation of GDD to predict bud burst, we found an RMSE of 3.0 days. For predicting full leaf, using 5 ^{o}C and DOY 95, we found an RMSE of 5.3 days. Lechowicz (1984) used GDD to predict bud burst with an RMSE between 2 and 5 days, similar to our findings. Raulier and Bernier (2000), however, were able to predict full leaf with a mean error of 1.5 days and Thomson and Moncrieff (1982) were able to predict flush date with an RMSE of 1.0 and bud burst with an error of 1.82, much lower than our predicted error. One possible reason for the discrepancy in predictive ability is the species distributions, our study includes eight species, where Thomson and Moncrieff included only one species. According to Raulier and Bernier (2000), another possible explanation is the difference in stand age, since phenology may be age dependent.

We found fall phenologies to be much more difficult to predict using climate variables than spring phenologies, similar to previous work by Menzel (2002). Our study

found the best climate predictors of fall phenologies were mean day adjusted for elevation (ρ=0.80; Figure 7).

One possibility for the difficulty in developing models that have good predictive ability for fall phenologies is the small variation in observed fall dates relative to spring phenology (White et al., 1997; White and Nemani, 2003). Richardson et al. (2006) found that spring phenologies varied by more than 20 days on average, but fall varied by no more than 10 days making it difficult to model. Additionally, fall phenologies may not be controlled as strongly by interannual variation in climate, though many studies do not clarify what does control them (Schaber and Badeck, 2003). Some studies have found genetic difference in fall phenologies, and others have shown strong relationships with photoperiod, though these results are rarely duplicated (Keskitalo et al., 2005). The more recent literature has found a potential link between fall phenology dates and the accumulation of carbohydrates. Fracheboud et al. (2009) considered that though fall phenology rate is controlled by photoperiod, the initiation of senescence is started once a tree reaches a carbohydrate total, indicating potential indirect relationships with climate.

PAR_C and Phenologies

PAR_C (i.e. the fraction of light hitting the forest floor) was strongly correlated with bud burst, color change and leaf fall (Figure 6). Models fit better for the lower elevation site than the higher elevation site, and elevation improved the estimation for color change and leaf fall. Bud burst had a strong relationship with PAR_C at S2 (ρ=0.89) and a moderately strong relationship at S4 (ρ=0.77; Figure 7). When the data from both

sites were combined, PAR_C and bud burst had a strong relationship with ρ=0.84 (Figure 8). When the data from both sites were combined, adding elevation as a predictor did not improve the correlation.

PAR_C was highly correlated with color change. There was a moderately strong relationship between PAR_C and color change at S4, with ρ=0.80, and a slightly weaker relationship at S2, with ρ=0.74. When sites were combined, the relationship weakened to ρ=0.65, showing the two sites developed different relationships between color change and PAR_C. This relationship was steeper at S4 than at S2, and therefore elevation did improve the model.

PAR_C was highly correlated with leaf fall. There was a strong relationship at S2, with ρ=0.91, and a moderately strong relationship at S4, with ρ=0.75. When the data from both sites were combined, the resulting model was moderately strong with ρ=0.73, signifying the relationship between PAR_C and leaf fall varies by elevation.

Though we could not find any literature that attempted to model phenological dates using PAR_C, we did find studies that used PAR_C to estimate LAI, via the Beer-Lambert Law (Larcher, 1983; Vose et al., 1995; Breda, 2003). Total LAI is related to phenological ratios. LAI increases from the date of leaf unfolding through the date of full leaf. In the fall LAI begins to decrease at leaf fall initiation and reaches full senescence at 100% leaf fall. Vose et al. (1995) applied the Beer- Lampert Law with poor results. Three of the five stands at CHL found 10% LAI error, but two of the five stands ranged

from -35% to 85% error. Jonckheere et al. (2004) found results within 5% of measured LAI results. Our models have an RMSE of 16%, well within the range found by Vose et al. (1995).

Additionally, Beer-Lampert studies can also be examined for potential problems with the use of PAR_C. Breda (2003) compared direct and indirect methods for estimating LAI, particularly Beer-Lambert, and found it underestimated LAI (25%- 50%) primarily due to the non-random distribution of leaves within the canopy, the clumping effect. If the below canopy PAR sensor is below a clump of leaves, the results will be different than if the sensor was below a gap, a potential impact on our models that should be considered.

LAI

LAI calculated from our terrain-based method (LAI_T) averaged 5.6 m^2 m^{-2} over the study watersheds. Maximum LAI_T averaged 7.1 m^2 m^{-2} and minimum LAI_T averaged 3.2 m^2 m^{-2}. Watersheds with the larger mean elevation had smaller mean LAI. In addition, watersheds with a larger range in elevation had a larger range in LAI values. Maximum LAI by watershed ranged from 5.9 m^2 m^{-2} to 8.8 m^2 m^{-2}, and minimums ranged from 1.4 m^2 m^{-2} to 7.3 m^2 m^{-2}.

LAI_T estimates of LAI were similar to ground based measurements of LAI reported from regional studies in the SA. Though we did not measure LAI on any watersheds for this study, measured LAI on WS15 was 5 m^2 m^{-2} (Day et al., 1977). Our

LAI_T estimates for WS15 averaged 6.6 m^2 m^{-2}, slightly higher than measured by Day et al. (1977). WS15 is a good watershed for analysis because it has gone without human disturbance for over 50 years, and has a species composition that is similar to our observed set. Additionally, LAI on WS15 was measured after canopy closure, when leaf area amounts were stabilized. A different study at CHL from Bolstad et al. (2001), measured LAI for the entire basin and found mean LAI=5.8 m^2 m^{-2}, with a range from 2.7 to 8.2 m^2 m^{-2}. LAI_T for WS15 fell within this range at 6.6 m^2 m^{-2}.

Even in similar forest types, LAI can vary substantially. Additional studies in the SA measured LAI for hardwood sites and showed significant variance. At Oak Ridge in eastern Tennessee, Wullschleger et al. (2001) measured 6.2 m^2 m^{-2}, similar to mean LAI_T, 5.63 m^2 m^{-2}. Three additional studies at Oak ridge found lower LAI than Wullschleger though they were measured in different stands. Chason et al. (1991) measured 4.89 m^2 m^{-2}, Hutchinson et al. (1986) measured 4.9 m^2 m^{-2}, and Scurlock et al. (2001) measured 5 m^2 m^{-2}. Variance in LAI measurements in similar forest stands may be a result of high variation in leaf distribution not accounted for by certain measurement techniques (Chason et al., 1991; Breda, 2003). Additionally, species composition is variable and may be responsible for the discrepancies (Breda, 2003).

ET Estimation

The error associated with estimating ET_{CWB} averaged across all methods, was 144 mm yr^{-1}, with an average RMSE of 220 mm yr^{-1} with significant differences among methods. Mean error was 15% of ET_{CWB}, and within the range of errors reported for

small-catchment studies of scaled sap flow ET (Wilson et al., 2001; Ford et al., 2007). Errors in estimating ET_{CWB} were smaller when using $PHEN_{LF}$ compared to ET estimates using $PHEN_C$ or $PHEN_{GF}$ (Table 4) showing us that given our ET model, the best estimates of ET_{CWB} result from using locally derived relationships predicting phenology with elevation.

Error results showed that the LAI method has a greater impact on ET estimation than the phenology method. Mean ET estimates varied on average by 2% among our three phenological methods, while ET estimates varied by more than 10% between the two LAI methods. For example, $PHEN_{LF}$ and $PHEN_{GF}$ ET was 1.2% and 3.2% greater than ET_{C_T}, respectively (Table 4). Estimated ET errors were much larger when using average reported leaf area estimates (LAI_M) for all three phenology estimation models tested. The three ET estimates using LAI_M, along with $PHEN_{LF}$, $PHEN_{GF}$, and $PHEN_C$ underestimated ET_{C_T} by -9.4%, -10.1% and -11.5% respectively. LAI_T models had lower mean error, percent error and RMSE compared to LAI_M models (Table 4). LAI_T model errors were smaller than LAI_M model errors with differences of up to 80 mm $year^{-1}$ in mean error and 39 mm $year^{-1}$ in RMSE. LAI_M percent error was correlated with mean annual runoff (ρ=0.63 to ρ=0.65) more than LAI_T percent error (ρ=0.48 to ρ=0.52). These results suggest that while it is important to get the phenology correct, it is more important to estimate LAI accurately.

Results differed by watershed, where some catchments performed poorly across all methods, including WS6-WS9, and WS13, while others performed particularly well

(Table 5). We were not able to identify the reason why some watersheds performed poorly across all methods, examining elevation, area, climate station network density, input estimates, and species composition as potential explanations.

Estimated ET varied significantly by watershed and year, with over three times higher mean error and RMSE in some years than in others (Figure 9). No explanations were found including relationships with climate variables to explain these high RMSE years. Error from estimating ET_{CWB} also varied significantly by watershed with mean percent error ranging from -7.8% to 22% for our six ET estimation methods (Table 5). Mean watershed errors were correlated with percent yield, with larger errors found on watersheds with lower percent yield (ρ=0.48). LAI_M ET errors from estimating ET_{CWB}, mean error, percent error, and RMSE, were also correlated with mean watershed runoff. LAI_M model mean ET error and percent ET error were also correlated with mean watershed percent yield (ρ=0.70).

Estimating ET using sap flow models requires estimates of LAI and phenological dates. Understanding the implications of these estimates on ET is essential to the development of accurate ET models and determining true ET error. Our study found that LAI estimates had a significant impact on ET, leading to differences of 78 mm $year^{-1}$ (11.5%). Phenological date estimates on the other hand led to differences of 20 mm $year^{-1}$ (3.1%), less than LAI impacts.

Natural variation in LAI and phenology are important to consider when examining the impact that each variable has on ET estimates and should be included in the discussion. The natural variation in LAI or phenology could be responsible for a greater proportion of change in the ET estimates compared to model variation. Since we did not measure LAI, we have to look to the literature for measurements of variation. Few articles have attempted to quantify the natural variation in LAI. Gower and Norman (1991) found coefficients of variation ranging between 0.6% and 1.7% whereas Chen (1996) found a much larger range of 4% to 8%. A range from 0.6% to 8%, results in a 0.6% to 8% change in ET estimates since LAI is a multiplicative factor in our ET equations. That corresponds to a maximum potential change in ET of 52 mm $year^{-1}$ on average.

Natural variation in phenological dates was documented in our data collected at CHL. The coefficient of variation for DOY of Budburst was 6% and 3% for both fall color change and leaf off, a 9% variation in the growing season length. A 9% change in the growing season length results in a maximum potential change in ET of 48 mm $year^{-1}$ on average, smaller to the change from the natural variation in LAI. Since natural variation in LAI and phenology result in a similar change to ET, we can still say that LAI has a greater impact on ET estimates than phenological dates.

Multiple studies have shown the significance of LAI on estimates of ET. Granier et al. (2000) found that LAI had a more significant impact of ET than species composition. Granier and Breda (1996) found LAI to be a main predictor in sap flow

derived ET estimates. Hogg and Hurdle (1997) found LAI was the main control in sap flow derived transpiration estimates. However, Ewers et al. (2002) found LAI was not a significant predictor of the variation in transpiration.

LAI_T estimated ET_{CWB} better than LAI_M. When comparing differences in LAI_T and LAI_M estimated ET, we expected LAI_T ET to be closer to ET_{CWB} than LAI_M ET, because LAI_T incorporates phenological variation leading to a more accurate ET variation. Both methods, however, varied similarly, but ET estimated using LAI_M was slightly smaller in all estimates than ET estimated using LAI_T. Sap flow models generally underestimate ET_{CWB} (Wilson et al., 2001; Wullschleger et al., 2001; Ford et al., 2007). Therefore, an increase in estimates may result in improved ET, regardless of whether the estimate is ecologically significant. ET estimates using LAI_T did not improve upon the estimation of ET beyond having larger values, variation in ET was not better modeled when using LAI_T. Ford et al. (2007) examined impacts of omitting LAI variation on sap flow derived ET and found there was a 6% impact on ET, however it is unknown if this was instead caused by a decrease in the mean LAI value. Alternatively, this study was for an even aged white pine watershed, so stand variation from species composition and structure could have increased the impact.

Phenological dates impacted ET estimates, although differences between methods were small. ET estimates of ET_{CWB} using both $PHEN_{LF}$ and $PHEN_{GF}$ resulted in smaller ET error than ET estimates using $PHEN_C$ even though $PHEN_C$ ET estimates were expected to be superior. On possible explanation is that $PHEN_{LF}$ and $PHEN_{GF}$ have

longer growing seasons than those calculated using $PHEN_C$. Longer growing seasons resulted in higher ET, and hence, improved the correspondence between sap flow ET and actual ET.

Conclusion

In all, we found the best method to estimate spring phenologies in the SA is thermal sums. Many studies use starting dates and threshold temperatures near DOY 1 and 0 ^oC respectively, however our results show that later starting dates and higher degree days than typically employed worked better for our data than values typically applied in the SA. For bud burst dates, we found the optimal degree day inputs were a threshold temperature of 2 ^oC and DOY 65. For Full leaf the optimal inputs were a threshold temperature of 5 ^oC and DOY 95. Fall phenology observations varied little between years and between the two observed elevations making it difficult to find relationships with climate variables.

We were able to use canopy PAR to estimate phenological ratios for spring initiation better than fall cessation. For both the high and low elevation sites, the strongest relationship on average was between canopy PAR and bud burst ratio with an average ρ of 0.84, though the relationship with leaf off was nearly similar with an average ρ of 0.83. The weakest was between canopy PAR and color change with an average ρ of 0.77. Canopy PAR can be used to model leaf phenology, though further studies are needed to examine potential impacts from species composition and spatial location.

Finally, we found the best phenological model is not as important as the best LAI model when estimating sap flow derived ET. LAI models contributed to a potential 11.5% change in ET estimate whereas phenological models contributed to a potential 3.1% change in ET. Though phenological models were not as significant in the ET process as LAI models, a 3.1% change is still large enough to be a consideration in the modeling process given that many published errors from sap flow derived ET are near 10%.

Further research is needed to examine the potential for elevation based phenological models, which would require gathering additional data at more elevations. Also, the possibility of species and site specific phenological models to be developed in concert with estimating LAI should be examined. Two critical variables for ecology and hydrology, strongly connected could be predicted simultaneously.

Watershed ID	County(s)	Area (sq km)	Average Temp (°C)	Mean Elevation (m)	Elevation Range (m)	Rainfall (mm/yr)	Runoff (mm/year)	Proportion Yield
1	Caldwell and Watauga	74.59	12.67	658	(368, 1183)	1332	596	43%
2	Clay and Macon	134.42	10.28	1212	(932, 1667)	2115	1347	63%
3	Burke	66.56	13.55	550	(343, 880)	1365	627	44%
4	Transylvania	104.64	11.52	975	(628, 1820)	1702	1068	61%
5	Buncombe	37.81	9.79	1287	(805, 1950)	1689	1010	59%
6	Buncombe	14.14	10.01	1243	(837, 1724)	1573	695	43%
7	Haywood	71.48	8.95	1458	(902, 1942)	1988	1249	62%
8	Haywood	86.76	9.25	1406	(864, 1942)	2010	1266	62%
9	Haywood	127.43	9.90	1213	(751, 1848)	1713	793	46%
10	Yancey	112.15	10.14	1192	(812, 2028)	1626	1099	66%
11	Macon	48.59	10.67	1190	(985, 1499)	2165	1486	68%
12	Transylvania	30.30	11.68	948	(687, 1230)	1781	1039	57%
13	Transylvania and Henderson	69.41	12.41	880	(767, 1151)	1637	1171	70%
14	Wilkes and Watauga	124.58	12.66	632	(329, 1248)	1299	673	50%
15	Macon	0.05	13.17	860	(726, 993)	2007	1001	49%

Table 1: Watershed characteristics for 15 watersheds (WS1-WS15) located in the southern Appalachians.

	Initiation			Cessation		
	Bud Burst	Color Change	Leaf Off	Full Leaf	Color Change	Leaf Off
Low Elevation Average DOY	86	273	293	131	303	313
High Elevation Average DOY	97	271	276	147	303	309

Table 2: Mean day of year (DOY) for phenological events at a low and high elevation site at the Coweeta Hydrological Laboratory (CHL). Average bud burst, color change, and leaf off initiation DOYs, and average full leaf, color change, and leaf off cessation DOYs were collected from 2003-2009.

	Annual soil moisture	Summer soil moisture	Late summer soil moisture	Sept. soil moisture	Average annual temp	Avg summer temp	Avg late summer temp	Avg Sept. temp	Avg min temp fall	Avg max temp late summer	Days below 12°C late summer	Days above 17°C summer
	Jan 1 - Oct 17	June 21 - Sept 21	August 1 - Oct 17	Sept 1 - Sept 30	Jan 1 - Oct 17	June 21 - Sept 21	August 1 - Oct 17	Sept 1 - Sept 30	August 1 - Oct 17	August 1 - Oct 17	August 1 - Oct 17	June 21 - Sept 21
Color Change Initiation	5.9	5.89	5.44	5.34	5.92	5.93	5.84	5.61	5.4	5.92	5.39	5.79
Leaf Off Initiation	8.24	8.48	5.97	7.99	5.63	7.21	6.33	5.49	6.81	5.8	6.28	5.24

Table 3: Root mean squared error (RMSE) of fall phenology climate predictors, units in days. Predicting fall color change and leaf off initiation at CHL. Predictors and date ranges were selected based on potential for predictive ability.

Simulation Name	Mean Error	Percent Error	RMSE	Difference from ET_{C_T}	Percent Difference from ET_{C_T}
ET_{C_T}	-112.5	-10.7%	204.1		
ET_{C_M}	-190.5	-22.0%	244.6	-78.0	-11.5%
ET_{LF_T}	-92.7	-7.8%	199.1	19.8	3.1%
ET_{LF_M}	-177.3	-20.1%	234.0	-64.8	-9.4%
ET_{GF_T}	-106.5	-9.9%	197.4	6.0	1.2%
ET_{GF_M}	-183.0	-20.9%	238.2	-70.5	-10.1%

Table 4: Error statistics from six ET estimation methods. Error statistics include mean error, percent error, RMSE (in relation to ET_{CWB}) and the mean percent difference between each ET simulation and ET_{C_T}. Three phenology estimates were used (GF = globally fixed, Locally fixed = LF, and Climate driven = C) along with two LAI estimates (Mean = M and Terrain-based = T). Data was computed for 15 watersheds (WS1-WS15) from 1986-2005.

Error (ET estimate -ET_{CWB})

WSID	ET_{C_T}	ET_{C_M}	ET_{LF_T}	ET_{LF_M}	ET_{GF_T}	ET_{GF_M}
1	-65.0	-251.2	-34.1	-222.8	-79.9	-248.9
2	-108.6	-150.4	-104.6	-136.8	-100.6	-132.4
3	-32.8	-246.1	-5.1	-220.4	-60.3	-250.5
4	34.9	-74.8	50.1	-53.1	36.0	-61.7
5	-108.5	-137.0	-118.7	-136.2	-113.3	-128.0
6	-316.7	-353.7	-328.3	-353.7	-323.2	-347.3
7	-194.5	-182.3	-200.6	-180.4	-190.0	-165.7
8	-178.7	-178.3	-185.8	-176.9	-177.2	-164.5
9	-347.1	-389.4	-337.4	-371.4	-335.8	-367.7
10	-40.0	-76.6	-28.9	-60.3	-29.8	-58.3
11	3.5	-43.8	-14.6	-49.2	-9.9	-44.9
12	-22.9	-146.6	-40.8	-147.7	-55.3	-157.7
13	250.8	106.6	228.6	103.2	207.6	89.0
14	56.3	-141.5	90.3	-111.3	40.3	-139.2
15	-78.0	-218.4	-51.9	-201.3	-79.9	-219.5
Average	-76.5	-165.6	-72.1	-154.6	-84.8	-159.8

Table 5: Average watershed ET error from six ET estimation methods using three phenology estimates (GF = globally fixed, Locally fixed = LF, and Climate driven = C) and two LAI estimates (Mean = M and Terrain-based = T). Calculated for 15 watersheds (WS1-WS15) from 1986-2005.

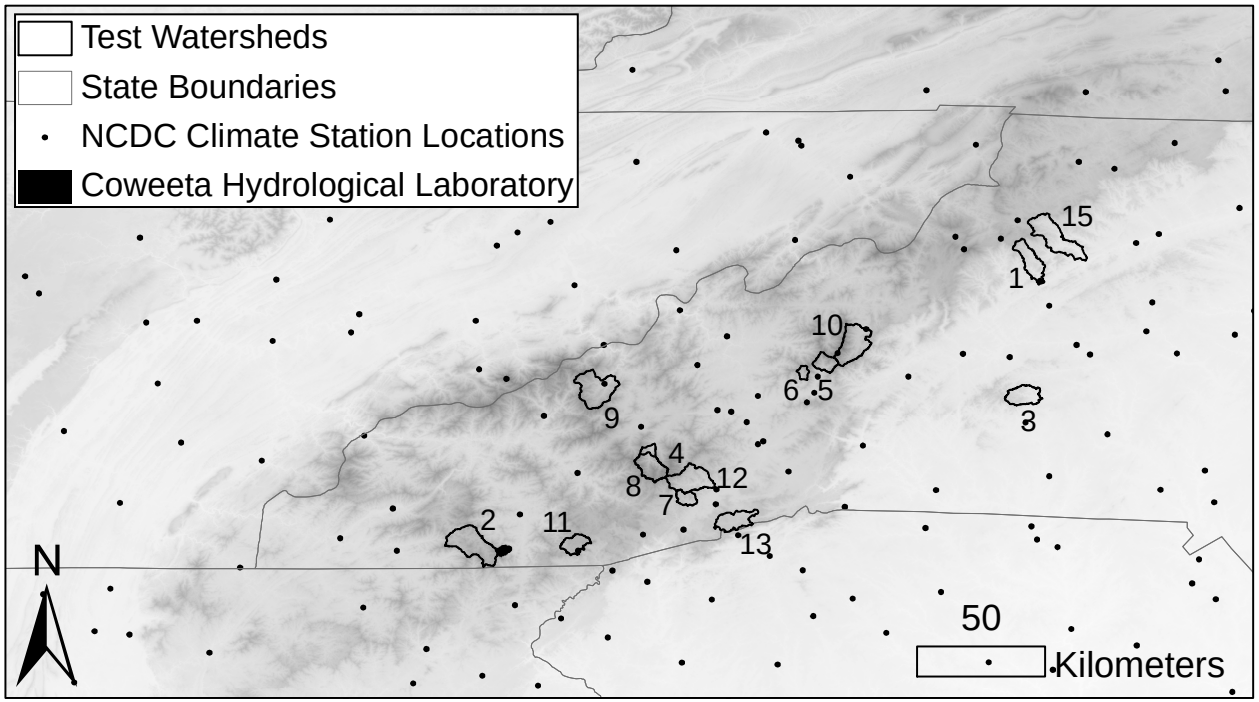

Figure 1: Study area, the southern Appalachian region (SAR). Fifteen test watershed boundaries, and 134 climate station locations.

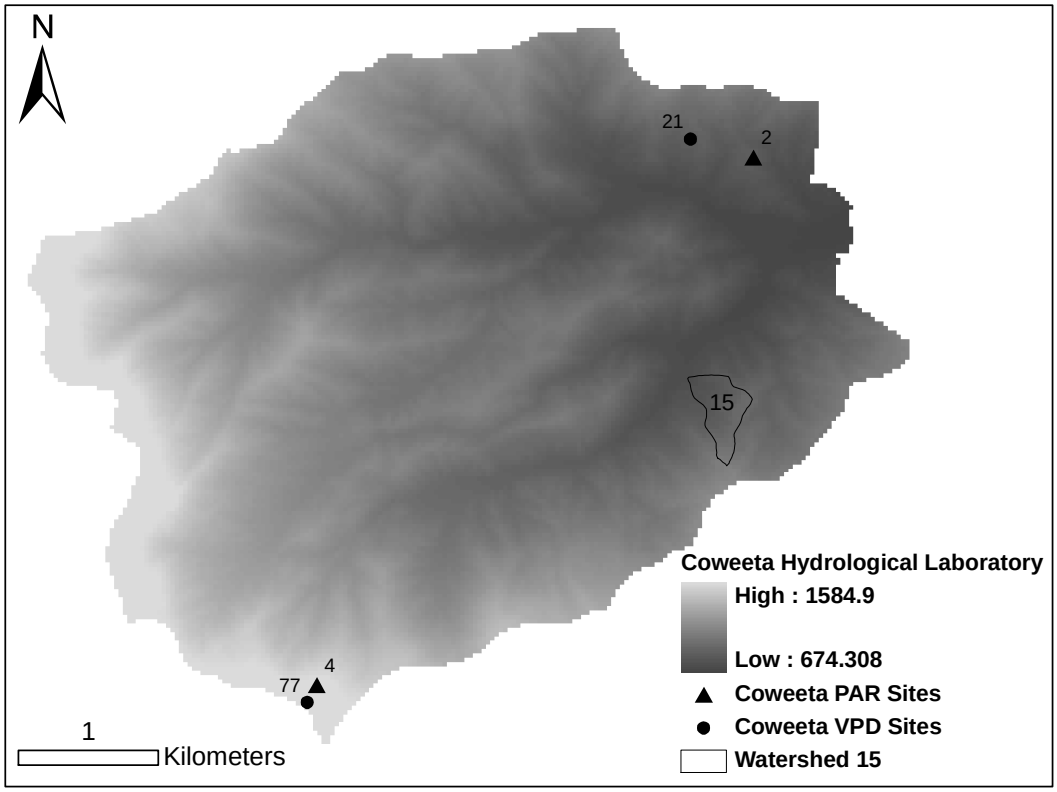

Figure 2: Coweeta Hydrological Laboratory digital elevation model with WS15, VPD climate station locations CS21 and CS77, and PAR locations S2 and S4.

.

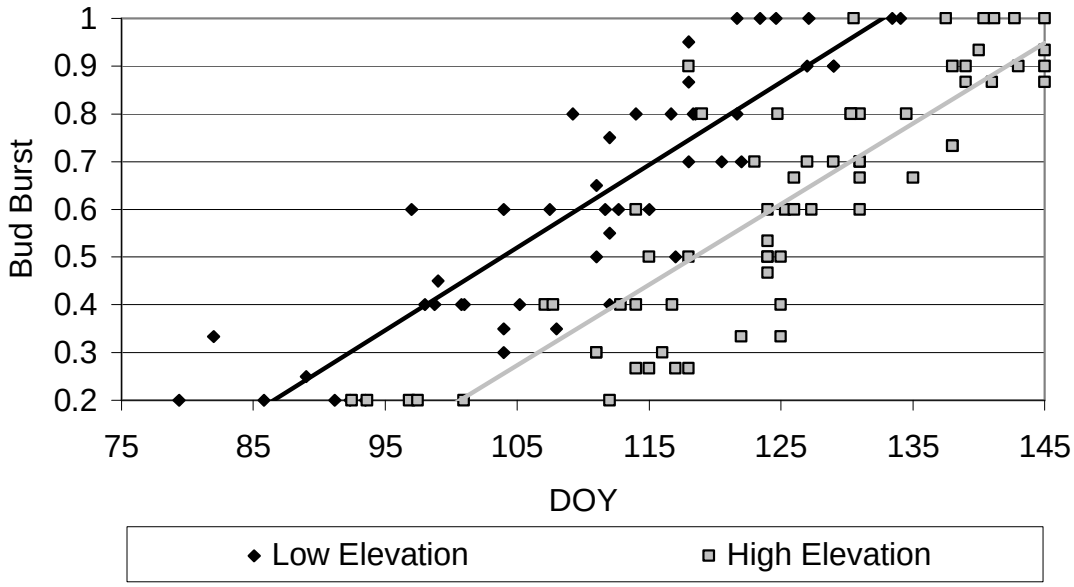

Figure 3: Spring bud burst versus DOY for high and low elevation sites at CHL. Bud burst is the proportion of the bud stage completed. Data collected from 2003-2008, minus 2005. Linear regression results:

High Elevation: BB = 0.0169 * DOY – 1.5, $R^2 = 0.74$

Low Elevation: BB = 0.0173 * DOY – 1.3, $R^2 = 0.79$

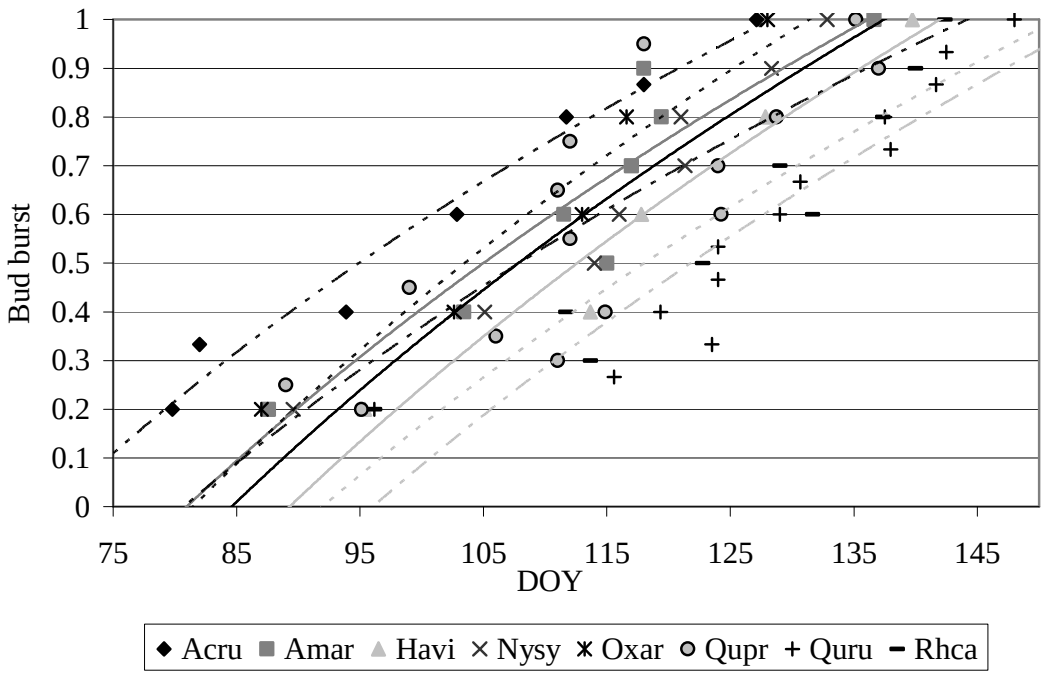

Figure 4: Bud burst versus DOY by species. Data collected from 2003-2008. Bud burst is the proportion of the bud stage completed. Acru = Acer rubrum, Nysy = Nyssa sylvatica, Quru = Quercus rubra, Qupr = Quercus prinus, Havi = Hammamelis virginiana, Oxar = Oxydendrum arboretum, Amar = Amelanchier arborea, Rhca = Rhododendron calendulaceum. Logarithmic equation results:

Acru = 29.488 * Ln(DOY) + 121.16, R^2 = 0.9286 (Black: line dot dot)
Amar = 1.9227 * Ln(DOY) - 8.4479, R^2 = 0.8559 (Dark Grey: solid)
Havi = 25.502 * Ln(DOY) + 135.51, R^2 = 0.9573 (Light Grey: solid)
Nysy = 2.0603 * Ln(DOY) - 9.1434, R^2 = 0.9258 (Black: solid)
Oxar = 2.0923 * Ln(DOY) - 9.2068, R^2 = 0.9413 (Black: dotted)
Qupr = 1.7226 * Ln(DOY) - 7.5637, R^2 = 0.6727 (Black: line dot line)
Quru = 2.1034 * Ln(DOY) - 9.6011, R^2 = 0.8448 (Light Grey: line dot line)
Rhca = 2.0041 * Ln(DOY) - 9.0617, R^2 = 0.8877 (Light Grey: dotted)

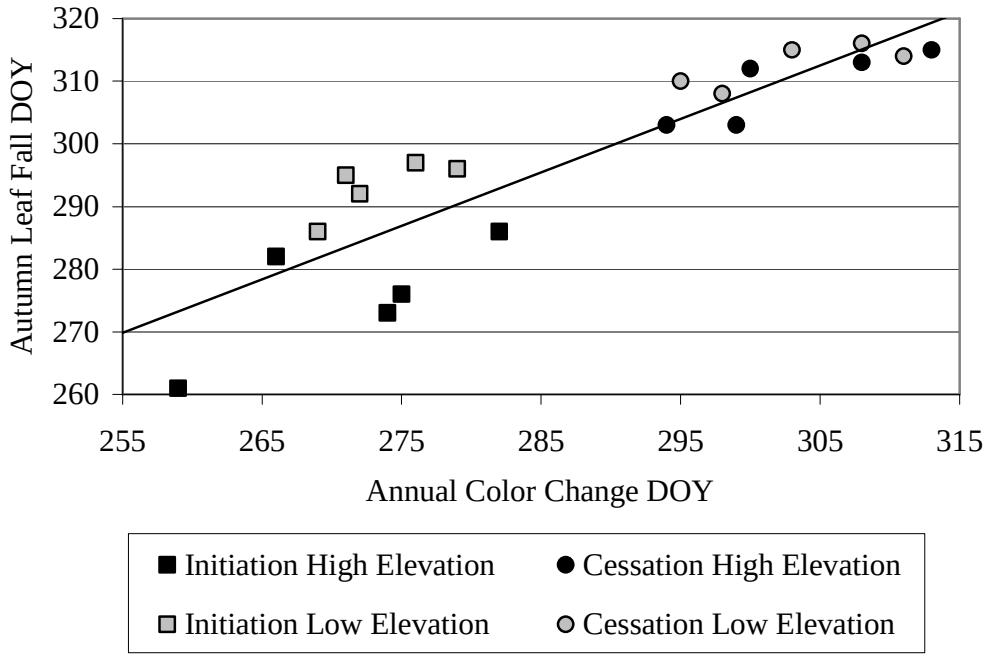

Figure 5: DOY of initiation and cessation of color change versus DOY of initiation and cessation of leaf fall from a high and a low elevation site collected from 2004-2009. Fall color change (CC = 100 – percentage of color change/100). Fall leaf fall (LF = 100 – percentage of leaves fallen)/100. Linear regression results:

$$CC\ DOY = 0.8536 * LF\ DOY + 52.15,\ R^2 = 0.8083$$

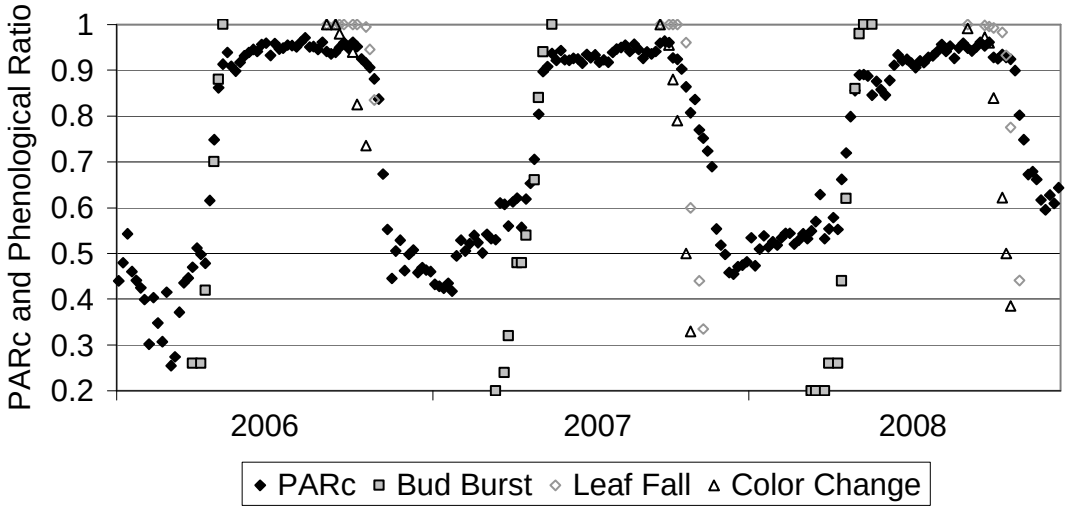

Figure 6: Site 2 PAR_C using a 5-day moving average with spring bud burst, autumn color change and leaf fall. PAR_C = Below canopy midday PAR/Above canopy midday PAR. Bud burst stage ranges from 0 to 5 where 0 = closed winter bud and 5 = full leaf. Bud burst = Bud stage / 5. Autumn color change = (100 – percentage of color change)/100. Autumn leaf fall = (100 – percentage of leaves fallen)/100.

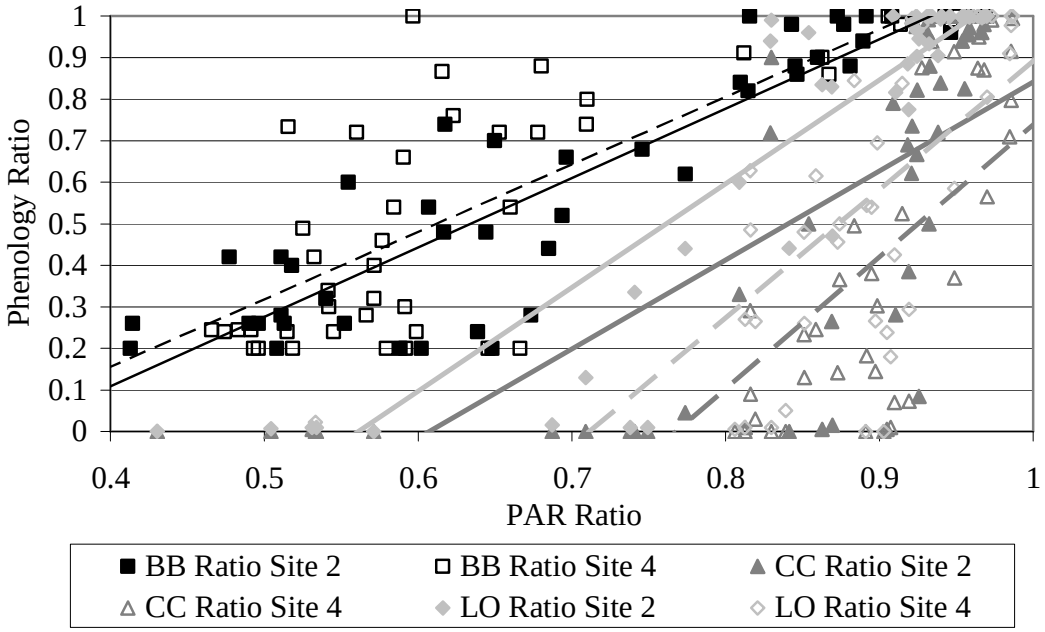

Figure 7: PAR_C versus three phenology ratios (Bud burst, Color change, Leaf off) for Site 2 (low elevation) and Site 4 (high elevation) including linear regressions (Site 2 represented by solid line, Site 4 representative by dashed line). BB Ratio = Bud burst ratio, CC Ratio = Color change ratio, LO Ratio = Leaf off ratio. Linear regression results:

Site 2: $BB = 1.67 * PAR_C - 0.56$, $R^2 = 0.80$
$CC = 2.14 * PAR_C - 1.3$, $R^2 = 0.55$
$LO = 2.5 * PAR_C - 1.4$, $R^2 = 0.82$

Site 4: $BB = 1.62 * PAR_C - 0.49$, $R^2 = 0.60$
$CC = 5.33 * PAR_C - 4.41$, $R^2 = 0.64$
$LO = 4.7 * PAR_C - 3.7$, $R^2 = 0.56$

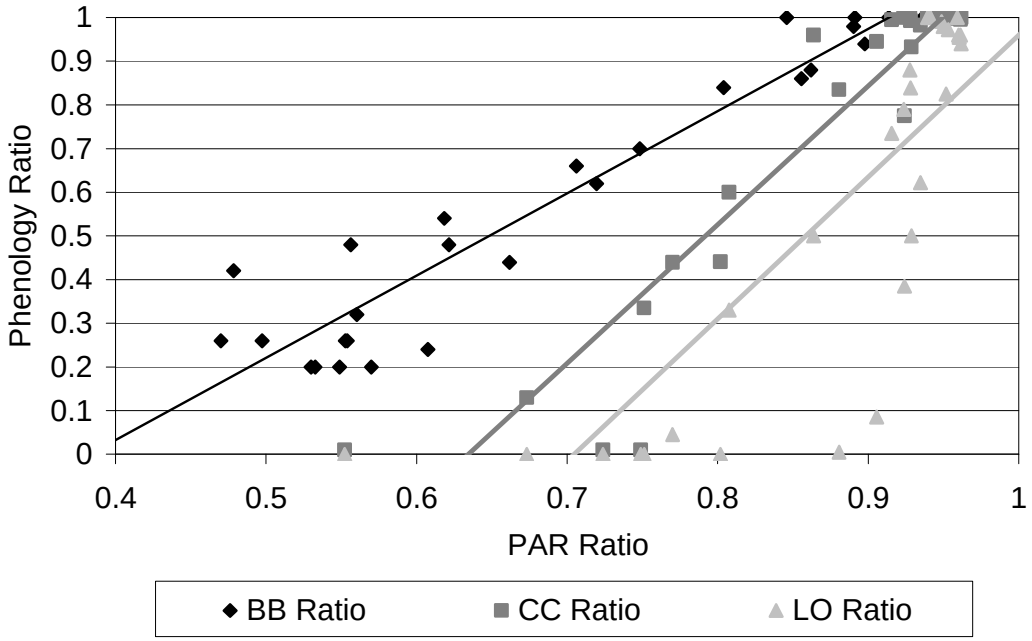

Figure 8: PAR_C versus three phenology ratios (Bud burst, Color change, Leaf off) for two combined sites, Site 2 (low elevation) and Site 4 (high elevation) from 2003-2008. BB = Bud burst, CC = Color change, LF = Leaf fall. Linear regression results:

$BB = 1.63 * PAR_C - 0.51$, $R^2 = 0.70$
$CC = 2.18 * PAR_C - 1.43$, $R^2 = 0.42$
$LF = 2.39 * PAR_C - 1.44$, $R^2 = 0.54$

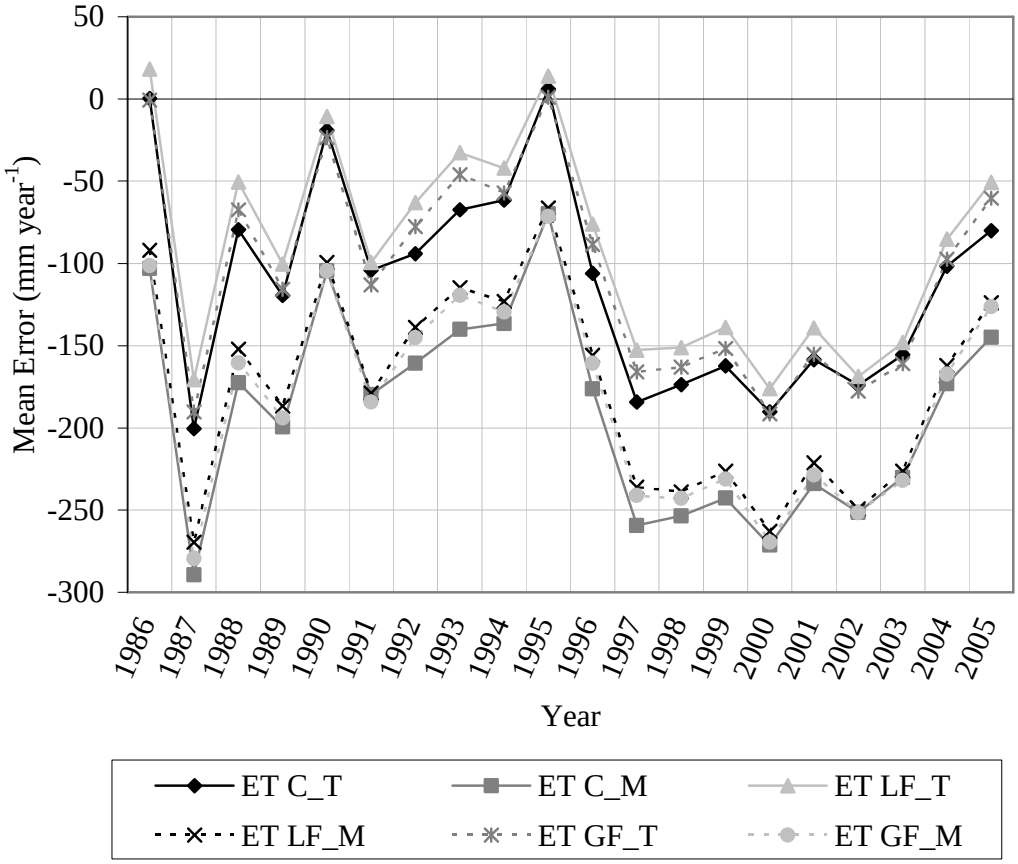

Figure 9: Annual mean error from six ET estimation methods using three phenology estimates (GF = globally fixed, Locally fixed = LF, and Climate driven = C) and two LAI estimates (Mean = M and Terrain-based = T). Computed on 15 watersheds (WS1-WS15) from 1986-2005.

Chapter 4 The effects of climate and species changes on water yield in the SA.

With over 55% forest cover, the southern Appalachians (SA) are a main water resource for the surrounding areas. These water resources are at risk due to changing climate and precipitation regimes as well as changes in forest cover. Understanding the implications of these risks will help to develop management strategies for an increasingly valuable resource. Though studies examining the impact of temperature increases are common, few have used sap flow ET models, primarily driven by temperature. Further, studies that examine the impact of species conversion on the hydrological cycle are rare. Most examine afforestation, deforestation, or a conversion between deciduous, non-deciduous and/or agricultural land, rather than shifts in mixed compositions. Additional studies are needed to examine the impact of potential temperature and compositional shifts on water yield, given the current threats to the SA and the importance of the water cycle in the southeast. Our study scaled up species specific sap flow models to 15 catchments in the SA and examined the impacts on ET estimates from three changes in temperature, two overall compositional shifts to more mesic or xeric species and two terrain-based compositional shifts on the coves and ridges. Temperature scenarios used include increases of 3.5 ^{o}C, 7 ^{o}C, and a night biased scenario which increased night temperature more than day temperature, keeping an average of 3.5 ^{o}C. We found large increases in ET when temperature increased evenly over day and night, 12% on average with a 3.5 ^{o}C temperature increase, and 20% on average under a 7 ^{o}C temperature increase. However, when we increased night temperatures more than day temperatures

we found a decrease of -2.8%. Our results show that changes to more mesic species will have a greater impact on our water resource than from xeric species. Changes in species composition to more mesic speices increased ET by 8% on average and a conversion to a more xeric stand decreased ET by 2% on average. When species conversions were performed according to terrain shape, converting coves to 100% *L. tulipifera* increased ET by 17% on average. For the ridge conversion to xeric species there was a slight decrease in ET, with a mean change of 4% on average.

Introduction

Fresh water resources are important for residential, commercial and ecological purposes, particularly across the southeastern United States (Kundzewicz et al., 2007). With over 55% forest cover, the southern Appalachians (SA) are a main water resource for the surrounding areas (Flather et al., 1989). These water resources are at risk due to changing climate and precipitation regimes as well as changes in forest cover (Arnell, 1999). Understanding the implications of these risks will help to develop management strategies for an increasingly valuable resource.

Both invasive species and climate change have altered forest composition and structure (Ellison et al., 2005). In North Carolina, the U.S. National Forest Service estimates 1,673,000 acres are at risk from at least 31 invasive insects, pathogens and diseases (FHM report: USDA, 2006). That comprises over 7% of the state's forest cover, with threats expected to increase (Simberloff, 2000; Stachowicz et al., 2002). Historically, invasive insects have altered forest composition and structure, diminished

biodiversity, decreased biomass and have led to species extinction (Ayres and Lombardero, 2000; Brown and Allen-Diaz; 2009; Holzmueller et al., 2010). Introduced pests in the eastern US include insects including gypsy moth (*Lymantria dispar)*, hemlock wooly adelgid (*Adelges tsugue*), balsam wooly adelgid (*Adelges picea*), Asian longhorned beetle (*Anoplophora glabripennis*) and the emerald ash borer (*Agrilus planipennis*), and pathogens, including chestnut blight (*Cryphonectria parasitica*), Dutch elm disease, butternut canker (*Sirococcus clavigignenti-juglandacearum*), dogwood anthracnose (*Discula* spp.), and sudden oak death (*Phytophthora ramorum*). Forest impacts from these pests have been substantial. American chestnut (*Castanea dentata*) was a dominant SA species, comprising up to 35% of the forests in the SA, but is now depleted due to the chestnut blight (Vandermast and Van Lear, 2002).

Impacts from introduced species and changing climate have the potential to alter watershed evapotranspiration (ET) (Simberloff, 2000; Stachowicz et al., 2002). ET characteristics vary by tree species and canopy structure, both of which can be altered by forest pests and changes in climate. Models that incorporate species composition in ET estimates may help us to understand how forest change affects our water resources. In this paper we use sap flow models, which can represent species contribution to ET, to provide ET estimates based on species composition and climate.

Studies that examine the impact of species losses on the hydrological cycle are rare. Most studies look at changes in water yield after afforestation, deforestation, or a conversion between deciduous, non-deciduous and/or agricultural land (Bosch and

Hewlett, 1982; Wattenbach et al., 2007; Gao et al., 2009). Few examine the impacts of species compositional changes on catchment runoff. One exception is Ford and Vose (2007). Using sap flow models, they found that the loss of Eastern hemlock (*Tsuga canadensis*) from the SA substantially affected the hydrological cycle, decreasing stand-level transpiration by 10-30% and thereby increasing discharge. Much of the decreased transpiration was due to lack of tree and hence overstory replacement of leaf area, caused by tree recruitment limitations at high Rhododendron densities.

Further studies are needed to examine the impact of potential compositional shifts on water yield, given the current threats to the SA and the importance of the water cycle in the southeast. Scaling up species specific sap flow models to a variety of catchments in the SA allows us to examine the impacts of species change on water yield, including shifts in species dominance.

Changing climates may also significantly alter water yield. Climate changes effects on runoff may be direct through modifications in precipitation amount or timing, or indirect through changes in temperature, thereby increasing plant water use, water stress, surface soil dryness, drought-induced differential recruitment, and changing species composition. Increases in temperature of 1.1 ^{o}C and precipitation by 2% in the last century demonstrate that climate change is currently occurring and potentially impacting our ecosystems (Lettenmaier et al., 1994; Jones and Hulme, 1996; Hulme et al., 1998; Karl and Knight, 1998; Groisman et al., 1999; IPCC, 2007). Predicted impacts of climate change include changes in species composition, decreased biodiversity

(Hansen et al., 2001), and increased herbivory (Bale et al., 2002). Projections from general circulation models (GCM) show that elevated greenhouse gas concentrations are expected to increase global mean temperatures from 2 ^{o}C to 6 ^{o}C over the next 100 years (Kattenberg et al., 1996; Houghton et al., 2001; IPCC, 2007). For the southeast US, projections rise to over 7 ^{o}C (Mearns et al., 2003). Projected changes in precipitation however, vary between GCM's with a range of +15% (Mitchell, 1989) for the southeast U.S. to -21% (Rowntree, 1988) for the Kenyan Rift Valley. These variations are most likely correlated with region, where some expect wet areas to become wetter and dry areas to become drier (Dore, 2005). Although many global and national GCMs exist, there are fewer studies projecting climate scenarios regionally for the SA. Two regional models, Mulholland et al. (1997) and Mearns et al. (2003) both show potential increases in temperature of 3-4 ^{o}C and up to 7 ^{o}C respectively for the southeast.

Though many climate projections assume equal shifts in minimum and maximum temperature, some studies show night time temperatures are increasing more than daytime temperatures (Easterling and Horton, 1997; Cheng et al., 2009). Using historical data, Loehle and LeBlanc (1996) and Ashcroft et al. (2009) have noted that minimum temperature may increase by up to three times more than maximum temperature. Higher night time humidity and cloud cover may reduce night time longwave radiation, increasing heat retention (Dai el al., 1999; Boyles and Raman, 2003). Few studies have examined the implications of these shifts on the ET of forested catchments.

Global climate change has been shown to alter species composition due to migration (Iverson et al., 1999; Iverson and Presad, 2002; Parmesan and Yohe, 2003; Lesica and McCune, 2004; Parmesan, 2006; Foden et al., 2007) and extinction (Thomas et al., 2004, Thuiller et al., 2008). Further changes to species ranges are forecast across the eastern United States following predicted increases in temperature. Iverson and Presad (1998) found that 36 of the 80 species studied had the potential for range shifts over 100 km, and seven over 250 km. Recently Woodall et al. (2009) found evidence that many species in the southeast are currently migrating at a rate of 100 km century^{-1}. Not only are species shifting their ranges north, they are also increasing their elevation ranges due to the temperature gradient (Pauli et al., 2007). These shifts in species composition may impact water yield.

Climate change will also impact forest phenologies (Lieth, 1974; Arnell, 1992; Gardenas and Jansson 1995; Kremer et al., 1996; Kellomaki and Vaisanen, 1997; Najjar, 1999; Stone et al., 2001; Guo et al., 2002; Sabate, 2002; Shenbin et al., 2006). Tree phenologies are the timing of bud burst and leaf development in the spring, and leaf senescence in the autumn. These phenological phases drive ecosystem processes because leaves produce energy through photosynthesis, thereby impacting annual growth (Kramer et al., 2000). Since phenologies determine growing season length, they are also primary factors in determining annual net primary production and annual water consumption (Linderholm, 2006).

The main drivers of tree phenology are temperature and photoperiod (Menzel, 2002). Spring leaf development is primarily controlled by growing degree-days, or the thermal sum, a sum of the variation in temperature above a threshold (Hunter and Lechowicz, 1992). Leaf senescence has added complexities, complicating models of autumn phenology (Fracheboud et al., 2009). Phenological events do not occur on the same calendar day each year because of trade-offs between the need to grow and store nutrients and the need to prevent damage from freezing temperatures and drought (Lopez et al., 2008). Consequently, variation in leaf phenology is primarily a result of climate variation, primarily temperature, but also precipitation, and will be impacted by changes in climate (Lechowicz, 1984). Phenology may also vary by species, and populations within species.

Climate change not only has the ability to alter species composition, but can also directly impact forest hydrology. Studies have shown that climate change can impact transpiration at the tree level (Gardenas and Jansson 1994; Kremer et al., 1996; Kellomaki and Vaisanen, 1997; Sabate, 2002; Shenbin et al., 2006) and thus ET and runoff at the catchment level (Arnell, 1992; Najjar, 1999; Stone et al., 2001; Guo et al., 2002). Under projected climate change, water yield has been predicted to increase (Najjar, 1999; Leipprand and Gerten, 2006), decrease (Mulholland et al., 1997; Chalecki and Gleick, 1999; Arnell and Liu, 2001; Trabucco et al., 2008), or do either (Goudie et al., 2006). Further studies are clearly needed to understand these differences and determine the potential impacts of climate change on forest hydrology.

Studies have examined the impacts of forest composition, primarily comparing conifers and hardwoods, on water yield (Bosch and Hewlett, 1982; Ewers et al., 2002; Wattenbach et al., 2007). Few studies have investigated the impacts on water yield from individual species. There are many factors that may change composition and hence aggregate water use by removing species. Threats to individual species include invasive insects, pathogens, disease or migration and extinction due to climate changes. In addition, the coupled impacts of changing species composition and climate on water yield have not been examined. By using species-specific sap flow models, we propose to address the following questions: 1) How would climate change affect ET on small catchments in the SA? 2) How would species compositional shifts affect ET? 3) How will combined changes in climate and species composition impact estimated ET?

Methods

Study Area

Our study area, herein called the southern Appalachian region (SAR), encompassed western North Carolina, northern Georgia, northwestern South Carolina, southern West Virginia, southwest Virginia, and eastern Tennessee (Figure 1). Climate across the SAR is temperate, moist, and humid. Average annual temperatures range from 10 ^{o}C in the north to 18 ^{o}C in the south, with average annual precipitation ranging from 850 mm to over 2500 mm. The region is composed of Paleozoic and Precambrian bedrock deposited approximately 800 million years ago (Sankovski and Pridnia, 1995). Overstory composition and forest communities vary strongly with terrain and elevation across the SA (Whittaker, 1956; Bolstad et al., 1998), and communities include mixed-

deciduous (*Q. alba*, *Q. rubra*, *R. psuedoaccacia*, and *Carya* spp.), northern hardwoods (*A. saccharum*, *Tilia spp*., *B. aleghaniensis*, *A. octandra*), xeric oak-pine (*Q. coccinea*, *Q. prinus*, *O. arboretum*, and *P. rigida*), and cove (*L. tulipifera*, *B. lenta*, *Magnolia* spp.). Understory most commonly includes *Rhododendron* spp. and *Kalmia* spp. (Bolstad et al., 2001). Soils in this region vary considerably even at small scales and are most often represented by ultisols in basins, ridges, and areas of gentle topography, and inceptisols are found on steeper slopes (Swank and Crossley, 1988).

Approach

We followed procedures common in similar studies (Arnell, 1992). Steps included: (1) model hydrology across the study region with historical time series of climatic data and species composition, (2) adjust historical climate data based on climate change scenarios and species composition maps based on species change scenarios, (3) simulate the hydrology using adjusted species and climate data across study basins, (4) compare the model simulations between the baseline and predicted annual ET for each scenario.

Data including streamflow, climate, and watershed properties were compiled for 15 watersheds located in the SAR (Figure 1). Study watersheds (WS1-WS14) were selected upstream from a USGS streamflow gauge site with at least 15 years of data, with the exceptions of WS11 (5 years) and WS13 (6 years), included for a more complete distribution of watershed size and location. Watersheds were also selected for their location (within the SA), size (less than 140 sq km), and percent forest cover (at least

95%). Fourteen watersheds were above USGS gauging stations, and one in the USDA Forest Service's Coweeta Hydrological Laboratory (CHL) situated near the southern edge of our study region. CHL is a 2185 ha watershed composed of a variety of gauged watersheds, with over 80 years of intact hydrological and climatologically data. Coweeta watershed 18 (WS15) was selected in part because the tested sap flow models were developed there.

Watersheds ranged in size from 0.13 km^2 to 134.4 $km^2$and in elevation from 329 m to 2038 m (Table 1). Precipitation and discharge varied based on elevation, with up to 2100 mm $year^{-1}$ of precipitation and 1350 mm $year^{-1}$ of discharge at higher elevations, and an average 1300 mm $year^{-1}$ precipitation and 600 mm $year^{-1}$ discharge at lower elevations (USGS, 2006; NCDC, 2006).

Watershed characteristics for our 14 USGS watersheds, including size, gauge elevation, and gauge locations were downloaded from a USGS website (USGS, 2006). WS15 watershed data were provided by CHL. Daily averaged instantaneous runoff was downloaded from the USGS and CHL, summed annually and divided by watershed size to find total annual runoff per unit area (R_t). All watersheds were delineated using ArcGIS 9.0 and data from the USGS. A depressionless elevation layer was created from USGS 30 m digital elevation models and flow direction and flow accumulation were computed in turn. Finally, pour points and flow accumulation layers determined watershed boundaries. Final watershed areas were compared to the USGS reported watershed areas.

Relevant climate variables for the SAR were downloaded from the National Climatic Data Center (NCDC) and interpolated across each watershed. Daily precipitation, minimum temperature and maximum temperature were obtained from the NCDC for 134 climate stations across the SAR from 1985-2005 (NCDC, 2006; Figure 1). The NCDC used a variety of instruments to measure temperature, including glass thermometers, thermistors and thermocouples. Daily maximum temperature and minimum temperature were recorded in degrees Fahrenheit and converted to degrees Celsius. Precipitation was recorded at 15-min intervals and summed over 24 hour periods by the NCDC. Precipitation measurements were most commonly made using either tipping bucket or standard weighing gauges and were presented by NCDC in hundredths of inches and converted to millimeters (NCDC, 2009). Gauge sites ranged in elevation from 100 m to 1980 m and range in annual precipitation from 854 mm $year^{-1}$ to 2418 mm $year^{-1}$.

Our general approach consisted of estimating spatial fields of climate driving variables across each study watershed, and applying those estimates to the ET models to estimate water flux. First, spatial estimation was required to determine precipitation and temperature across each watershed. Several techniques were examined and compared for our region to determine the best method for interpolation. Numerous studies have shown the advantages to using kriging with external drift to interpolate both precipitation and maximum and minimum temperature (Phillips et al., 1992; Skirvin et al., 2003; Carrera-Hernandez and Gaskin, 2007; Haberlandt, 2007). Other studies have found regional

regression (Bolstad et al., 1998) and ordinary kriging (Goovaerts, 2000) provide better estimates. To identify the best method for our study region, regional regression, kriging, and kriging with external drift estimates were compared to point based daily estimates across the study area for precipitation, minimum temperature, and maximum temperature. Leave-one-out cross validation was implemented using all available climate stations for each day (Kove and Bolstad, in prep). Kriging with external drift was used because it provided the best daily interpolations of precipitation, minimum temperature, and maximum temperature. Annual precipitation (P) for each catchment was calculated using the estimated daily total precipitation, interpolated for each cell, summed annually and divided by catchment size. Daily maximum and minimum temperature were used in calculating VPD and PAR for use in our ET models.

Photosynthetically active radiation (PAR) is not measured consistently across the SA, and thus had to be estimated. Most commonly, PAR is estimated from temperature, latitude, and day of year (DOY). To estimate PAR, daily extraterrestrial solar radiation, R_e (MJ m^{-2} s^{-1}), was calculated from Bristow and Campbell (1984) using latitude and DOY. Global solar radiation, R_g (MJ m^{-2} s^{-1}) was found by calculating the transmittance, T_t, using the difference between maximum and minimum temperature, ΔT , and multiplying by R_e, where:

$$T_t = 0.7 \cdot \left(1 - \exp\left(-0.004 \cdot \Delta T^{2.4}\right)\right)$$

The Bristow and Campbell (1984) transmittance model was used because it was found to be superior over the modified Hargreaves-Samani model(Annandale et al.,

2002) when compared to daily measured PAR data on CHL, particularly during the summer months (Kove and Bolstad, in prep). PAR was converted from R_g assuming 4.608 umol quanta J^{-1} (Campbell and Norman, 1998) and that 50% of global solar radiation fell in the range of 400-700 nm (Landsberg and Waring, 1997; Ford et al., 2007).

Additional meteorological variables and fluxes were estimated using the best available models. Vapor pressure deficit (VPD) was also not measured sufficiently across our study area and was estimated from temperature using the temperature based method of Yoder et al. (2005). Soil evaporation was assumed to be zero due to the closed canopy and thick forest floor (Essery, 1992; Ford et al., 2007). Forest interception, $\sum I$, however is very high in the SA relative to precipitation (Helvey, 1967) and was estimated using the equation derived for mature hardwoods in the CHL Basin from Helvey and Patric (1965) based on total annual precipitation, $\sum P$ and number of storms over 1.5 mm, *n*:

$$\sum I = 0.083\left(\sum P\right) + 0.036(n).$$

Sap flow models require that we estimate LAI and composition cell by cell across each watershed, though there are no good estimates or agreements on the best methods to use. Optimal methods used to estimate LAI and species composition saturate in high LAI areas, common for the SAR. Allometric methods are generally considered one of the most accurate methods when using site-specific measurements (Law et al., 2001; Levia,

2008), however watershed-level diameter and height data were not available for this study. Instead, we applied a regression approach estimating LAI from elevation. Leaf area in deciduous taxa has been reported to be strongly correlated with elevation and to a lesser extent with terrain shape in the SA (Bolstad et al., 2001). A linear relationship developed from Bolstad et al., (2001) was developed to estimate LAI for each grid cell across the catchments using elevation, where as elevation increased LAI generally decreased.

Forest community composition varies spatially and can affect sap flow estimates of ET. Estimating forest composition is difficult at the resolution required, particularly in areas we never visit by foot. Remote sensing methods are applicable for the region, but would designate stands as deciduous or coniferous, not detailed enough for our sap flow models. We collected community composition from county level forest inventory and analysis data (FIA) downloaded from the USDA forest service website (USDA, 2007), and applied a single composition to each watershed. If a watershed covered more than one county, area-based weighted averages were used.

Annual ET was calculated in two different ways. First, annual ET was calculated using the catchment water balance method, $ET_{CWB} = P - R_o$. ET_{CWB} was used as our estimate for the "true" ET in all subsequent comparisons. Ground water storage and losses due to deep flow were assumed insignificant over annual time scales due to steep slopes and impenetrable bedrock (Ford et al., 2007). We also assume that the net ground water storage change over our annual time step was negligible (Essery, 1992). Since we

are averaging over 20 years of data, we are not overly concerned with violating this assumption (Winter, 1981).

Second, annual ET was calculated from scaled sap flow equations (ET_{SAP}) developed by Ford (Ford, in prep). ET_{SAP} was found by multiplying El_{sp} by our species-specific LAI totals, described earlier. Daily values were summed across the watershed and across the year to compute annual catchment ET_{SAP}. Ford measured sap flow on eight species (*A. rubrum, B. lenta, Tsuga Canadensis, P. strobus, Q. prinus, Q. rubra, L. tulipifera and Carya spp*.) within CHL. Transpiration was estimated at 15 second intervals and averaged every 30 minutes (Granier, 1985). Daily totals were then used to find species-specific transpiration equations based on VPD, PAR and day of year (DOY). Detailed methods are described in Ford et al. (2007) with EL_{sp} equations defined as follows:

$$EL_{chestnut\_oak} = \left(1 - e^{(-0.3055 \times VPD)}\right) - 0.00015 \times PAR + e^{(-0.00954 \times DOY)}$$

$$EL_{red\_oak} = \left(1 - e^{(-0.07728 \times VPD)}\right) + 0.000009264 \times PAR + e^{(-0.015151 \times DOY)}$$

$$EL_{hickory} = \left(1 - e^{(-0.49504 \times VPD)}\right) - 0.00031 \times PAR + e^{(-0.006435 \times DOY)}$$

$$EL_{tulip\_tree} = \left(1 - e^{(-0.2538 \times VPD)}\right) + 0.000136 \times PAR + e^{(-0.007702 \times DOY)}$$

$$EL_{white\_pine} = 0.21677 \times \left(1 - e^{(-0.79411 \times VPD)}\right) + 0.000179 \times PAR$$

$$EL_{birch} = 0.5943 \times \left(1 - e^{(-3.4558 \times VPD)}\right)$$

$$EL_{hemlock} = 0.1698 \times \left(1 - e^{(-2.9216 \times VPD)}\right)$$

$$EL_{red\_maple} = 0.3978 \times \left(1 - e^{(-2.0029 \times VPD)}\right)$$

Species scenarios were used to examine the implications from compositional shifts of the overstory from insects, pathogens and changes in climate. Since the potential for changes in species-specific basal area (BA) varies, shifts to both more xeric and more mesic species were examined. We classified xeric species as *Q. prinus*, and *P. strobus*, and mesic species as *L. tulipifera*, *B. lenta*, *Q. rubra*, and *Tsuga canadensis.* Scenarios shifted the base species composition to 80% xeric or 80% mesic while holding constant the relative proportions within mesic and xeric species.

Because species segregate by landform, we also altered species scenarios based on terrain shape. Digital terrain shape was determined using 100 m DEMs from the USGS (2006). A modified McNab's (1989) 9-cell weighted average was used, further described in Bolstad et al. (1998). Negative index values indicated the center cell was a depression or cove, positive values indicated a peak or ridge. Cells were subsequently divided into cove, slope, and ridge. Two species scenarios were used. First, cove cells were converted to 100% *L. tulipifera* and both ridge and slope sites remained unchanged. Second, ridge cells were converted to 100% xeric species, and both cove and slope sites remained unchanged. Annual ET was calculated with each species scenario and compared to ET_{SAP}.

Climate scenarios were also implemented. Given a regional climate prediction for a 1 ^{o}C -7 ^{o}C increase from Mearns et al. (2003), and global predictions from 2.4 ^{o}C – 6.4 ^{o}C (IPCC, 2007), mean temperature increases of 3.5 ^{o}C and 7 ^{o}C degrees were

implemented, with the increase uniformly distributed of diurnal and annual intervals. Because minimum temperatures may increase more than maximum temperatures (Kukla and Karl, 1993; Easterling et al., 1997) we added a scenario which increased the mean temperature by 3.5 ^{o}C but proportionally increased the minimum temperature three times more than the maximum temperature, hereafter called the 3.5n ^{o}C. This third scenario increased minimum temperature by 5.25 ^{o}C and maximum temperature by 1.75 ^{o}C. All scenarios were compared using simulated runoff. By subtracting precipitation by our estimated ET, from our climate and species scenarios, we were able to compare the relative impacts that changes in these variables and levels will have on runoff.

Baseline scenarios were run for years 1986-2005 for WS1-WS15 to verify applicability of the hydrological model. For each climate scenario, minimum and maximum temperature for the control range 1986-2005 were modified, in turn affecting VPD and PAR, and these were used to compute subsequent transpiration. As described above, interception was added to transpiration to compute ET.

Results and Discussion

Our analysis highlights the potential importance of climate and species changes on watershed water balance. We found large declines in runoff when temperature increased evenly over day and night. We also found the relative night time to daytime change substantially affects the changes in water yield. When night time temperatures increased more than day time temperatures, runoff changed little, and increased, on average. Overall, impacts on transpiration from changes in species composition were

significant and slightly lower than the impact from changes in temperature. Impacts on transpiration from changes in species varied and were dependent on the original species and the converted species compositions.

Increased temperatures from our climate scenarios impacted transpiration in two main ways, first, by shifting phenology, and second by altering climatic inputs to our transpiration models. Increased temperatures shifted the estimated dates for bud burst and full leaf expansion through more rapid accumulation in growing degree days. Scenario 3.5 ^{o}C and 3.5n ^{o}C resulted in the same phenological dates because both models use the same mean increase in temperature, 3.5 ^{o}C. Full leaf DOY was affected more than bud burst DOY by temperature increases. Bud burst DOY occurred on average 10 days earlier for a 3.5 ^{o}C temperature rise, and 16 days earlier for a 7 ^{o}C mean temperature rise, corresponding to an increase in growing season of 5% and 7% respectively. Similarly, full leaf DOY was on average 13 days earlier for a 3.5 ^{o}C increase and 22 days earlier for a 7 ^{o}C increase, corresponding to an increase in growing season of 6% and 10%, respectively. Models for leaf-off were dependent primarily on the distribution of annual precipitation, and therefore could have both positive and negative impacts on growing season length depending on if there were warmer or drier falls. Precipitation distribution estimates are more complicated and substantially less supported, so we assumed they were unchanged, and so fall phenologies did not vary in our scenarios.

A uniform increase in maximum and minimum temperature of either 3.5 ^{o}C or 7 ^{o}C leads to increased ET (Table 2). Baseline ET averaged 593 mm year^{-1}, and increased

by 12% to 666 mm year^{-1} with a 3.5 ^{o}C temperature increase, and 20% to 708 mm year^{-1} under a 7 ^{o}C temperature increase, when averaged across all years and watersheds. Increased ET was observed individually for all watersheds, and increases were largest at higher temperatures, higher elevations (F-test, P<0.001; Figure 2), and lower precipitation (F-test, P<0.01; Figure 3). Since temperature decreases and mean precipitation increases as elevation increases, it is difficult to separate these related impacts. Interannual variation occurred with mean annual increases in variation of more than 10% for a 3.5 ^{o}C temperature increase, 15% for a 7 ^{o}C temperature increase, and decreased between 0 to 5% for a 3.5^{o}C night time bias temperature increase. Estimated ET decreased for the night time bias 3.5 ^{o}C temperature increases, in contrast with our findings of increased ET with uniform temperature increases (Figure 2 and 3). Decreases were between 0 and 5%, and showed no trend with mean watershed elevation, temperature, or precipitation.

Trends and differential scenario responses may be explained by changes in VPD, and plant response to VPD. Mean VPD averaged 0.62 $\mu mol\ m^{-2}s^{-1}$ during the growing season for the original climate data, and decreased with mean watershed elevation (Figure 4). Mean growing season VPD increased to 0.76 $\mu mol\ m^{-2}s^{-1}$ for the uniform 3.5 ^{o}C mean temperature increase, and VPD increased to 0.93 $\mu mol\ m^{-2}s^{-1}$ with an increase of 7 ^{o}C. However, with the 3.5n biased increase in temperature, mean annual VPD was slightly lower than observed for the original climate data, with a mean of 0.61 $\mu mol\ m^{-2}s^{-1}$ (Figure 5).

Our study watersheds spanned a range of mean temperatures and initial mean VPDs. Changes in VPD were consistent across watersheds within a scenario, shifting these relationships upward or downward (Figure 5). Lower mean VPD and lower ET demands were observed at lower temperatures (higher elevations) relative to higher temperatures (lower elevations) at any given climate scenario. The lines shifted upward due to higher uniform temperature increases, but were basically unchanged at the night-biased temperature increase. When we combine these two results we find the impacts on ET should be greatest for higher increases in temperature at lower elevations, under the uniform temperature increases. This results in the greatest change in VPD, and hence the greatest estimated increase in ET.

However, impacts on ET from fluctuating VPD values will vary by species (Figure 6). Most species show a curve-linear increase in daily ET in response to increases in VPD (e.g., *B. lenta, T. Canadensis, Q. prinus*), while other species are less sensitive across the range of VPD (e.g., *P. strobus*). ET estimated for *B. lenta* is not affected like the other species because VPD values are already high enough to be on the asymptote section of the curve for the 3.5 ^{o}C and 7 ^{o}C increase in temperature, reducing the impacts of changes in VPD. However, for other species it has a greater impact, particularly *Q. prinus*, and *L. tulipifera* both of which increase steadily throughout the range of VPD values observed.

Our results are similar to others, where increases in temperature lead to increases in ET, or subsequent decreases in runoff (Murakami et al., 2000; Gordon and Famiglietti, 2004). Other studies have shown significantly greater impacts from similar or smaller increases in temperature than ours (Nash and Gleick, 1991; Gardenas and Jansson, 1995; Rosenberg et al., 1999). Though most studies show increasing temperatures lead to increased ET (or subsequent decreases in streamflow) other studies have shown contradictory results, primarily in water limited regions (Kremer et al., 1996). Differences in study results are controlled by the main factors that drive potential ET including sunlight and dry air, and they are meditated by species and water availability. Different results are therefore a result of how site characteristics and climate affect these factors.

Jha et al. (2006) found increases in temperature led to decreases in streamflow on the Mississippi basin. Increases of 2 ^{o}C, 4 ^{o}C, and 6 ^{o}C led to decreases of 7%, 14%, and 21% in water yield primarily resulting from increases in ET. We had similar results for our uniform day/night temperature increases even though our study areas differed considerably. The Mississippi basin is lower in elevation with less precipitation, and has less forested land than the SA. Lower water availability coupled with lower VPD gave us similar results in a different climate.

Similarly, Najjar's(1999) study of the Susquehanna River found a wider range, with a 24% increase in streamflow and a range of +/- 13% for a 2.5 ^{o}C increase in temperature. The Susquehanna River is a similar ecoregion, but with a somewhat cooler

and drier climate. These factors result in a wider range of outcomes from similar changes in temperature. With a cooler climate, when temperatures are increased, evaporative demand may be impacted more than in an already warm climate. Further differences in our model and study area may also explain these deviations. First, their ET models were driven only by climate, using precipitation and temperature, whereas our models included species-specific LAI. Further differences with our study include a longer study period, a lower elevation range and differences in landcover. The Susquehanna River is only 67% forest and 29% farmland (Boyer et al. 2002), and is on average 10 ^{o}C with approximately 1000 mm of annual precipitation. Furthermore they used over 100 years of data for their study, leading to a wider range in climate than our study.

Studies with more extreme differences are still comparable because of our interest in the magnitude and direction of change and in the author's causative explanations. For instance, Nash and Gleick (1991) found an increase in ET of 9%-21% from a 4 ^{o}C increase in temperature in the Colorado Basin. This result is only slightly higher than ours even though the Colorado basin is a significantly different region. Drier conditions, wider ranges in elevation and landcover differences distinguish this study area from the SA and could explain why smaller increases in temperature may result in larger increases in ET compared to our results.

Rosenberg et al. (1999) studied the impacts of climate change to the Ogallala or High Plains aquifer, nearly 450,000 km^2, a significantly drier area than the SA. As expected they found a larger impact than our study, of up to a 25% increase in ET from a

1 ^{o}C increase in temperature. Greater climate sensitivities may be due to differences in base climate and the lower water availability of the region. From their examination of storage recharge, they found that even in increased precipitation, ET decreased because increased water recharged the aquifer making it unavailable to plants.

A study in another water limited environment was done by Kremer et al. (1996). They found that higher temperatures led to lower ET for arid sagebrush in south-central Washington, most likely due to low precipitation. Increased temperature and subsequent increases in VPD caused decreased stomatal conductance and hence transpiration. Moreover, in arid regions, limited water availability can limit transpiration even in elevated temperatures (Cienciala et al., 1994; Bernier et al., 2006; Zeppel et al., 2008), not a concern for the SA.

Gardenas and Jansson (1995) studied potential climate change impacts on small Scots pine stands in Sweden. They found an increase in transpiration between 30-50% for modest increases in temperature. Given their cooler, boreal climate, any increase in temperature could increase ET due to their limited temperature environment. Further, they simultaneously increased precipitation in the climate scenario making it difficult to distinguish between impacts from temperature increases and the increased water availability.

The variation in results may also be due to differences in climate regime. The SA are a temperate climate with high precipitation and high humidity, potentially alleviating

the impact to climate change (Guo et al., 2002). High humidity decreases the leaf to air water potential gradient and hence transpiration. On the other hand, leaf areas are higher, so we might expect increased aggregate transpiration, but high sub-canopy humidity, even on warmer days, effectively reduces the impacts of higher leaf areas. Also, a higher number of cloudy days reduces ET demand relative to more arid climates (Oishi et al., 2010). However, this only holds true if all other variables are equal. Given the differences in other factors including temperature, species composition, and climate regimes, they are too difficult to isolate. Some studies suggest humid regions may be less vulnerable to impacts from climate change, both Gardenas and Jansson (1995) and Rosenberg et al. (1999) are drier and less humid regions than the SA. Catchment water availability may also alter the impact of changes in climate on ET. Arnell (1992) found drier catchments, defined by a low percent yield, were more impacted by increases in temperatures than wetter catchments, though our watershed results show no correlation.

The impact from increases in mean daily temperature on ET depends on how the warming occurs, results differ when night temperatures increase relatively more than day temperatures. Increased temperature more heavily weighted to night time caused a slight decrease in ET that averaged -3%. These results are generally consistent across watersheds and years, with exceptions of WS4 and year 1997, where ET increased slightly. Unlike uniform increases in day and night temperature, there were no correlations between changes in ET and mean annual precipitation or mean watershed elevation.

The small decrease in ET is a result of and supported by the 1.5% average decrease in VPD from the night time temperature scenario (Figure 4). We adopted the common assumption that VPD saturates at night during the growing season (Glassy and Running, 1994). We tested our assumption on VPD data that was measured at CHL in 1991 and 1992. Results confirm that nearly 80% of nights saturate during the growing season. Therefore, VPD decreased which decreased transpiration due to the increased night temperatures.

There are few studies that investigate differential day/night temperature impacts on forested catchments, particularly for a humid area such as the SA. Most studies focused on productivity instead of water use. Higher water use is often found during high productivity within any give species or vegetation type, but the linkage is not strong, in part because differential day/night temperatures may affect photosynthesis and respiration balances, and hence productivity. Studies have shown impacts on productivity from changes to night time temperatures. Two studies found increases in night time temperature decreased rice yields by up to 90% (Peng et al., 2004; Mohammed and Tarpley, 2009). Rice physiology is different from tree physiology in that water is not limited and transpiration resistance and atmospheric humidity are of lesser importance. The decrease in yield is primarily a result of increased respiration, due to increased night temperatures. Previous work has shown that increases in night time respiration decreased retention of photosynthate to be used for the maintenance of current foliage (Lawrence et al., 2005). Therefore, higher respiration may be responsible for lowered rates of ET. Our models did not represent photosynthesis or respiration, and depended primarily on VPD

calculated from minimum and maximum temperature, so increasing minimum temperature significantly decreased VPD thereby decreasing ET.

Species Scenarios

Changes in species composition altered transpiration, depending on the species conversion. Species scenarios showed that changes to more mesic species increased ET and changes to more xeric species decreased ET. Baseline ET averaged 593 mm $year^{-1}$. ET increased by 7.8% to 639 mm $year^{-1}$ for the mesic species scenario, and decreased by 2.4% to 579 mm $year^{-1}$ for the xeric species scenario.

Change in ET with change in species composition varied across watersheds (Figure 7). The mesic species scenario resulted in an increased mean ET for all watersheds, whereas the xeric species scenario resulted in a decrease for 13 of the 15 watersheds. WS2 had the largest percentage change in the XS scenario and correspondingly the highest initial MS proportion, though there was not a relationship with proportion of MS and percentage difference from the baseline for all of the watersheds. WS10 ET increased, and had a higher percentage change from the baseline than any other watershed for the MS scenario. WS10 had the highest initial XS proportion. There was not a relationship with proportion of MS or XS and percentage ET difference from the baseline for all of the watersheds. The impact on ET from a shift to xeric species was greater on higher elevation watersheds (ρ=0.71; Figure 8). This was a result of the relationship between elevation and proportion of MS. Higher elevation watersheds had higher proportions of MS so higher elevation watersheds changed more

in composition. Since the XS species had lower ET rates over the environmental conditions we observed than the MS species they replaced, there were greater changes at higher elevations. For the MS scenario, there were greater changes to ET at lower elevations, though the relationship was not significant (Figure 8). However, removal of an outlier for WS10 (+2 standard deviations) made the regression significant (F-test, $P<0.01$).

Average annual ET estimated for MS species scenario was higher than baseline ET observed in all years from 1986-2005. Average annual ET estimated for XS species scenario was lower than baseline ET observed in all years from 1986-2005.

We found, on average that xeric species use less water than mesic species, though this isn't always true. Studies have shown that given unlimited water supply, xeric species can use more water than mesic species (Tipton, 1994). When examining the response curves for the sap flow models, the xeric species were not the lowest water users (Figure 6). We found that *L. tulipifera* and *B. lenta* were the highest water users, followed by the xeric species, *P. strobes* and *Q. prinus*. The lowest water users, nearly half the rate as the xeric species, were *Q. rubra* and *T. canadensis*. Lower proportions of *Q. rubra* and *T. Canadensis* relative to the proportions of *L. tulipifera* and *B. lenta* kept the overall MS transpiration higher than the XS transpiration. Additionally, converting to more xeric species had less of an impact on the original ET than the conversion to more mesic species potentially due to the higher transpiration rates from *L. tulipifera* and *B.*

lenta and the current composition. Our estimated forest cover is originally more xeric, so a shift to more mesic species would have a greater impact on transpiration.

When species conversions were performed according to terrain shape, converting coves to 100% *L. tulipifera* increased ET by 17% on average, ranging from 8% to 29%, with a standard deviation of 7%. Higher elevation watersheds were less impacted by the conversion, with low elevation watersheds showing the highest percentage increases. The proportion of coves in a watershed does not vary by elevation, so this cannot be the explanation. *L. tulipifera* had the highest transpiration, particularly at higher VPD and warmer temperatures, which occur more frequently at lower elevation sites. Cove conversions increased ET the most in years with low precipitation (ρ=0.96; Figure 9). The opposite was true for the ridge conversion to xeric species. The ridge conversion decreased ET more in years with higher precipitation (ρ=0.94). The ridge conversion decreased ET by 4% on average ranging from -0.2% to -10%, with a standard deviation of 5%.

Studies confirm transpiration varies among tree taxa on a leaf and tree basis where consistent differences in rates have been measured between conifers and hardwoods (Ewers et al., 2002). Conifers have higher transpiration rates than deciduous species due to higher LAIs, and increased spring and fall transpiration, when leaves are not present but needles are. Transpiration rates have been measured across a variety of species, including red and silver birch (*Betula lenta and B. pendula*) (Kelliher et al., 1992), willow (*Salix spp.*) (Lindroth et al., 1995), oak (*Quercus spp.*) (Granier et al.,

1996), beech (*Fagus spp.*) (Granier et al., 2000), cottonwood (*Populus spp.*) (Schaeffer et al., 2000) red maple (*Acer rubrum*), loblolly pine (*Pinus taeda*), chestnut oak (*Q. prinus*), white oak (*Q. alba*), red oak (*Q. rubra*), yellow-poplar (*Liriodendron tulipifera*) (Wilson et al., 2001), black gum (*Nyssa sylvatica*) (Wullschleger et al., 2001), Japanese cedar (*Cupressus japonica*) (Kumagai et al., 2005), apricot (*Prunus armeniaca*) (Nicolas et al., 2005) and white pine (*Pinus strobus*) (Ford et al., 2007). This variation between species results from differences in physiological factors, including stomatal conductance and responsiveness to climate, and in structural characteristics such as rooting depth, leaf area, canopy architecture, and the amount and permeability of sapwood (Ewers et al., 2002; Vose et al., 2003; Kumagai et al., 2005; Ford et al., 2007). Differences in transpiration rates among woody species may impact total catchment transpiration and alter streamflow. Previous studies have shown that changes in species composition can impact stand ET and total catchment yield (Bosch and Hewlett, 1982; Hornbeck et al., 1993; Ewers et al., 2002; Wattenbach et al., 2007).

Comparisons to other studies that examine impacts on ET from changing or different species composition are difficult because no known study used a similar species set to ours. However, we can compare results generally. For example, Hornbeck et al. (1993) found a 21% decrease in water yield on stands that had converted from equal amounts of beech, birch, and maple species to 80% birch and pin cherry with the remainder divided between beech and maple. Though this result was higher than our average changes, it fell within the range for our conversion of coves to *L. tulipifera*, 8%-29%.

Ewers et al. (2002) examined differences in canopy transpiration by species composition in northern Wisconsin. They found northern hardwoods had the lowest daily canopy transpiration, with wetland cover types and conifers in second just shy of twice that of the northern hardwoods. Aspen/fir had the highest, nearly three times higher than northern hardwoods. Aspen is in some ways similar to L. tulipifera, with higher water use and productivity per unit leaf, but tree size, leaf area, and other factors are substantially different among these species, as are tree-level, water-use, and response to climate. We did not find differences this large, possibly because our different set of species. Our conifers were dominated by white pine, with little fir. Climate differences between northern Wisconsin and the SA could also explain the difference in magnitude, including warmer temperatures, higher precipitation, and increased humidity in the SA.

Bosch and Hewlett (1982) reviewed 94 catchment studies examining the impacts of basal area reduction and species changes on water yield. Studies examining the species conversion primarily went from hardwoods to conifers and results varied from a 14% to 54% reduction in water yield. The larger values were found in areas of high precipitation and in studies that converted a higher proportion of the watershed to conifer. The average change across similar studies was approximately a 30% reduction in water yield. Our study did not convert hardwoods to conifers, though it is important to note converting to conifer would probably be a greater impact on ET than converting within hardwood species, as our study shows.

Combined Scenarios

Temperature changes, when combined with species compositional shifts, impacted baseline ET with a cumulative effect (Figure 10). As we have discovered, increasing temperature uniformly increased baseline ET and increasing temperature more at night decreased ET. Additionally, conversion to greater xeric species decreased ET and the conversion to more mesic species increased ET. As expected, when we combined mesic species conversion and uniform temperature increases, ET increased, more so for greater temperature increases. Additionally, for uneven increases in night temperature in combination with a conversion to mesic species, ET increased, but less than temperature increases. Results for the conversion to more xeric species shows the combinatorial effect of a decrease from the species shift and an increase from the uniform temperature increase. Converting to more xeric species will lessen the impact from uniform increases in temperature. For night biased increases in temperature, the xeric species conversion amplified the decrease in ET.

Model Limitations

Limitations from our models may play a role in our estimates of climate change impacts and species change impacts. Sap flow derived ET estimates are strongly driven by LAI (Scanlon and Albertson, 2003). Both differences in LAI duration, phenologies, and LAI maximums will impact sap flow ET estimates. Dates used for the initiation of budburst, full leaf, and leaf senescence in this study were estimated using regionally developed relationships with climate variables and elevation (Kove and Bolstad, in prep). Our models were developed at CHL with data from 2003 through 2009 using 8 species at

two different locations. Though the RMSE of the models on CHL averaged around 3 days, error may be larger for our study due to higher species diversity, wider ranges of elevation, and wider ranges of latitude. Therefore, variation in watershed error may be a result of the differences in phenological dates across the SAR unexplained by our phenological models.

LAI maximums will also impact ET estimates. Bolstad et al's (2001) terrain driven LAI model was developed in the region with R^2=0.58. Error in estimates of LAI may explain the differences in RMSE among watersheds. A Monte Carlo analysis shows increased error in ET due to LAI parameter variability (Kove and Bolstad, in prep). ET mean error and mean LAI were significantly correlated, though that may be a result of the strong relationship with LAI and elevation (Bolstad et al., 2001)

Further, species composition was estimated using county-level FIA data, and given some of our small watersheds and elevation ranges, accuracy could be questioned. Species composition and distribution may affect ET estimates from sap flow models and give different results under our changing landscape. Combining nonlinear ET models and linear species composition models will give us different ET values depending on our initial species composition. We used the most accurate, current, widely-available data on species composition, though accuracy of species compositions was not analyzed. Our observed differences in transpiration from the species sap flow models, run individually and in our MCMC tests shows a change in composition may result in larger changes in ET. For example, daily *L. tulipifera* transpiration estimated with our sap flow models

was nearly three times larger than all other species under equal climate conditions and LAI. Shifts in species composition could possibly impact sap flow estimates of ET significantly.

Further, our models assume there is zero net ground storage change. Any bias should diminish over time, because the longer time periods average the net change over many years. When averaging results over the 20 year period, overall error statistics are significantly decreased for a majority of the watersheds and years than compared to individual years on individual watersheds. Extreme maxima and minima range between -48% and 192% error. Ground water storage changes over the annual water year are most likely not zero, as commonly assumed (Wilson et al., 2001; Ford et al., 2007; Oishi et al., 2008), although in most years in the SA, winter rainfall brings soils to near saturation. One study examined the relationship between catchment water balance error and soil water storage level and found that at the monthly and seasonal time scale, there was a significant relationship between error and soil moisture (Essery, 1992). However, at the annual time scale and for all study watersheds, there were no significant relationships between catchment water balance error and ground water storage level, suggesting that at the annual time scale, the assumption of negligible net storage differences is valid.

Additionally, we only examined changes in overstory species composition. Most studies have been conducted on extremely small watersheds where a large percentage of the trees are measured, including understory trees and shrubs. Understory transpiration

was ignored in our models since the only accessible estimate of LAI was that of the canopy. A closed canopy should result in low understory transpiration. However, Wullschleger et al. (2001) found in a deciduous stand at Oak Ridge, Tennessee that understory transpiration was 17% of the total stand transpiration. Species conversion was only performed for overstory species, so estimates of change may be impacted by not including the understory.

Another limitation to our model was the exclusion of soil moisture, since plants can respond to soil moisture differently (Xu and Singh, 2005). Our mesic species may be more sensitive to dry soils, particularly on upper coves or side-slopes. However, our models assume there were no differences because the best measurement data did not show a great deal of soil response in individual plant ET at our measurement sites. Ignoring this may lead to higher ET estimates with MS replacement that are warranted, particularly at low elevations.

Our transpiration models also do not include precipitation timing. Both seasonal timing and daily timing were not considered in our model and may impact transpiration. Further, they might have a species affect. Rainfall all through the growing season may be more effective than concentrated early in the growing season. Rainfall in the afternoon may decrease transpiration more than morning rainfall. Species may respond to rainfall differently as well, though we do not resolve precipitation timing, nor enter it into our model.

Conclusion

In conclusion, we find that temperature matters, at least according to our models. More importantly, relative night time and daytime temperatures matter, changing the impacts of changing climate on transpiration from a positive to a negative, even with an equal mean increase. Changes in temperature, however, may also interact with cloudiness, which our model does not account for. Cloudiness affects insolation, a driving force of ET. Another important consideration is the assumption our model used to estimate VPD. Our results are based on the theory that in an area of high humidity, saturation vapor pressure occurs at the minimum daily temperature. Our tests confirm this is true at CHL for approximately 80% of the growing season nights. If this assumption is wrong for the rest of SAR then daytime VPD may be greater than we estimate when we increase night time temperatures more than daytime temperatures and hence we may be underestimating ET under higher night time temperatures relative to daytime.

Species conversion results may be impacted by shifts in LAI. Changes in species composition may affect LAI, even if equal basal area remained. For example, stands of white pine generally have higher LAI than stands of birch, so a conversion to more white pine would come with an increase in LAI, further increasing ET. However, since LAI was estimated using an elevation based relationship, converting LAI with our species compositional shifts was beyond the reach of our study.

Regarding species conversion, the literature has shown that changes in species composition impact ET. We found similar results, where species changes were significant to ET and varied based on the species changes. The largest response was from mesic species. Our results examined the most important impacts. However, the incomplete knowledge of species and their distribution, LAI, and soil storage could have impacts on our results though none were significant in our sap flow equations, and are generally not significant in other sap flow equations. We found that the day/night balance in temperature change is important to examine, that species composition is also significant, and the change in species composition across space and through time can be significant. Further studies are needed to better quantify these impacts.

Further investigation to examine the night biased temperature scenarios are needed to determine the parameters required for a decrease in ET including ranges in temperature, VPD, PAR, species, and elevation. Also, the impact on ET from potential changes in understory species would improve on this analysis. Finally, including precipitation in our sap flow models would allow us to examine the impacts from the variable timing of precipitation events.

Watershed ID	County(s)	Area (sq km)	Avg Temp (^{o}C)	Mean Elevation (m)	Elevation Range (m)	Percent Forested (%)
1	Caldwell and Watauga	74.6	12.7	658	(368, 1183)	100
2	Clay and Macon	134.4	10.3	1212	(932, 1667)	100
3	Burke	66.6	13.6	550	(343, 880)	99
4	Transylvania	104.6	11.5	975	(628, 1820)	98
5	Buncombe	37.8	9.8	1287	(805, 1950)	100
6	Buncombe	14.1	10.0	1243	(837, 1724)	100
7	Haywood	71.5	8.9	1458	(902, 1942)	100
8	Haywood	86.8	9.3	1406	(864, 1942)	100
9	Haywood	127.4	9.9	1213	(751, 1848)	100
10	Yancey	112.1	10.1	1192	(812, 2028)	100
11	Macon	48.6	10.7	1190	(985, 1499)	98
12	Transylvania	30.3	11.7	948	(687, 1230)	99
13	Transylvania and Henderson	69.4	12.4	880	(767, 1151)	98
14	Wilkes and Watauga	124.6	12.7	632	(329, 1248)	100
15	Macon	0.1	13.2	860	(726, 993)	100

Table 1 (Continued on next page): Watershed characteristics from 1986-2005 for 15 watersheds (WS1-WS15), where percent yield = runoff/rainfall*100 averaged for each watershed.

Watershed ID	Rainfall (mm/yr)	Runoff (mm/year)	Water Yield (%)	Cove Landform (%)	Side Slope Landform (%)	Ridge Landform (%)
1	1332	596	43	42	21	37
2	2115	1347	63	40	27	33
3	1365	627	44	35	31	34
4	1702	1068	61	39	26	34
5	1689	1010	59	39	28	33
6	1573	695	43	41	25	34
7	1988	1249	62	38	27	34
8	2010	1266	62	39	27	34
9	1713	793	46	41	22	36
10	1626	1099	66	37	31	32
11	2165	1486	68	31	43	26
12	1781	1039	57	42	23	35
13	1637	1171	70	31	41	27
15	1299	673	50	40	23	37
CS18	2007	1001	49	31	35	34

Table 1 (Continued from previous page): Watershed characteristics from 1986-2005 for 15 watersheds (WS1-WS15), where percent yield = runoff/rainfall*100 averaged for each watershed.

	Run Description	*Average ET (mm year^{-1})*	*Difference (mm year^{-1})*	*Percent Difference (%)*
	control	592.8		
Temperature Changes	*3.5*	665.6	72.8	12.27
	7	708.4	115.7	19.56
	3.5 night time	576.3	-16.5	-2.81
Species Changes	*MS*	638.5	45.8	7.75
	XS	578.7	-14.1	-2.38

Table 2: Average ET run results for our six tested temperature and species scenarios compared to ET_{C_T}. Difference is the averaged annual difference between each run result and ET_{C_T}, and percent difference = estimated ET/ ET_{C_T}*100. MS = conversion to 80% mesic species, and XS = conversion to 80% xeric species. 3.5 = ET simulation increasing mean temperature 3.5 ^{o}C. 7 = ET Simulation increasing mean temperature 7 ^{o}C. 3.5 night = ET simulation increasing night temperature more than day temperature with a mean increase of 3.5 ^{o}C.

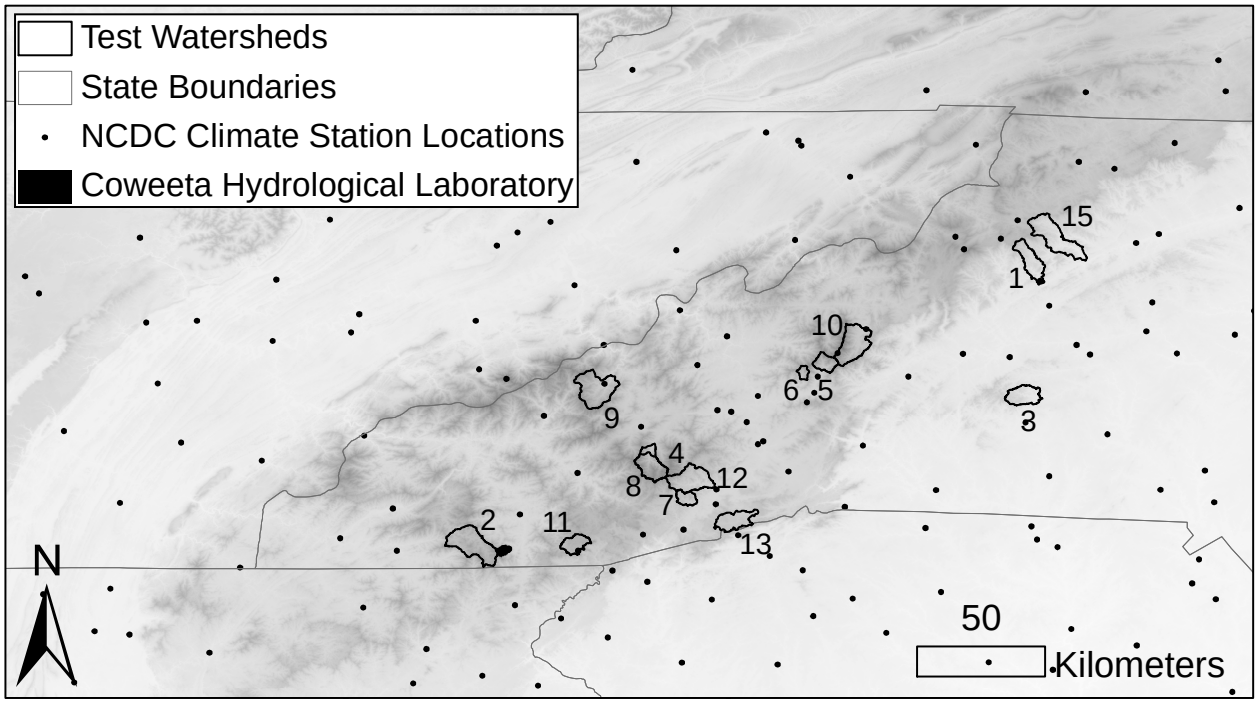

Figure 1: Study area, the southern Appalachian region (SAR). Fifteen test watershed boundaries, and 134 climate station locations.

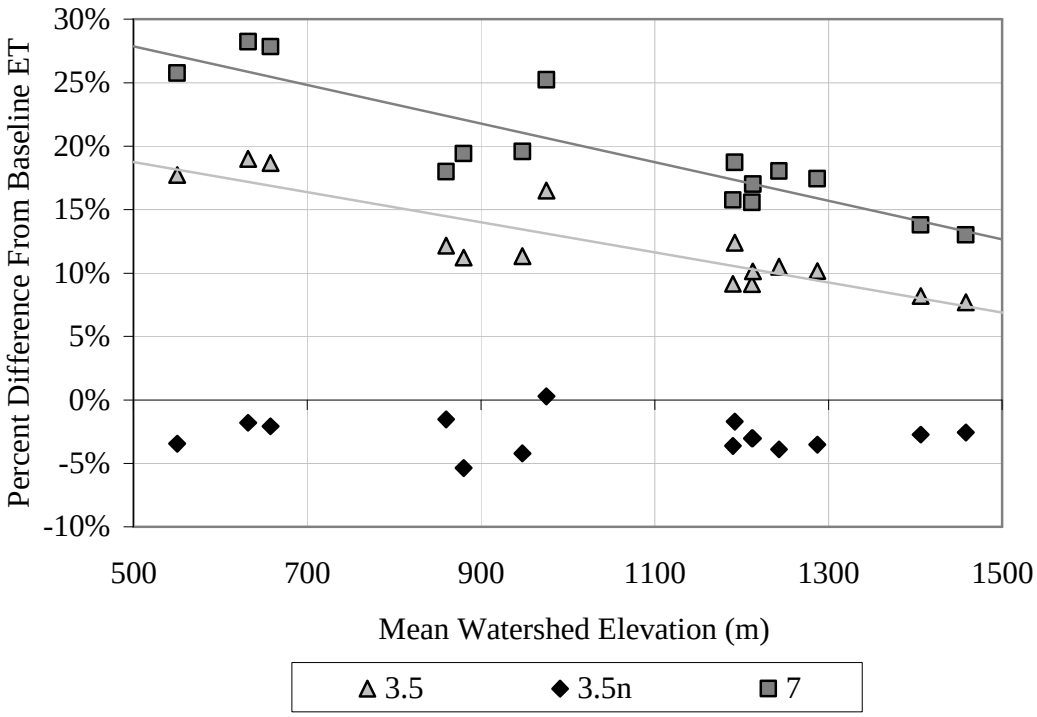

Figure 2: Relationship between ET estimation response to temperature scenarios and mean watershed elevation. There were 15 watersheds analyzed (WS1-WS15) from 1986-2005. Significant relationships were found for temperature increases of 3.5 ^{o}C and 7 ^{o}C, but not for the night biased 3.5n ^{o}C increase. 3.5 = ET simulation increasing mean temperature 3.5 ^{o}C. 7 = ET Simulation increasing mean temperature 7 ^{o}C. 3.5 n = ET simulation increasing night temperature more than day temperature with a mean increase of 3.5 ^{o}C.

3.5 ^{o}C: $Y = -0.0002 \cdot X + 0.3548$; $R^2 = 0.78$

7 ^{o}C: $Y = -0.0001 \cdot X + 0.2469$; $R^2 = 0.78$

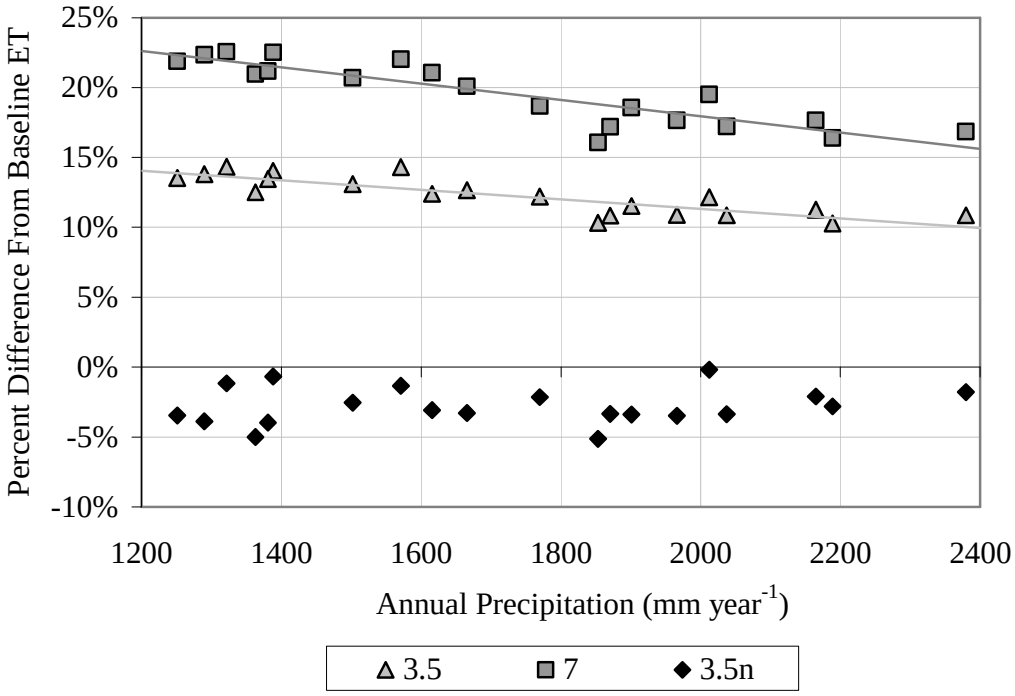

Figure 3: Relationship between ET estimation response to temperature scenarios and annual precipitation. There were 15 watersheds analyzed (WS1-WS15) from 1986-2005. Significant relationship found for temperature increases of 3.5 ^{o}C and 7 ^{o}C, but not for the minimum temperature bias 3.5 ^{o}C increase. 3.5 = ET simulation increasing mean temperature 3.5 ^{o}C. 7 = ET Simulation increasing mean temperature 7 ^{o}C. 3.5 n = ET simulation increasing night temperature more than day temperature with a mean increase of 3.5 ^{o}C.

7 ^{o}C:	$Y = 0.00006 \cdot X + 0.2962;$	$R^2 = 0.78$
3.5 ^{o}C:	$Y = 0.00005 \cdot X + 0.1817;$	$R^2 = 0.72$

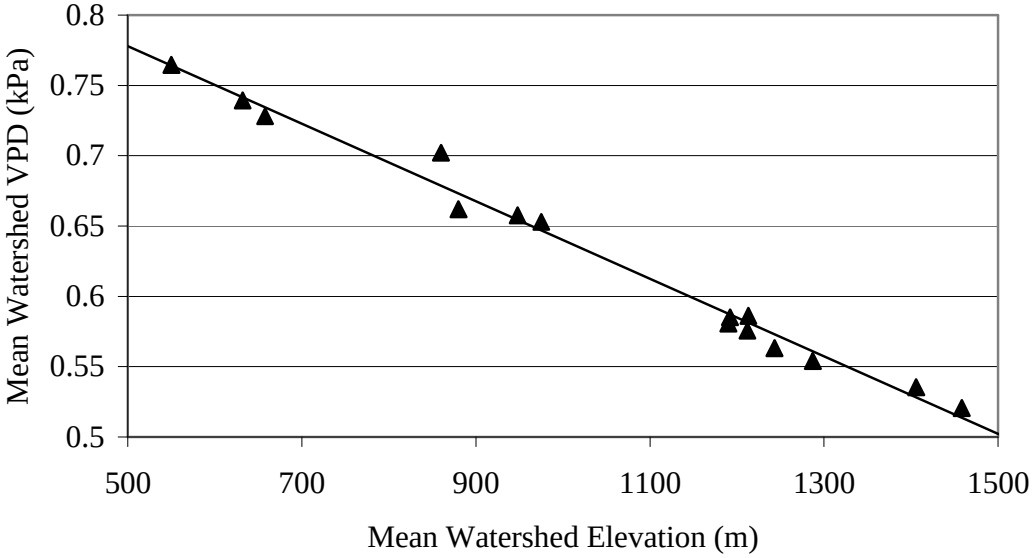

Figure 4: Mean watershed elevation versus mean daytime VPD (kPa) for the growing season, averaged over our 20 year study period (1986-2005) under the originally measured climate.

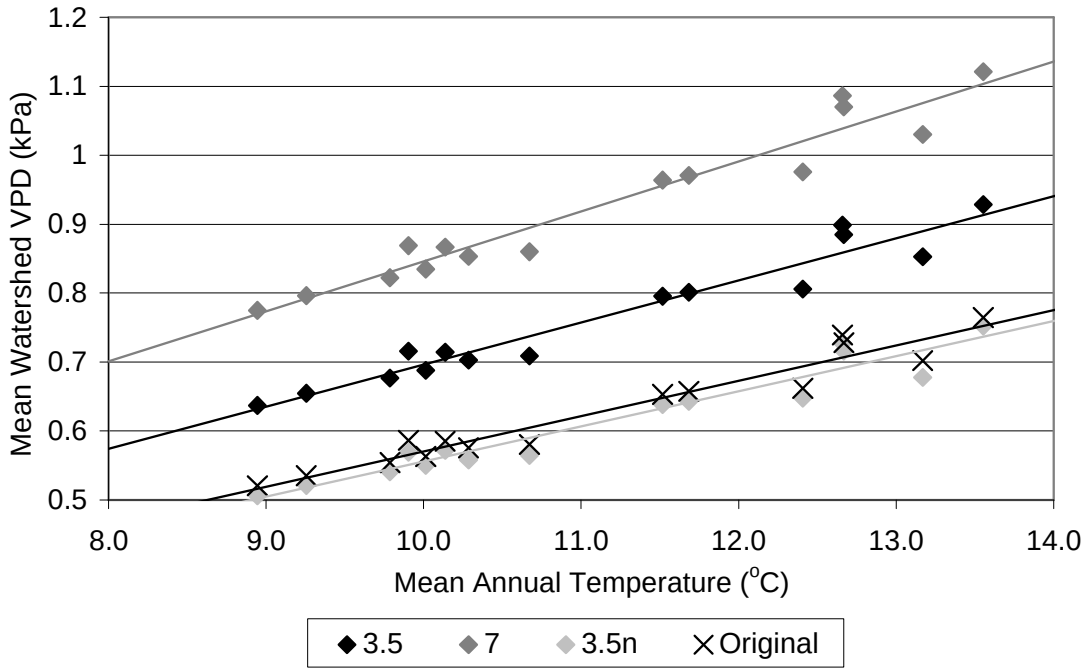

Figure 5: Mean annual temperature versus mean watershed daytime VPD for the growing season, averaged over our 20 year study period (1986-2005) under the originally measured climate. 3.5 = ET simulation increasing mean temperature 3.5 ^{o}C. 7 = ET Simulation increasing mean temperature 7 ^{o}C. 3.5n = ET simulation increasing night temperature more than day temperature with a mean increase of 3.5 ^{o}C. Original = original temperature.

3.5 ^{o}C:	$Y = 0.0611 \cdot X + 0.0857$; $R^2 = 0.94$
7 ^{o}C:	$Y = 0.0725 \cdot X + 0.1205$; $R^2 = 0.94$
3.5n ^{o}C:	$Y = 0.051 \cdot X + 0.0454$; $R^2 = 0.93$
Original:	$Y = 0.05121 \cdot X + 0.0585$; $R^2 = 0.94$

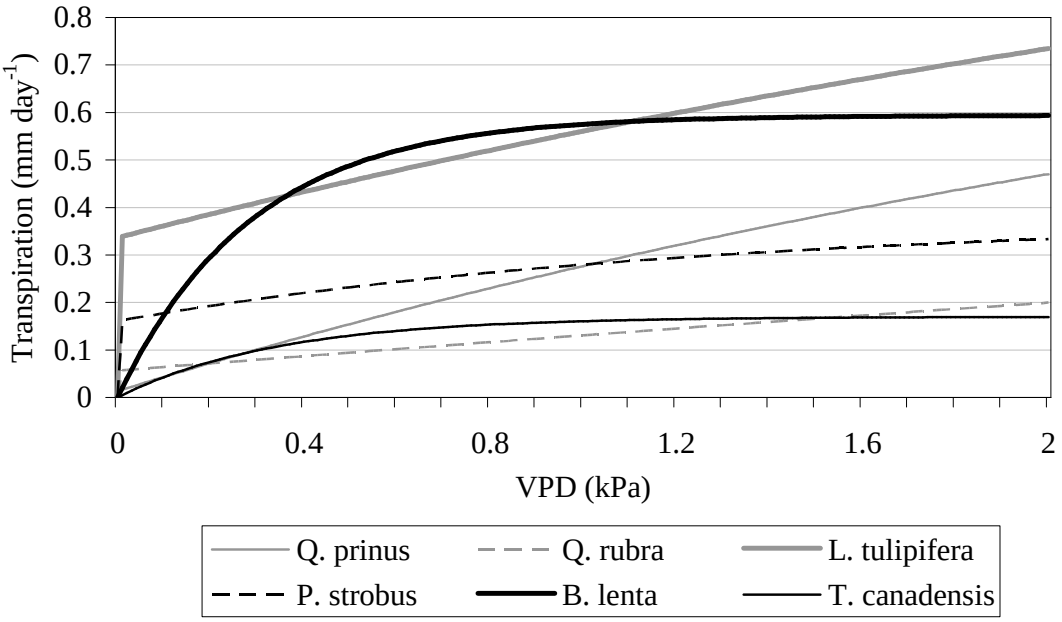

Figure 6: Comparison of daily transpiration relationship with VPD by species. Day of year 200 and PAR value of 900 μmol m^{-2} s^{-1} were used in the transpiration sap flow equations.

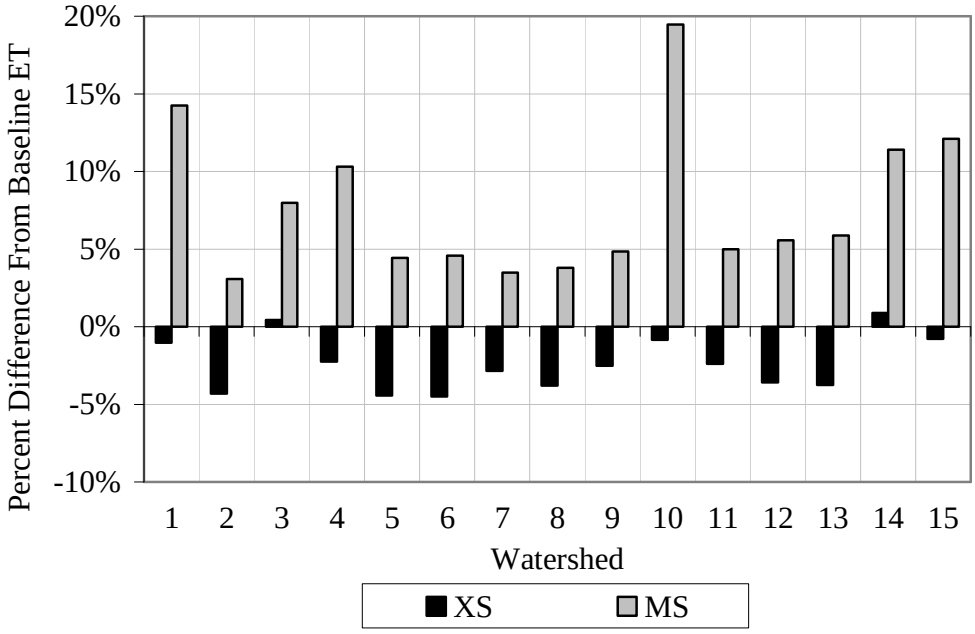

Figure 7: Percentage differences between baseline values of ET and species scenario estimates of ET by watershed, averaged over 1986-2005. MS = conversion to 80% mesic species, and XS = conversion to 80% xeric species.

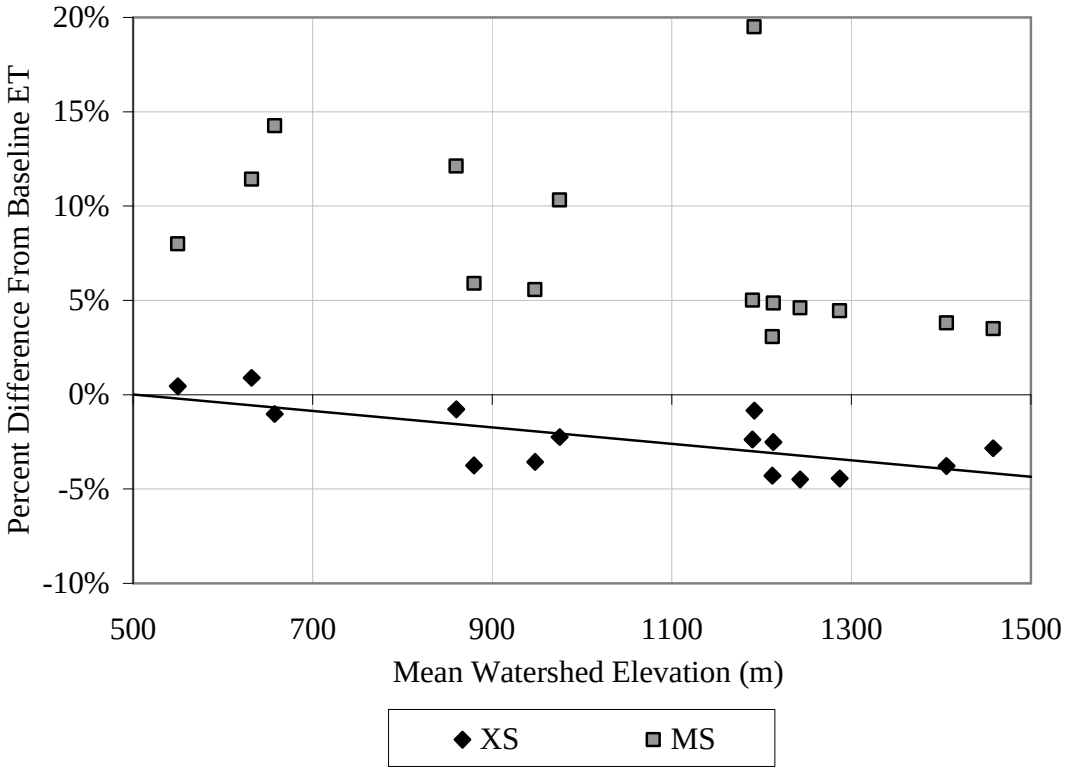

Figure 8: Relationship between mean watershed elevation and percentage difference from baseline ET of species scenario estimated ET averaged over 1986-2005. Significant relationship found for XS scenario. MS = conversion to 80% mesic species, and XS = conversion to 80% xeric species.

MS: $Y = -0.00008 \cdot X + 0.1618$; $R^2 = 0.23$

XS: $Y = -0.00005 \cdot X + 0.0219$ $R^2 = 0.50$

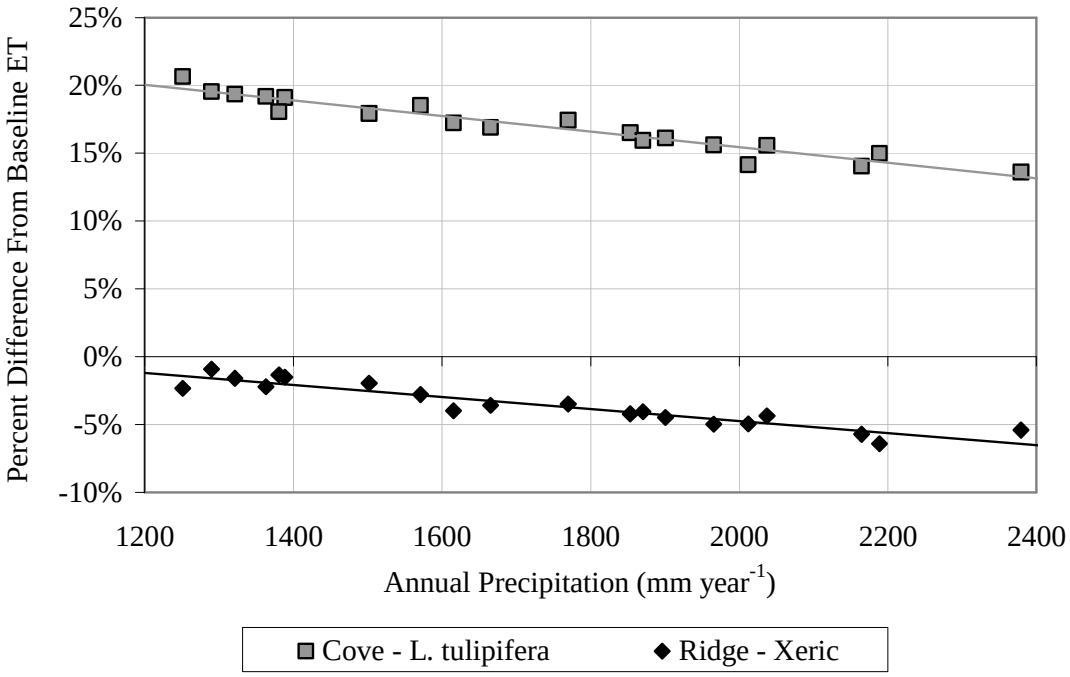

Figure 9: Annual precipitation plotted against estimated ET difference from baseline ET, averaged from 1986-2005. Estimated ET from the terrain shape analysis conversion of cove cells to *L. tulipifera* and ridge cells to xeric species. Transpiration was calculated with new conversion and compared to the baseline ET.

Cove: $Y = -0.00006 \cdot X + 0.2695$; $R^2 = 0.93$

Ridge: $Y = -0.00004 \cdot X + 0.0416$ $R^2 = 0.88$

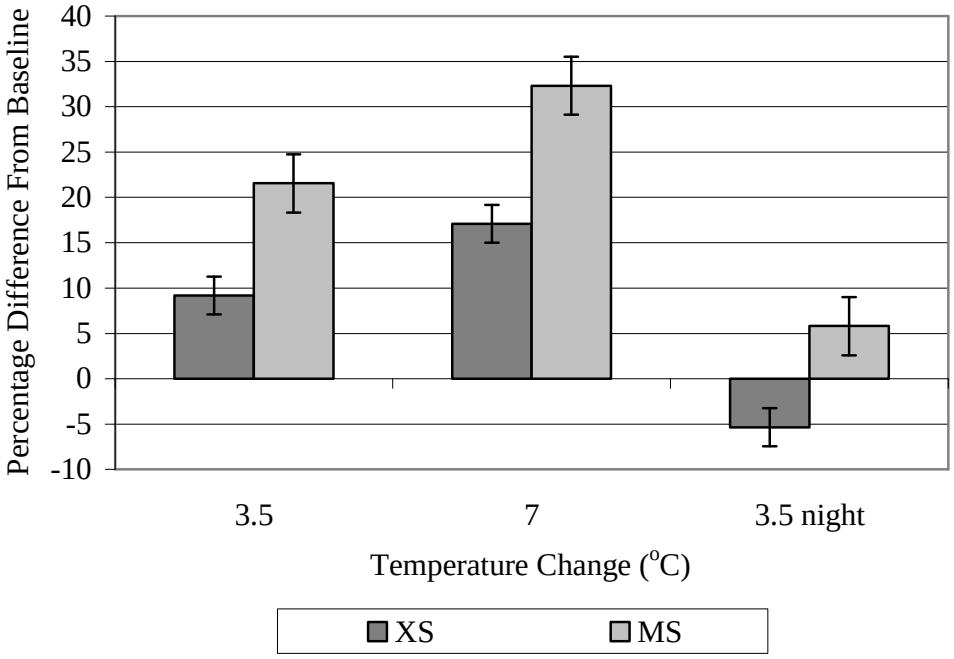

Figure 10: Percentage difference from baseline ET of the six combined temperature and species scenarios calculated and averaged across 15 watersheds (WS1-WS15) from 1986-2005. MS = conversion to 80% mesic species, and XS = conversion to 80% xeric species. 3.5 = ET simulation increasing mean temperature 3.5 ^{o}C. 7 = ET Simulation increasing mean temperature 7 ^{o}C. 3.5 night = ET simulation increasing night temperature more than day temperature with a mean increase of 3.5 ^{o}C. Error bars represent +/- 2 standard deviations.

Bibliography

Abraha, M.G., and M.J. Savage. 2008. Comparison of estimates of daily solar radiation from air temperature range from application in crop simulations. Agricultural and Forest Meteorology 148:401-416.

Adeck, F.W., A. Bondeau, K. Bottcher, D. Doktor, W. Lucht, J. Schaber, and S. Sitch. 2004. Responses of spring phenology to climate change. New Phytologist 162:295-309.

Ahrens, B. 2006. Distance in spatial interpolation of daily rain gauge data. Hydrology and Earth System Sciences 10:197-208.

Alados, I., I. Foyo-Moreno, and L. Alados-Arboledas. 1996. Photosynthetically active radiation: Measurements and modelling. Agricultural and Forest Meteorology 78:121-131.

Alley, W.M., R.W. Healy, J.W. Labaugh. 2002. Flow and storage in groundwater systems. Science 296:1985-1991.

Amatya D.M., and C. Trettin. 2007. Annual evapotranspiration of a forested wetland watershed, SC. In: 2007 ASABE Annual International Meeting, 17-20 June. 16 p.

Annandale, T. 1999. The eastern water wars. Governing (August): 30-34.

Annandale, J.G., N.Z. Jovanic, N. Benade, and R.G. Allen. 2002. Software for missing data error analysis of Penman-Monteith reference evapotranspiration. Irrigation Science 21:57-67.

Antonio, B.M., E. Caetano, V. Magana, R.B. Silveira, and R. Dominguez. 2009. Rainfall estimation from a combination of TRMM precipitation radar and GOES multispectral satellite imagery through the use of an artificial neural network. Atmosfera 22:299-313.

Arnell, N.W. 1992. Factors controlling the effects of climate change on river flow regimes in a humid temperate environment. Journal of Hydrology 132:321-342.

Arnell, N.W., and Liu C. 2001. Hydrology and water resources. P. 191-233 *in* Climate Change 2001: Impacts, Adaptation and Vulnerability. Contribution of Working Group II to the Third Assessment Report of the Intergovernmental Panel on Climate Change. Canziani, O.F., D.J. Dokken, N.A. Leary, J. J. McCarthy, and K.S. White (eds.). Cambridge University Press, Cambridge, U.K.

Arrandale, T. 1999. The eastern water wars. Governing Magazine Feature, 30-33 pp.

Ashcroft, M.B., L.A. Chrisholm, and K.O. French. 2009. Climate change at the landscape scale: predicting fine grained spatial heterogeneity in warming and potential refugia for vegetation. Global Change Biology 15:656-667.

Ayres, M.P., and M.J. Lonbardero. 2000. Assessing the consequences of global change for forest disturbance from herbivores and pathogens. The Science of the Total Environment 262:263-286.

Bale, J.S., G. J. Masters, I. D. Hodkinson, C. Awmack, T.M. Bezemer, V.K. Brown, J. Butterfield, A. Buse, J.C. Coulson, J. Farrar, J.E.G. Good, R. Harrington, S. Hartley, T.H. Jones, R.L. Lindroth, M.C. Press, I. Symrnioudis, A.D. Watt, and J.B. Whittaker. 2002. Herbivory in global climate change research: direct effects of rising temperature on insect herbivores. Global Change Biology 8:1-16.

Ball, R.A., L.C. Purcell, and S.K. Carey. 2004. Evaluation of solar radiation prediction models in North America. Agronomy Journal 96:391–397.

Battaglia, M., and P.J. Sands. 1998. Process-based forest productivity models and their application in forest management. Forest Ecology and Management 102:13-13-32.

Bedient, P.B., and W.C. Huber. 1992. Hydrology and Floodplain Analysis. Addison-Wesley Publishing Co., New York. 816 p.

Bellerby, T., M. Todd, D. Kniveton, and C. Kidd. 2000. Rainfall estimation from a combination of TRMM precipitation radar and GOES multispectral satellite imagery through the use of an artificial neural network. Journal of Applied Meteorology 39:2115-2128.

Bernier, P.Y., P. Bartlett, T.A. Black, A. Barr, N. Klijun, and J.H. McCaughey. 2006. Drought constraints on transpiration and canopy conductance in mature aspen and jack pine stands. Agricultural and Forest Meteorology 140:64-78.

Beven, K. 1989. Changing ideas in hydrology - The case of physically-based models. Journal of Hydrology 105:157-172.

Biftu, G.F., and T.Y. Gan. 2000. Assessment of evapotranspiration models applied to a watershed of Canadian prairies with mixed land-uses. Hydrological Processes 14:1305-1325.

Blackburn, W.J., and J.T.A. Proctor. 1983. Estimating photosynthetically active radiation from measured solar irradiance. Solar Energy 31:233-234.

Bois, B., P. Pieri, C. Van Leeuwen, L. Wald, L. Huard, J.P. Gaudillere, and E. Saur. 2008. Using remotely sensed solar radiation data for references evapotranspiration estimation at a daily time step. Agricultural and Forest Meteorology 148:619-630.

Bolstad, P.V., W.T. Swank, and J.M. Vose. 1998. Predicting southern Appalachian overstory vegetation with digital terrain data. Landscape Ecology 13:271-283.

Bolstad, P.V., L.W. Swift Jr., F. Collins, and J. Regniere. 1998. Measured and predicted air temperature at basin to regional scales in the southern Appalachian mountains. Agricultural and Forest Meteorology 91:161-176.

Bolstad, P.V., J.M. Vose, and S.G. McNulty. 2001. Forest productivity, leaf area, and terrain in southern Appalachian deciduous forests. Forest Science 47:419-427.

Borga, M., and A. Vizzaccaro. 1997. On the interpolation of hydrologic variables: formal equivalence of multiquadratic surface fitting and kriging. Journal of Hydrology 195:160-171.

Bosch, J.M., and J.D. Hewlett. 1982. A review of catchment experiments to determine the effect of vegetation changes on water yield and evapotranspiration. Journal of Hydrology 55:3-23.

Boyer, E.W., C.L. Goodale, N.A. Jaworski, and R.W. Howarth. 2002. Anthropogenic nitrogen sources and relationships to riverine nitrogen export in the northeastern USA. Biogeochemistry 57-58:137-169.

Boyles, R.P., and S. Raman. 2003. Analysis of climate trends in North Carolina (1949–1998). Environment International 29:263-275.

Breda, N., H. Cochard, E. Dreyer, and A. Granier. 1993. Water transfer in a mature oak stand (*Quercus petraea*): seasonal evolution and effects of a severe drought. Canadian Journal of Forestry Research 23:1136-1143.

Breda, N.J.J. 2003. Ground-based measurements of leaf area index: a review of methods, instruments and current controversies. Journal of Experimental Botany 54:2403-2417.

Bristow, K.L., and G.S. Campbell. 1984. On the relationship between incoming solar radiation and daily maximum and minimum temperature. Agricultural and Forest Meteorology 31:159-166.

Brown, L.B., and B. Allen-Diaz. 2009. Forest stand dynamics and sudden oak death: Mortality in mixed-evergreen forests dominated by coast live oak. Forest Ecology and Management 257:1271-1280.

Budyko, M.I. 1956. The heat balance of the earth's surface. U.S. Dept. of Commerce, Weather Bureau, Washington. 259 p.

Buytaert, W., R. Celleri, P. Willems, and B. De Bievre. 2006. Spatial and temporal rainfall variability in mountainous areas: A case study from the south Ecuadorian Andes. Journal of Hydrology 329:413-421.

Calder, I.R., and M.D. Newson. 1979. Land use and upland water resources in Britain - a strategic look. Water Resources Bulletin 16:1628-1639.

Campbell, G.S., and J.M. Norman. 1998. An introduction to environmental biophysics. Springer-Verlag, New York. 286 p.

Cannell, M.G.R., and R.I. Smith. 1983. Thermal time, chill days and prediction of budburst in *Picea sitchensis*. Journal of Applied Ecology 20:951-963.

Carpenter, T.M., K.P. Georgakakos, and J.A. Sperfslagea. 2001. On the parametric and NEXRAD-radar sensitivities of a distributed hydrologic model suitable for operational use. Journal of Hydrology 253:169-193.

Carrera-Hernandez, J.J., and S.J. Gaskin. 2007. Spatio temporal analysis of daily precipitation and temperature in the Basin of Mexico. Journal of Hydrology 336:231-249.

Carter, G.A., W.K. Smith, and J.L. Hadley. 1988. Stomatal conductance in three conifer species at different elevations during summer in Wyoming. Canadian Journal of Forestry Research 18:242-246.

Castellvi, F., P.J. Perez, J.M. Villar, and J.I. Rosell. 1996. Analysis of methods for estimating vapor pressure deficits and relative humidity. Agricultural and Forest Meteorology 82:29-45.

Cellier, P., and A. Olioso. 1993. A simple system for automated long term Bowen ratio measurement. Agricultural and Forest Meteorology 66:81-92.

Cermak, J., E. Cienciala, J. Kucera, A. Lindroth, and E. Bednafova. 1995. Individual variation of sap flow rate in large pine and spruce trees and stand transpiration: a pilot study at the central NOPEX site. Journal of Hydrology 168:17-27.

Chalecki, E.L., and P.H. Gleick. 1999. A framework of ordered climate effects on water resources: a comprehensive bibliography. Journal of the American Water Resource Association 35:1657-1665.

Chason, J.W., D.D. Baldocchi, and M.A. Huston. 1991. A comparison of direct and indirect methods for estimating forest canopy leaf area. Agricultural and Forest Meteorology 57:107-128.

Chen, H., S. Guo, C. Xu, and V.P. Singh. 2007. Historical temporal trends of hydro-climatic variables and runoff response to climate variability and their relevance in water resource management in the Hanjiang basin. Journal of Hydrology 344:171-184.

Chen, J.M. 1996. Optically-based methods for measuring seasonal variation of leaf area index in boreal conifer stands. Agricultural and Forest Meteorology 80:135-163.

Cheng, W., H. Sakai, K. Yagi, and T. Hasegawa. 2009. Interactions of elevated [CO_2] and night temperature on rice growth and yield. Agricultural and Forest Meteorology 149:51-58.

Chiew, F.H.S., P.H. Whetton, T.A. McMahon, and A.B. Pittock. 1995. Simulation of the impacts of climate change on runoff and soil moisture in Australian catchments. Journal of Hydrology 167:121-147.

Chmura, D.J. 2006. Phenology differs among Norway spruce populations in relation to local variation in altitude of maternal stands in the Beskidy Mountains. New Forests 32:21-31.

Chmura, D.J., and R. Rozkowski. 2002. Variability of beech provenances in spring and autumn phenology. Silvae Genet 51:123-127.

Chua, S.H., and R.L. Bras. 1982. Optimal estimators of mean areal precipitation in regions of orographic influence. Journal of Hydrology 57:23-48.

Chuine, I., G. Cambon, and P. Comtois. 2000. Scaling phenology from the local to the regional level: advances from species-specific phenological models. Global Change Biology 6:943-952.

Chuine, I., O. Cour, and D.D. Rousseau. 1999. Selecting models to predict the timing of flowering of temperate trees: implications for tree phenology modeling. Plant, Cell & Environment 22:1-13.

Cienciala, E., H. Eckersten, A. Lindroth, and J. E. Hallgren. 1994. Simulated and measured water uptake by *Picea abies* under non-limiting soil water conditions. Agricultural and Forest Meteorology 71:147-164.

Clark, M.P., and A.G. Slater. 2006. Probabilistic quantitative precipitation estimation in complex terrain. Journal of Hydrometeorology 7:3-22.

Clearwater, M.J., F.C. Meinzer, J.L. Andrade, G. Goldstein, and N.M. Holbrook. 1999. Potential errors in measurement of non-uniform sap flow using heat dissipation probes. Tree Physiology 19:681-687.

Cliff, A., and J.K. Ord. 1981. Spatial processes, model and applications. Pion, London. 260 p.

Clinton, B.D. 2003. Light, temperature, and soil moisture responses to elevation, evergreen understory, and small canopy gaps in the southern Appalachians. Forest Ecology and Management 186:243-255.

Closs, R.L. 1958. The heat pulse method for measuring rate of sap flow in a plant stem. New Zealand Journal of Science 1:281-288.

Cohen, Y., M. Fuchs, and G.C. Green. 1981. Improvement of the heat pulse method for determining sap flow in trees. Plant, Cell & Environment 4:391-391-397.

Cooter, E. J., and G.B. Dhakhwa. 1995. A solar radiation model for use in biological applications in the South and Southeastern USA. Agricultural and Forest Meteorology 78:31-51.

Copeland, L. March 17, 2008. Drought eases, water wars persist. USA Today Feature: http://www.usatoday.com/news/nation/environment/2008-03-17-water-wars_N.htm.

Costa, M. H., and J. A. Foley. 1997. The water balance of the Amazon basin: Dependence on vegetation cover and canopy conductance. Journal of Geophysical Research 102:973-989.

Court, A., and D. Waco. 1965. Means and midranges of relative humidity. Monthly Weather Review 93:517-522.

Cressie, N. 1993. Statistics for spatial data. Wiley-Interscience, New York. 928 p.

Dai, A., K.E. Trenberth, and T.R. Karl. 1999. Effects of clouds, soil moisture, precipitation, and water vapor on diurnal temperature range. Journal of Climate 12:2451-2473.

Day, F.P., and C.D. Monk. 1977. Net primary production and phenology on a southern Appalachian watershed. American Journal of Botany 64:1117-1125.

Day, M.E., J.L. Schedlbauer, W.H. Livingston, M.S. Greenwood, A.S. White, and J.C. Brissette. 2005. Influence of seedbed, light environment, and elevated night temperature on growth and carbon allocation in pitch pine (*Pinus rigida*) and jack pine (*Pinus banksiana*) seedlings. Forest Ecology and Management 205:59-71.

Dellapenna, J.W. 2005. Interstate struggles over rivers: The southeastern states and the struggle over the hooch. N.Y.U. Environmental Law Journal 12:828-900.

DeRocher, T.R., and R.J. Tausch. 1994. Predicting potential transpiration of single leaf pinyon: an adaptation of the potometer method. Forest Ecology and Management 63:169-180.

Diodato, N., and G. Bellocchi. 2007. Modeling solar radiation over complex terrains using monthly climatological data. Agricultural and Forest Meteorology 144:111-126.

Dirks, K.N., J.E. Hay, C.D. Stow, and D. Harris. 1998. High-resolution studies of rainfall on Norfolk Island; Part II, Interpolation of rainfall data. Journal of Hydrology 208:187-193.

Dittmar, C., and W. Willing. 2006. Phenological phases of common beech (*Fagus sylvatica* L.) and their dependence on region and altitude in southern Germany. European Journal of Forest Research:181-188.

Donohue, R.J., M.L. Roderick, and T.R. McVicar. 2007. On the importance of including vegetation dynamics in Budyko's hydrological model. Hydrology and Earth System Sciences 11:983-995.

Dore, M.H.I. 2005. Climate change and changes in global precipitation patterns: What do we know? Environmental International 31:1167-1181.

Douglass, J.E. 1965. Effects of species and arrangement of forests on evapotranspiration. National Science Foundation Advanced Science Seminar, International Symposium of Forest Hydrology Proceedings. 451-461 pp.

Easterling, D.R., and B. Horton. 1997. Maximum and minimum temperature trends for the globe. Science 277:364-367.

Efron, B., and G. Gong. 1983. A leisurely look at the bootstrap, the jackknife, and cross-validation. The American Statistician 37:36-48.

Eisenbies, M.H., W.M. Aust, J.A. Burger, and M.B. Adams. 2007. Forest operations, extreme flooding events, and considerations for hydrologic modeling in the Appalachians - A review. Forest Ecology and Management 242:77-98.

Ellison, A.M., M.S. Bank, B.D. Clinton, E.A. Colburn, K.J. Elliott, C.R. Ford, and B.D. Kloeppel. 2005. Loss of foundation species: consequences for the structure and dynamics of forested ecosystems. Front Ecol Environ 3:479-486.

Ellsworth, D.S. 2000. Seasonal CO_2 assimilation and stomatal limitations in a *Pinus taeda* canopy. Tree Physiology 20:435-445.

Engel, V.C., M. Stieglitz, M. Williams, and K.L. Griffin. 2002. Forest canopy hydraulic properties and catchment water balance: observations and modeling. Ecological Modelling 154:263-288.

Essery, C.I. 1992. Influence of season and balance period on the construction of catchment water balances. Journal of Hydrology 140:171-187.

Ewers, B.E., D.S. Mackay, S.T. Gower, D.E. Ahl, S.N. Burrows, and S.S. Samanta. 2002. Tree species effects on stand transpiration in northern Wisconsin. Water Resources Research 38:8.1-8.11.

Ewers, B.E., D.S. Mackay, J. Tang, P.V. Bolstad, and S. Samanta. 2008. Intercomparison of sugar maple (*Acer saccharum* Marsh.) stand transpiration responses to environmental conditions from the Western Great Lakes Region of the United States. Agricultural and Forest Meteorology 148:231-246.

Falusi, M., and R. Calamassi. 1990. Bud dormancy in beech (*Fagus sylvatica* L.). Effect of chilling and photoperiod on dormancy release of beech seedlings. Tree Physiology 6:429-438.

Federer, C.A., and L.D. Brook. A hydrologic simulation model for eastern forests. Res. Rep. No. 19. Water Resource Research Center, University of New Hampshire. 84 pp.

Fekete, B.M., C.J. Vorosmarty, J.O. Roads, and C.J. Willmott. 2004. Uncertainties in precipitation and their impacts on runoff estimates. Journal of Climate 17:294-304.

Feldman, D.L. 2001. Tennessee's inter-basin water transfer act: a changing water policy agenda. Water Policy 3:1-12.

Fitzjarrald, D.R., O.C. Acevedo, and K.E. Moore. 2001. Climatic consequences of leaf presence in the eastern United States. Journal of Climate 14:598-614.

Flather, C.H., L.A. Joyce, and R.M. King. 1989. Linking multiple resources analysis to land use and timber management: application and error considerations. USDA, Forest Service, Pacific Northwest Forest Experimental Station, General Technical Report PNW GTR-263.

Flint, H.L. 1974. Phenology and genecology of woody plants. P. 83-97 *in* Phenology and seasonality modeling, Lieth, H. (ed.). Springer-Verlag, New York.

Foden, W., G.F. Midgley, G. Hughes, W.J. Bond, W. Thuiller, M.T. Hoffman, P. Kaleme, L.G. Underhill, A. Rebelo, and L. Hannah. 2007. A changing climate is eroding the geographical range of the Namib Desert tree Aloe through population declines and dispersal lags. Diversity and Distributions 13:645-653.

Ford, C.R., R.M. Hubbard, B.D. Kloeppel, and J.M. Vose. 2007. A comparison of sap flux-based evapotranspiration estimates with catchment-scale water balance. Agricultural and Forest Meteorology 145:176-185.

Ford, C.R., and J.M. Vose. 2007. *Tsuga Canadensis* (L.) Carr. mortality will impact hydrologic processes in southern Appalachian forest ecosystems. Ecological Applications 17:1156-1167.

Fracheboud, Y., V. Luquez, L. Bjorken, A. Sjodin, H. Tuominen, and S. Jansson. 2009. The control of autumn senescence in European aspen. Plant Physiology 149:1982-1991.

Freese, F. 1960. Testing Accuracy. Forest Science 6(2):139-145.

Frei, C., and C. Schar. 1998. A precipitation climatology of the Alps from high-resolution rain-gauge observations. International Journal of Climatology 18:873-900.

Gao, Z., Z. Zhang, and X. Zhang. 2009. Responses of water yield to changes in vegetation at a temporal scale. Frontiers of Forestry in China 4:53-59.

Gardenas, A.I., and P. Jansson. 1995. Simulated water balance of scots pine stands in Sweden for different climate change scenarios. Journal of Hydrology 166:107-125.

Garbrecht, J. D., M. Van Liew, and G.O. Brown. 2004. Trends in precipitation, streamflow, and evapotranspiration in the great plains of the United States. Journal of Hydrological Engineering 9:360-367.

Germann, U., M. Berenguer, D. Sempere-Torres, and M. Zappa. 2009. REAL – Ensemble radar precipitation estimation for hydrology in a mountainous region. Quarterly Journal of Royal Meteorological Society 135:445-456.

Gerten, D., S. Schaphoff, U. Haberlandt, W. Lucht, and S. Sitch. 2004. Terrestrial vegetation and water balance—hydrological evaluation of a dynamic global vegetation model. Journal of Hydrology 286:249-270.

Glassy, J.M., and S.W. Running. 1994. Validating diurnal climatology logic of the MT-CLIM model across a climatic gradient in Oregon. Ecological Applications 4:246-257.

Gomez, J.D., J.D. Etchevers, A.I. Monterroso, C. Gay, J. Campo, and M. Martinez. 2008. Spatial estimation of mean temperature and precipitation in areas of scarce meteorological information. Atmosfera 21:35-56.

Goovaerts, P. 1997. Geostatistics for natural resources evaluation. Oxford, New York. 496 p.

Goovaerts, P. 2000. Geostatistical approaches for incorporating elevation into the spatial interpolation of rainfall. Journal of Hydrology 228:113-129.

Gordon, W.S., and J.S. Famiglietti. 2004. Response of the water balance to climate change in the United States over the 20th and 21st centuries: Results from the VEMAP Phase 2 model intercomparisons. Global Biogeochemical Cycles 18:1-16.

Gowda, P.H., J.L. Chavez, P.D. Colaizzi, S.R. Evett, T.A. Howell, and J.A. Tolk. 2007. Remote sensing based energy balance algorithms for mapping ET: Current status and future challenges. American Society of Agriculture and Biological Engineers 50:1639-1644.

Gower, S.T. and J.M. Norman. 1991. Rapid estimation of leaf area index in conifer and broad-leaf plantations. Ecology 72:1896-1900.

Goudie, A.S. 2006. Global warming and fluvial geomorphology. Geomorphology 79:384-394.

Granier, A. 1985. A new method of sap flow measurement in tree stems. Annales des Sciences Forestieres 42:193-200.

Granier, A., P. Biron, B. Kostner, L. W. Gay, and G. Najjar. 1996. Comparisons of xylem sap flow and water vapour flux at the stand level and derivation of canopy conductance for scots pine. Theoretical and Applied Climatology 53:115-122.

Granier, A., P. Biron, and D. Lemoine. 2000. Water balance, transpiration and canopy conductance in two beech stands. Agricultural and Forest Meteorology 100:291–308.

Granier, A., and N. Breda. 1996. Modelling canopy conductance and stand transpiration of an oak forest from sap flow measurements. Ann. Sci. For. 53:537-546.

Green, S.R., and B.E. Clothier. 1988. Water use of kiwifruit vines and apple trees by the heat-pulse technique. Journal of Experimental Botany 39:115-123.

Groisman, P.Y., T.R. Karl, D.R. Easterling, R.W. Knight, P.F. Jamason, K.J. Hennessy, R. Suppiah, C.M. Page, J. Wibig, K. Fortuniak, V. N. Razuvaev, A. Douglas, E.

Forland, and P. M. Zhai. 1999. Changes in the probability of heavy precipitation: Important indicators of climatic change. Climate Change 42:243-283.

Gue, S.L., H. Chen, H.G. Zhang, L.H. Xiong, P. Liu, B. Pang, G.C. Wang, and Y.Z. Wang. 2005. A semi-distributed monthly water balance model and its application in a climate change impact study in the middle and lower Yellow River basin. Water International 30:250-260.

Guo, S., J. Wang, L. Xiong, A. Ying, and D. Li. 2002. A macro-scale and semi-distributed monthly water balance model to predict climate change impacts in China. Journal of Hydrology 268:1-15.

Haberlandt, U. 2007. Geostatistical interpolation of hourly precipitation from rain gauges and radar for a large-scale extreme rainfall event. Journal of Hydrology 332:144-157.

Hamon, W.R. 1963. Computation of direct runoff amounts from storm rainfall. International Association of Scientific Hydrology 63:52-62.

Hansen, A.J., R.P. Neilson, V.H. Dale, C.H. Flather, L.R. Iverson, D.J. Currie, S. Shafer, R. Cook, and P. J. Bartlein. 2001. Global change in forests: Responses of species, communities, and biomes. BioScience 51:765-779.

Hargreaves, G.H. 1975. Moisture availability and crop production. Transactions of the ASAE 18: 980-984.

Hargreaves, G.H., and Z.A. Samani. 1982. Estimating potential evapotranspiration. Journal of the Irrigation and Drainage Division 108:223-230.

Hashimoto, H., J.L. Dungan, M.A. White, F. Yang, A.R. Michaelis, S.W. Running, and R. R. Nemani. 2008. Satellite-based estimation of surface vapor pressure deficits using MODIS land surface temperature data. Remote Sensing of Environment 112:142-155.

Heide, O.M. 1993. Daylength and thermal time responses of budburst during dormancy release in some northern deciduous trees. Plant Physiology 88:531-540.

Helvey, J.D. 1967. Interception by eastern white pine. Water Resources Research 3:723-729.

Helvey, J.D., and J.H. Patric. 1965. Canopy and litter interception of rainfall by hardwoods of eastern United States. Water Resources Research 1:193-206.

Helvey, J.D. Rainfall interception by hardwood forest litter in the southern Appalachians. Research Paper SE-8. Asheville, NC: U.S. Department of Agriculture, Forest Service, Southeastern Forest Experiment Station. 11 p.

Hevesi, J.A., A.L. Flint, and J.D. Istok. 1992. Precipitation estimation in mountainous terrain using multivariate geostatistics; Part II, Isohyetal maps. Journal of Applied Meteorology 31:677-688.

Hogg, E.H., and P.A. Hurdle. 1997. Sap flow in trembling aspen: implications for stomatal responses to vapor pressure deficit. Tree Physiology 17:501-509.

Holzmueller, E.J., S. Jose, and M.A. Jenkins. 2010. Ecological consequences of an exotic fungal disease in eastern U.S. hardwood forests. Forest Ecology and Management 259:1347-1353.

Hornbeck, J.W., M.B. Adams, E.S. Corbett, E.S. Verry, J.A. Lynch. 1993. Long-term impacts of forest treatments on water yield: a summary for northeastern USA. Journal of Hydrology 150:323-344.

Houghton, J.T., Y. Ding, D.J. Griggs, M. Noguer, P.J. van der Linden, and D. Xiaosu. Climate Change 2001: The scientific basis: Contributions of working group I to the third assessment report of the intergovernmental panel on climate change. 881 p.

Houghton, J.T., Y. Ding, D.J. Griggs, M. Noguer, P.J. van der Linden, and D. Xiaosu. Climate Change 2001: The scientific basis: Contributions of working group I to the third assessment report of the intergovernmental panel on climate change. 881 p.

Howell, T.A., and D.A. Dusek. 1995. Comparison of vapor-pressure deficit calculation methods—Southern high plains. Journal of Irrigation and Drainage Engineering 121:191-198.

Hulme, M., T.J. Osborn, and T.C. Johns. 1998. Precipitation sensitivity to global warming: Comparison of observations with HadCM2 simulations. Geophysical Research Letters 25:3379-3382.

Hunter, A.F., and M.J. Lechowicz. 1992. Predicting the timing of budburst in temperate trees. Journal of Applied Ecology 29:597-604.

Hursh, C.R. 1948. Local climate in the copper basin of Tennessee as modified by the removal of vegetation. U.S. Dept. of Agriculture. Washington, D.C. 38 p.

Hutchinson, B.A., D.R. Matt, R.T. McMillen, L.J. Gross, S.J. Tajchman, and J.M. Norman. 1986. The architecture of a deciduous forest canopy in eastern Tennessee, U.S.A. Journal of Ecology 74:635-646.

IPCC. 2007. Climate Change 2007: Impacts, adaptation and vulnerability. Contribution of working group II to the fourth assessment report of the intergovernmental panel on climate change. Cambridge University Press, Cambridge, UK.

Ishida, T., and S. Kawashima. 1993. Use of cokriging to estimate surface air temperature from elevation. Theoretical and Applied Climatology 47:147-157.

Iverson, L.R., and A.M. Prasad. 1998. Predicting abundance of 80 tree species following climate change in the eastern United States. Ecological Monographs 68:465-485.

Iverson, L.R., and A.M. Prasad. 2002. Potential redistribution of tree species habitat under five climate change scenarios in the eastern US. Forest Ecology and Management 155:205-222.

Iverson, L.R., A.M. Prasad, and M.W. Schwartz. 1999. Modeling potential future individual tree-species distributions in the eastern United States under a climate change scenario: a case study with *Pinus virginiana*. Ecological Modelling 115:77-93.

Johnson, D., M. Smith, V. Koren, and B. Finnerty. 1999. Comparing mean areal precipitation estimates from NEXRAD and rain gauge networks. Journal of Hydrologic Engineering 4:117-124.

Jolly, W.M., J.M. Graham, A. Michaelis, R. Nemani, and S.W. Running. 2005. A flexible, integrated system for generating meteorological surfaces derived from point sources across multiple geographic scales. Environmental Modeling & Software 20:873-882.

Jonckheere, I., S. Fleck, K. Nackaerts, B. Muys, P. Coppin, M. Weiss, and F. Baret. 2004. Review of methods for in situ leaf area index determination Part I. Theories, sensors and hemispherical photography. Agricultural and Forest Meteorology 121:19-35.

Jones, P.D., and M. Hulme. 1996. Calculating regional climatic time series for temperature and precipitation: Methods and illustrations. International Journal of Climatology 16:361-377.

Jones, R.N., F.H.S. Chiew, W.C. Boughton, and L. Zhang. 2006. Estimating the sensitivity of mean annual runoff to climate change using selected hydrological models. Advances in Water Resources 29:1419-1429.

Karl, T.R., and R.W. Knight. 1998. Secular trends of precipitation amount, frequency, and intensity in the United States. Bulletin of the American Meteorological Society 79:231-241.

Kattenberg, A., E. Giorgi, H. Grassl, G.A. Meehl, J.F.B. Mitchell, R.J. Stouffer, T. Tokioka, A.J. Weaver, and M.L. Wigley. 1996. Climate models-Projections of future climate. P. 289-357 *in* Climate Change 1995: The Science of Climate Change. Report of IPCC Working Group I, Houghton, J. T., L. G. M. Filho, B. A. Callander, N. Harris, A. Kattenberg, and K. Maskell (eds.). Cambridge University Press, Cambridge, UK.

Kay, A.L., and H.N. Davies. 2008. Calculating potential evaporation from climate model data: A source of uncertainty for hydrological climate change impacts. Journal of Hydrology 358:221-239.

Kelliher, F.M., B.M.M. Kostner, D.Y. Hollinger, J.N. Byers, J.E. Hunt, T.M. McSeveny, R. Meserth, P.L. Weir, and E.D. Schulze. 1992. Evaporation, xylem sap flow, and tree transpiration in a New Zealand broad-leaved forest. Agricultural and Forest Meteorology 62:53-73.

Kellomaki, S., and H. Vaisanen. 1997. Modelling the dynamics of the forest ecosystem for climate change studies in the boreal conditions. Ecological Modelling 97:121-140.

Kergoat, L. 1998. A model for hydrological equilibrium of leaf area index on a global scale. Journal of Hydrology 212-213:268-286.

Keskitalo, J., G. Bergquist, P. Gardestrom, and S. Jansson. 2005. A cellular timetable of autumn senescence. Plant Physiology 139:1635-1648.

Kimball, J.S., S.W. Running, and R.R. Nemani. 1997. An improved method for estimating surface humidity from daily minimum temperature. Agricultural and Forest Meteorology 85:87-98.

Kjelgaard, J.F., C.O. Stockle, R.A. Black, and G.S. Campbell. 1997. Measuring sap flow with the heat balance approach using constant and variable heat inputs. Agricultural and Forest Meteorology 85:239-250.

Konikov, L.F., E. Kendy. 2005. Groudwater depletion: A global problem. Hydrogeology Journal 13:317-320.

Koren, V.I., B.D. Finnerty, J.C. Schaake, M.B. Smith, D.J. Seo, and Q.Y. Duan. 1999. Scale dependencies of hydrologic models to spatial variability of precipitation. Journal of Hydrology 217:285-302.

Kostner, B., A. Granier, and J. Cermak. 1998. Sap flow measurements in forest stands-methods and uncertainties. Annales des Sciences Forestieres 55:13-27.

Kostner, B.M.M., P. Biron, R. Siegwolf, and A. Granier. 1996. Estimates of water flux and canopy conductance of scots pine at tree level utilizing different xylem sap flow methods. Theoretical and Applied Climatology 53:105-113.

Krajewski, W.F., V. Lakshmi, K.P. Georgakakos, and S.C. Jain. 1991. A Monte Carlo study of rainfall sampling effect on a distributed catchment model. Water Resources Research 27:119-128.

Kramer K., I. Leinonen, and D. Loustau. 2000. The importance of phenology for the evaluation of impact of climate change on growth of boreal, temperate and Mediterranean forests ecosystems: an overview. International Journal of Biometeorology 44:67-75.

Kremer, R.G., E.R. Hunt Jr., S.W. Running, and J.C. Coughlan. 1996. Simulating vegetational and hydrologic responses to natural climatic variation and GCM-predicted climate change in a semi-arid ecosystem in Washington, U.S.A. Journal of Arid Environments 33:23-38.

Kubota, M., J. Tenhunen, R. Zimmermann, M. Schmidt, S. Adiku, and Y. Kakubari. 2005. Influences of environmental factors on the radial profile of sap flux density in *Fagus crenata* growing at different elevations in the Naeba Mountains, Japan. Tree Physiology 25:545-556.

Kucharika, C.J., C.C. Barforda, M.E. Maayar, S.C. Wofsyc, R.K. Monsond, and D.D. Baldocchie. 2006. A multiyear evaluation of a dynamic global vegetation model at three AmeriFlux forest sites: Vegetation structure, phenology, soil temperature, and CO2 and H2O vapor exchange. Ecological Modelling 196:1-31.

Kukla, G., and T. Karl. 1993. Night time warming and the greenhouse effect. Environmental Science and Technology 27:1468-1474.

Kumagai, T., H. Nagasawa, T. Mabuchi, S. Ohsaki, K. Kubota, K. Kogi, Y. Utsumi, S. Koga, and K. Otsuki. 2005. Sources of error in estimating stand transpiration using allometric relationships between stem diameter and sapwood area for *Cryptomeria japonica* and *Chamaecyparis obtusa*. Forest Ecology and Management 206:191–195.

Kundzewicz, Z.W., L.J. Mata, N. Arnell, P. Döll, P. Kabat, B. Jiménez, K. Miller, T. Oki, Z. Şen, and I. Shiklomanov. 2007. Freshwater resources and their management. P. 173-210 *in* Climate change 2007: Impacts, adaptation and vulnerability. Contribution of working group II to the fourth assessment report of the intergovernmental panel on climate change, Parry, M.L., O. F. Canziani, J. P. Palutikof, P. J. van der Linden and C. E. Hanson (eds.). Cambridge University Press, Cambridge, UK.

Kyriakidis, P.C., J. Kim, and N.L. Miller. 2001. Geostatistical mapping of precipitation from rain gauge data using atmospheric and terrain characteristics. Journal of Applied Meteorology 40:1855-1877.

Landsberg, J.J., and R.H. Waring. 1997. A generalised model of forest productivity using simplified concepts of radiation-use efficiency, carbon balance and partitioning. Forest Ecology and Management 95:209–228.

Larcher, W. 1983. Physiological plant ecology. Springer-Verlag, Germany. 513 p.

Law, B.E., S. Van Tuyl, A. Cescatti, and D.D. Baldocchi. 2001. Estimation of leaf area index in open-canopy ponderosa pine forests at different successional stages and management regimes in Oregon. Agricultural and Forest Meteorology 108:1-14.

Lawrence, G.B., A.G. Lapenis, D. Berggren, B.F. Aparin, K.T. Smith, W.C. Shortle, S.W. Bailey, D.L. Varlyguin, and B. Babikov. 2005. Climate dependency of tree growth suppressed by acis deposition effects on soils in northwest Russia. Environmental Science & Technology 39:2004-2010.

Lechowicz, M.J. 1984. Why do temperate deciduous trees leaf out at different times? Adaptation and ecology of forest communities. The American Naturalist 124:821-842.

Leipprand, A., and D. Gerten. 2006. Global effects of doubled atmospheric CO_2 content on evapotranspiration, soil moisture and runoff under potential natural vegetation. Hydrological Sciences 51:171-185.

Lesica, P., and B. McCune. 2004. Decline of arctic-alpine plants at the southern margin of their range following a decade of climatic warming. Journal of Vegetation Science 15:679-690.

Lettenmaier, D.P., E.F. Wood, and J.R. Wallis. 1994. Hydro-climatological trends in the continental United States, 1948-88. Journal of Climate 7:586-607.

Levia, D.F. 2008. A generalized allometric equation to predict foliar dry weight on the basis of trunk diameter for eastern white pine (*Pinus Strobus* L.). Forest Ecology and Management 255:1789-1792.

Lieth, H. 1974. Phenology and seasonality modeling. Springer-Verlag, New York. 444 p.

Linderholm, H.W. 2006. Growing season changes in the last century. Agricultural and Forest Meteorology 137:1-14.

Lindroth, A., J. Cermak, J. Kucera, E. Cienciala, and H. Eckersten. 1995. Sap flow by the heat balance method applied to small size salix trees in a short-rotation forest. Biomass and Bioerrergy 8:7-15.

Linkosalo, T., R. Hakkinen, and H. Hanninen. 2006. Models of the spring phenology of boreal and temperate trees: is there something missing? Tree Physiology 26:1165-1172.

Lloyd, C.D. 2005. Assessing the effect of integrating elevation data into the estimation of monthly precipitation in Great Britain. Journal of Hydrology 308:128-150.

Loehle, C., and D. LeBlanc. 1996. Model-based assessments of climate change effects on forests: a critical review. Ecological Modelling 90:1-31.

Lopez, O.R., K. Farris-Lopez, R.A. Montgomery, and T.J. Givnish. 2008. Leaf phenology in relation to canopy closure in southern Appalachian trees. American Journal of Botany 95:1395-1407.

Lu, J., G. Sun, S.G. McNulty, and D.M. Amatya. 2003. Modeling Actual Evapotranspiration from forested watersheds across the southern United States. Journal of the American Water Resources Association 39:887-896.

Lu, J., G. Sun, S.G. McNulty, and D.M. Amatya. 2005. A comparison of six potential evapotranspiration methods for regional use in the southeastern United States. Journal of the American Water Resources Association 41:621-633.

Mackay, D.S., D.E. Ahl, B.E. Ewers, S.T. Gower, S N. Burrows, S. Samanta, and K.J. Davis. 2002. Effects of aggregated classifications of forest composition on estimates of evapotranspiration in a northern Wisconsin forest. Global Change Biology 8:1253-1265.

Malek, E., and G.E. Bingham. 1993. Comparison of the Bowen ratio-energy balance and the water balance methods for the measurement of evapotranspiration. Journal of Hydrology 146:209-220.

Martin, T.A. 2000. Winter season tree sap flow and stand transpiration in an intensively-managed loblolly and slash pine plantation. Journal of Sustainable Forestry 10:155-163.

McMaster, G.S., and W.W. Wilhelm. 1997. Growing degree-days: one equation, two interpretations. Agricultural and Forest Meteorology 87:291-300.

McNab, W.H. 1989. Terrain shape index: Quantifying effect of minor landforms on tree height. Forest Science 35:91-104.

Mearns, L.O., F. Giorgi, L. McDaniel, and C. Shields. 2003. Climate scenarios for the southeastern U.S. based on GCM and regional model simulations. Climatic Change 60:7-35.

Menzel, A. 2002. Phenology: It's importance to the global change community. Climatic Change 54:379-385.

Milly, P.C.D. 1994. Climate, soil water storage, and the average annual water balance. Water Resources Research 30:2143-2156.

Mitchell, J.F.B. 1989. The "greenhouse"effect and climate change. Reviews of Geophysics 27:113-139.

Mohammed, A.R., and L. Tarpley. 2009. High night time temperatures affect rice productivity through altered pollen germination and spikelet fertility. Agricultural and Forest Meteorology 149:999-1008.

Monteith, J.L. 1965. Evaporation and environment, In: Proceedings of he 19th Symposium of the Society for Experimental Biology. Cambridge University Press, New York, NY pp. 205-233.

Moorhead, K.K. 2003. Effects of drought on the water-table dynamics of a southern Appalachian mountain floodplain and associated fen. Wetlands 23:792-799.

Morton, F.I. 1983. Operational estimates of areal evapotranspiration and their significance to the science and practice of hydrology. Journal of Hydrology 66:1-76.

Mowbray, T.B., and H.J. Oosting. 1968. Vegetation gradients in relation to environment and phenology in a southern Blue Ridge Gorge. Ecological Monographs 38:309-344.

Mulholland, P.J., G.R. Best, C.C. Coutant, G.M. Hornberger, J.L. Meyer, P.J. Robinson, J.R. Stenberg, R.E. Turner, F. Vera-Herrera, and R.G. Wetzel. 1997. Effects of climate change on freshwater ecosystems of the southeastern United States and the Gulf of Mexico. Hydrological Processes 11:949-970.

Mulligan, M., and J. Wainwright. 2004. Environmental modelling: Finding simplicity in complexity. John Wiley & Sons Ltd., West Sussex, England, UK. 430 p.

Murakami, S. 2007. Application of three canopy interception models to a young stand of Japanese cypress and interpretation in terms of interception mechanism. Journal of Hydrology 342:305-319.

Murakami, S., Y. Tsuboyama, T. Shimizu, M. Fujieda, and S. Noguchi. 2000. Variation of evapotranspiration with stand age and climate in a small Japanese forested catchment. Journal of Hydrology (Amsterdam) 227:114-127.

Murdock, N.A. 1994. Rare and endangered plants and animals of southern Appalachian wetlands. Water, Air and Soil Pollution 77:385-405.

Murray, F.W. 1967. On the computation of saturation vapor pressure. Journal of Applied Meteorology 6:203-204.

Najjar, R.G. 1999. The water balance of the Susquehanna River Basin and its response to climate change. Journal of Hydrology 219:7-19.

Nash, L.L., and P.H. Gleick. 1991. Sensitivity of streamflow in the Colorado basin to climatic changes. Journal of Hydrology 125:221-241.

National Climatic Data Center (NCDC). 1985-2010. Daily Totals/Averages for Southeast United States Stations. US Climate Normals. Available from <http://cdo.ncdc.noaa.gov>.

Nicolas, E., A. Torrecillas, M.F. Ortuno, R. Domingo, and J.J. Alarcon. 2005. Evaluation of transpiration in adult apricot trees from sap flow measurements. Agricultural Water Management 72:131-145.

Nie, D., I.D. Flitcroft, and E.T. Kanemasu. 1992. Performance of Bowen ratio systems on a slope. Agricultural and Forest Meteorology 59:165-181.

Nienstaedt, H. 1974. Genetic variation in some phenological characteristics of forest trees. P. 389-400 *in* Phenology and seasonality modeling, Leith, H. (ed.). Springer-Verlag, New York.

Nizinski, J.J., and B. Sauguer. 1988. Model of leaf budding and development for a mature *Quercus* forest. Journal of Applied Ecology 25:643-652.

Norby, R.J., J.D. Sholtis, C.A. Gunderson, and S.S. Jawdy. 2003. Leaf dynamics of a deciduous forest canopy: no response to elevated CO_2. Oecologia 136:574-584.

Oishi, A.C., R. Oren, K.A. Novick, S. Palmroth, G.G. Katul. 2010. Interannual invariability of forest evapotranspiration and its consequence to water flow downstream. Ecosystems 13:421-436.

Oishi, A.C., R. Oren, and P.C. Stoy. 2008. Estimating components of forest evapotranspiration: A footprint approach for scaling sap flux measurements. Agricultural and Forest Meteorology 148:1719-1732.

Oudin, L., F. Hervieu, C. Michel, C. Perrin, V. Andreassian, F. Anctil, and C. Loumagne. 2005. Which potential evapotranspiration input for a lumped rainfall-runoff model? Part 2: Towards a simple and efficient potential evapotranspiration model for rainfall-runoff modelling. Journal of Hydrology (Amsterdam) 303:290-306.

Pacl, J., 1972. Orographic influences on distribution of precipitation; Physiographic factors and hydrologic approaches. Ib: Distribution of Precipitation in Mountainous Areas, Volume I. Proceedings of the World Meteorological Organization Symposium. Geilo, World Meteorological Organization, Geneva, WMO No. 326, pp. 67-72.

Parmesan, C. 2006. Ecological and evolutionary responses to recent climate change. Annual Review of Ecology Evolution Systematics 37:637-669.

Parmesan, C., and G. Yohe. 2003. A globally coherent fingerprint of climate change impacts across natural systems. Nature 421:37-42.

Pauli, H., M. Gottfried, K. Reiter, C. Klettner, and G. Grabherr. 2007. Signals of range expansions and contractions of vascular plants in the high Alps: observations (1994–2004) at the GLORIA*master site Schrankogel, Tyrol, Austria. Global Change Biology 13:147-156.

Peng, S., J. Huang, J.E. Sheehy, R.C. Laza, R.M. Visperas, X. Zhong, G.S. Centeno, G. S. Khush, and K.G. Cassman. 2004. Rice yields decline with higher night temperature from global warming. Proceedings of the National Academy of Sciences 101:9971-9975.

Perez, P.J., F. Castellvi, M. Ibanez, and J.I. Rosslee. 1999. Assessment of reliability of Bowen ratio method for partitioning fluxes. Agricultural and Forest Meteorology 97:141-150.

Perry, T.O. 1971. Dormancy of trees in winter. Science 171:29-36.

Phillips, D.L., J. Dolph, and D. Marks. 1992. A comparison of geostatistical procedures for spatial analysis of precipitation in mountainous terrain. Agricultural and Forest Meteorology 58:119-141.

Pike, J.G. 1964. The estimation of annual runoff from meteorological data in a tropical climate, Journal of Hydrology 2:116-123.

Piri, J., S. Amin, A. Moghaddamnia, A. Keshavarz, D. Han, and D. Remesan. 2009. Daily pan evaporation modeling in a hot and dry climate. Journal of Hydrological Engineering 14:803-811.

Ponce, V.M., and A.V. Shetty. 1995. A conceptual model of catchment water balance: 1. Formulation and calibration. Journal of Hydrology 173:27-40.

Priestley, C.H.B., and R.J. Taylor. 1972. On the assessment of surface heat flux and evaporation using large-scale parameters. Monthly Weather Review 100:81-92.

Prueger, J.H., J.L. Hatfield, J.K. Aase, and J.L. Pikul Jr. 1997. Bowen-ratio comparisons with lysimeter evapotranspiration. Agronomy Journal 89:730-736.

Raichle, B.W., and W.R. Carson. 2009. Wind resource assessment of the southern Appalachian ridges in the southeastern United States. Renewable and Sustainable Energy Reviews 13:1104-1110.

Rana, G., and N. Katerji. 2000. Measurement and estimation of actual evapotranspiration in the field under Mediterranean climate: a review. European Journal of Agronomy 13:125-153.

Ranzi, R., and R. Rosso. 1995. Distributed estimation of incoming direct solar radiation over a drainage basin. Journal of Hydrology 166:461-478.

Raspa, G., M. Tucci, and R. Bruno. 1997. Reconstruction of rainfall fields by combining ground rain gauges data with radar maps using external drift method. P. 941-950 *in* Geostatistics Wollongong '96, Baafi, E.Y., and N. A. Schofield, (eds.). Kluwer Academic Publishers, Dordrecht.

Raulier, F., and P.Y. Bernier. 2000. Predicting the date of leaf emergence for sugar maple across its native range. Canadian Journal of Forestry Research 30:1429-1435.

Richardson, A.D., A.S. Bailey, E.G. Denny, C.W. Martin, and J. O'Keefe. 2006. Phenology of northern hardwood forest canopy. Global Change Biology 12:1174-1188.

Riekerk, H. 1985. Water quality effects of pine flatwoods silviculture. Journal of Soil and Water Conservation 40:306-309.

Robinson, A.P., R.E. Froese. 2004. Model validation using equivalence tests. Ecological Modelling 176:349-358.

Rosenberg, N.J., D.J. Epstein, D. Wang, L. Vail, R. Srinivasan, and J.G. Arnold. 1999. Possible impacts of global warming on the hydrology of the Ogallala aquifer region. Climatic Change 42:677-692.

Rotzer, T., and F.M. Chmielewski. 2001. Phenological maps of Europe. Climate Research 18:249-257.

Rowntree, P.R. 1988. Review of general circulation models as a basis for predicting the effects of vegetation change on climate. P. 162-196 *in* Forests, Climate and Hydrology - Regional Impacts. Reynolds, E.R.C. and F.B. Thompson (eds.). Keff Press.

Russo, J.M., A.M. Liebhold, and J.G.W. Kelley. 1993. Mesoscale weather data as input to a gypsy moth (*Lepidoptera: Lymantriidae*) phenology model. Journal of Economic Entomology 86:838-844.

Rutter, J., K.A. Kershaw, P.C. Robins, and A.J. Morton. 1971. A predictive model of rainfall interception in forests, 1. Derivation of the model from observations in a plantation of corsican pine. Agricultural Meteorology 93:367-384.

Sabate, S., C.A. Gracia, and A. Sanchez. 2002. Likely effects of climate change on growth of *Quercus ilex*, *Pinus halepensis*, *Pinus pinaster*, *Pinus sylvestris* and *Fagus sylvatica* forests in the Mediterranean region. Forest Ecology and Management 162:23-37.

Samani, Z. 2000. Estimating solar radiation and evapotranspiration using minimum climatological data (Hargreaves-Samani Equation). Journal of Irrigation and Drainage Engineering 126:265-267.

Sankovski, A., and M. Pridnia. 1995. A comparison of the southern Appalachian (U.S.A.) and southwestern Caucasus (Russia) forests: influences of historical events and present environment. Journal of Biogeography 22:1073-1081.

Scanlon, T.M., and J.D. Albertson. 2003. Inferred controls on tree/grass composition in a savanna ecosystem: combining 16-Year NDVI data with a dynamic soil moisture model. Water Resources Research 39:1224.

Schaber, J., and F.W. Badeck. 2005. Plant phenology in Germany over the 20th century. Regional Environmental Change 5:37-46.

Schaeffer, S.M., D.G. Williams, and D.C. Goodrich. 2000. Transpiration of cottonwood/willow forest estimated from sap flux. Agricultural and Forest Meteorology 105:257–270.

Schreiber, P. 1904. Uber die Beziehungen zwischen dem Niederschlag und der Wasserfu¨hrung der Flu¨ße in Mitteleuropa. Meteorology 21:441-452.

Schuirmann, D.L. 1981. On hypothesis testing to determine if the mean of a normal distribution is contained in a known interval. Biometrics 37:617.

Scurlock, J.M.O., G.P. Asner, and S.T. Gower. 2001. Worldwide historical estimates of bibliography leaf area index, 1932-2000. ORNL Technical Memorandum ORNL/TM-2001/268. Oak Ridge National Laboratory, Oak Ridge, TN.

Shah, S. M. S., P. E. O'Connell, and J. R. M. Hosking. 1996. Modelling the effects of spatial variability in rainfall on catchment response. Journal of Hydrology 175:89-111.

Shenbin, C., L. Yunfeng, and A. Thomas. 2006. Climate change on the Tibetan platuae: Potential evapotranspiration trends from 1961-2000. Climate Change 76:291-319.

Simberloff, D. 2000. Global climate change and introduced species in United States forests. The Science of the Total Environment 262:253-261.

Singh, V.P. 1997. Effect of spatial and temporal variability in rainfall and watershed characteristics on stream flow hydrograph. Hydrological Processes 11:1649-1669.

Sivapalan, M. 2005. Pattern, process and function: Elements of a unified theory of hydrology at the catchment scale. P. 193-219 *in* Encyclopedia of Hydrological Sciences, Anderson, M.G., (ed.). John Wiley & Sons Ltd.

Skirvin, S.M., S.E. Marsh, M.P. McClaran, and D.M. Meko. 2003. Climate spatial variability and data resolution in a semi-arid watershed, south-eastern Arizona. Journal of Arid Environments 54:667-686.

Spittlehouse, D.L., and T.A. Black. 1980. Evaluation of the Bowen ratio/energy balance method for determining forest evapotranspiration. Atmosphere-Ocean 18:98-116.

Stachowicz, J.J., J.R. Terwin, R.B. Whitlatch, and R.W. Osman. 2002. Linking climate change and biological invasions: Ocean warming facilitates nonindigenous species invasions. Proceedings of the National Academy of Sciences 99:15497-15500.

Stellman, K.M., and H.E. Fuelberg. 2001. An examination of radar and rain gauge–derived mean areal precipitation over Georgia watersheds. American Meteorological Society 16:133-144.

Stone, M.C., R.H. Hotchkiss, C.M. Hubbard, T.A. Fontaine, L.O. Mearns, and J.G. Arnold. 2001. Impacts of climate change on Missouri River Basin water yield. Journal of the American Water Resources Association 37:1119-1130.

Stoy, P.C., G.C. Katul, M.B.S. Siqueira, J.Y. Juang, K.A. Novick, H.R. McCarthy, A.C. Oichi, J.M. Uebelherr, H.S. Kim, and R. Oren. 2006. Separating the effects of climate and vegetation on evapotranspiration along a successional chronosequence in the southeastern US. Global Change Biology 12:2115-2135.

Sun, G., J. Lu, D. Gartner, M. Miwa, and C. Trettin. 2000. Water budgets of two forested watersheds in South Carolina. P. 199-202 *in* Proceedings of the spring special conference. Higgins, R.W. (ed.). American Water Resources Association, Miami, Florida.

Swank, W.T., and D.A. Crossley. 1988. Forest hydrology and ecology at Coweeta. Springer-Verlag, New York, New York. 469 p.

Tanner, B.D. 1990. Automated weather stations. Remote Sensing Reviews 5:73-98.

Thiessen, A.H. 1911. Precipitation averages for large areas. Monthly Weather Review 39:1082-1089.

Thomas, C.D., A. Cameron, R.E. Green, M. Bakkenes, L.J. Beaumont, Y.C. Collingham, B.F.N. Erasmus, M. Ferreira de Siqueira, A. Grainger, L. Hannah, L. Hughes, B. Huntley, A.S. Van Jaarsveld, G.F. Midgley, L. Miles, M.A. Ortega-Huerta, A.T. Peterson, O.L. Phillips, and S.E. Williams. 2004. Extinction risk from climate change. Nature 427:145-148.

Thomson, A.J., and S.M. Moncrieff. 1982. Prediction of bud burst in douglas-fir by degree-day accumulation. Canadian Journal of Forestry Research 12:448-452.

Thornthwaite, C.W. 1948. An approach toward a rational classification of climate. Geographical Review 38:55-94.

Thornton, P.E., and S.W. Running. 1999. Agricultural and Forest Meteorology 93:211-228.

Thornton, P.E., S.W. Running, and M.A. White. 1997. Generating surfaces of daily meteorological variables over large regions of complex terrain. Journal of Hydrology 190:214-251.

Thuiller, W., C. Albert, M.B. Araujo, P.M. Berry, M. Cabeza, A. Guisan, T. Hickler, G. F. Midgley, J. Paterson, F.M. Schurr, M.T. Sykes, and N.E. Zimmermann. 2008. Predicting global change impacts on plant species' distributions: Future challenges. Perspectives in Plant Ecology, Evolution and Systematics 9:137-152.

Tipton, J. L. 1994. Relative drought resistance among selected southwestern landscape plants. Journal of Arboriculture 20:151-155.

Trabucco, A., R.J. Zomer, D.A. Bossio, O. Van Straaten, and L.V. Verchot. 2008. Climate change mitigation through afforestation/reforestation: A global analysis of hydrologic impacts with four case studies. Agriculture, Ecosystems and Environment 126:81-97.

Turc, L. 1961. Estimation of irrigation water requirements, potential evapotranspiration: A simple climatic formula evolved up to date. Annual Agronomy 12:13-49.

Udo, S.O. 2002. Contribution to the relationship between solar radiation and sunshine duration in the Tropics: a case study of experimental data at Ilorin, Nigeria. Turkish Journal of Physics 26:229-236.

Udo, S.O., and T.O. Aro. 2000. New empirical relationships for determining global par from measurements of global solar radiation, infrared radiation or sunshine duration. International Journal of Climatology 20:1265–1274.

U.S. Geological Survey. 2006. National Water Information System (NWISWeb) data available on the World Wide Web, accessed January 20, 2006 at URL *http://waterdata.usgs.gov/nwis/*.

USDA Forest Service. 2007. The forest inventory and analysis database: Database description and users guide version 2.1. National Forest Inventory and Analysis Program, U.S. Department of Agriculture, Forest Service, Washington, DC.

USDA Forest Service: Forest Health Protection. Forest Insect and Disease Conditions in the United States 2006. 1 p.

Vandermast, D.B., and D.H. Van Lear. 2002. Riparian vegetation in the southern Appalachian mountains (USA) following chestnut blight. Forest Ecology and Management 155:97-106.

Valentine, H.T. 1983. Budbreak and leaf growth functions for modeling herbivory in some gypsy moth hosts. Forest Science 29:607-617.

Vaughan, P.J., T.J. Trout, and J.E. Ayars. 2007. A processing method for weighing lysimeter data and comparison to micrometeorological ET_o predictions. Agricultural Water Management 88:141-146.

Vest, R. 1993. Water wars in the southeast: Alabama, Florida, and Georgia square off over the Apalachicola-Chattahoochee-Flint river basin. Georgia State University Law Review 9:689-716.

Vitasse, Y., A.J. Porte, A. Kremer, R. Michalet, and S. Delzon. 2009. Responses of canopy duration to temperature changes in four temperate tree species: relative contributions of spring and autumn leaf phenology. Oecologia 161:187-198.

von Wuehlisch G., D. Krusche, and H. J. Muhs. 1995. Variation in temperature sum requirement for flushing of beech provenances. Silvae Genetica 44:5-6.

Vose, J.M., G.J. Harvey, K.J. Elliott, and B.D. Clinton. 2003. Measuring and modeling tree and stand level transpiration. P. 263-282 *in* Phytoremediation: Transformation and control of contaminants, McCutcheon, S. C. and J. L. Schnoor, (eds.). John Wiley & Sons Ltd., Hoboken, NJ.

Wattenbach, M., M. Zebisch, F. Hattermann, P. Gottschalk, H. Goemann, P. Kreins, F. Badeck, P. Lasch, F. Suckow, and F. Wechsung. 2007. Hydrological impact assessment of afforestation and change in tree-species composition - A regional case study for the Federal State of Brandenburg (Germany). Journal of Hydrology 346:1-17.

Wellek, S. 2003. Testing Statistical Hypotheses of Equivalence. Chapman & Hall, London. 284pp

Westlake, W.J. 1981. Response to T.B.L. Kirkwood: bioequivalence testing - a need to rethink. Biometrics 37:589-594.

Whigham, D.F. 1999. Ecological issues related to wetland preservation, restoration, creation and assessment. The Science of the Total Environment 240:31-40.

White, J.D., S.W. Running, R. Nemani, R.E. Keane, and K.C. Ryan. 1997. Measurement and remote sensing of LAI in Rocky Mountain montane ecosystems. Canadian Journal of Forest Research 27:1714-1727.

White, M.A., and R.R. Nemani. 2003. Canopy duration has little influence on annual carbon storage in the deciduous broad leaf forest. Global Change Biology 9:967-972.

Whittaker, R.H. 1956. Vegetation of the Great Smoky Mountains. Ecological Monographs 26:1-80.

Willmott, C.J., S.M. Robeson, and J.J. Feddema. 1991. Influence of spatially variable instrument networks on climate averages. Geophysical Research Letters 18:2249-2251.

Willmott, C.J., S.M. Robeson, and M.J. Janis. 1996. Comparison of approaches for estimating time-averaged precipitation using data from the USA. International Journal of Climatology 16:1103-1115.

Wilson, K.B., P.J. Hanson, P.J. Mulholland, D.D. Baldocchi, and S.D. Wullschleger. 2001. A comparison of methods for determining forest evapotranspiration and its components: sap flow, soil water budget, eddy covariance and catchment water balance. Agricultural and Forest Meteorology 106:153-168.

Winter, T.C. 1981. Uncertainties in estimating the water balance of lakes. Water Resources Bulletin 17:82-115.

Woodall, C.W., C.M. Oswalt, J.A. Westfall, C.H. Perry, M.D. Nelson, and A.O. Finley. 2009. An indicator of tree migration in forests of the eastern United States. Forest Ecology and Management 257:1434-1444.

Woodcock, D.W. 1989. Significance of ring porosity in analysis of a Sangamon flora. Palaeogeography, Palaeoclimatology, Palaeoecology 73:197-204.

Wullschleger, S.D., P.J. Hanson, and D.E. Todd. 2001. Transpiration from a multi-species deciduous forest estimated by xylem sap flow techniques. Forest Ecology and Management 143:205-213.

Xu, C., L. Tuneman, Y.D. Chen, and V.P. Singh. 2006. Evaluation of seasonal and spatial variations of lumped water balance model sensitivity to precipitation data errors. Journal of Hydrology 324:80-93.

Xu, C.Y., V.P. Singh. 2005. Evaluation of three complementary relationship evapotranspiration models by water balance approach to estimate actual regional evapotranspiration in different climatic regions. Journal of Hydrology 308:105-121.

Yang, D., B.E. Goodison, I. Ishida, and C.B. Benson. 1998. Adjustment of daily precipitation at 10 climate stations in Alaska: Application of WMO Intercomparison results. Water Resources Research 34:241-256.

Yoder, R.E., L.O. Odhiambo, and W.C. Wright. 2005. Calculation methods on accuracy of standardized Penman-Monteith equation in a humid climate. Journal of Irrigation and Drainage Engineering 131:228-237.

Zeppel, M.J.B., C.M.O. Macinnis-Ng, I.A.M. Yunusa, R.J. Whitley, and D. Eamus. 2008. Long term trends of stand transpiration in a remnant forest during wet and dry years. Journal of Hydrology 349:200-213.

Zhang, L., W.R. Dawes, and G.R. Walker. 2001. Response of mean annual evapotranspiration to vegetation changes at catchment scale. Water Resources Research 37:701-708.

Zhang, L., K. Hickel, W.R. Dawes, F.H.S. Chiew, A.W. Western, and P.R. Briggs. 2004. A rational function approach for estimating mean annual evapotranspiration. Water Resources Research 40:W02502.

Zhang, S.B., Z.K. Zhou, H. Hu, K. Xu, N. Yan, and S.Y. Li. 2005. Photosynthetic performances of *Quercus pannosa* vary with altitude in the Hengduan Mountains, southwest China. Forest Ecology and Management 212:291-301.

Zhang, X., Y. Zhang, and Y. Zhoub. 2000. Measuring and modelling photosynthetically active radiation in Tibet Plateau during April–October. Agricultural and Forest Meteorology 102:207-212.

Zhou, G., G. Sun, X. Wang, C. Zhou, S.G. McNulty, J.M. Vose, and D.M. Amatya. 2008. Estimating forest ecosystem evapotranspiration at multiple temporal scales with a dimension analysis approach. Journal of the American Water Resource Association 44:208-222.

Zierl B. 2001. A water balance model to simulate drought in forested ecosystems and its application to the entire forested area in Switzerland. Journal of Hydrology 242:115-136.